UNIVERSIDADE FEDERAL DO PARANÁ

ELIANE LEAL DE LARA

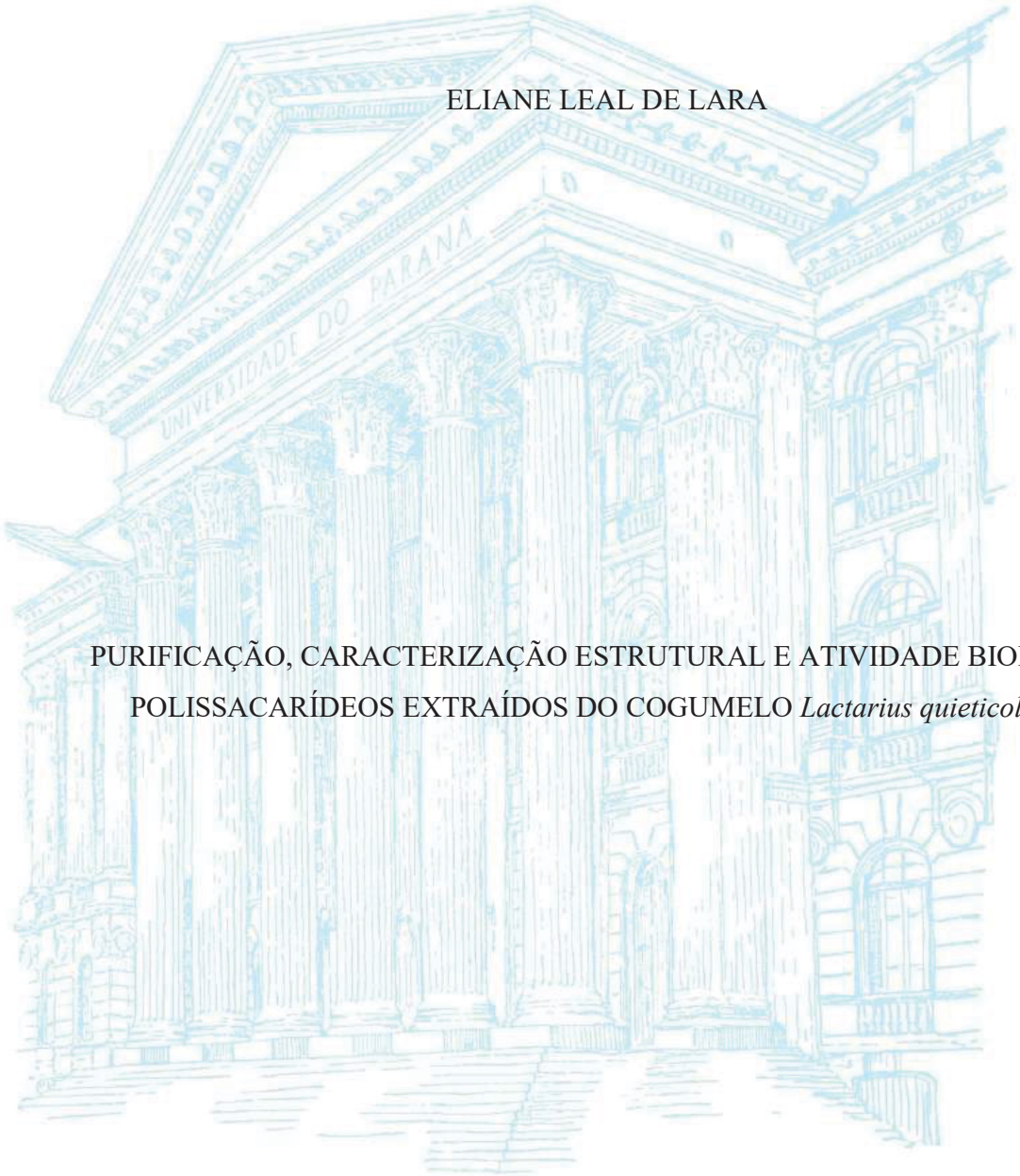

PURIFICAÇÃO, CARACTERIZAÇÃO ESTRUTURAL E ATIVIDADE BIOLÓGICA DE POLISSACARÍDEOS EXTRAÍDOS DO COGUMELO *Lactarius quieticolor*

Curitiba-PR
2024

ELIANE LEAL DE LARA

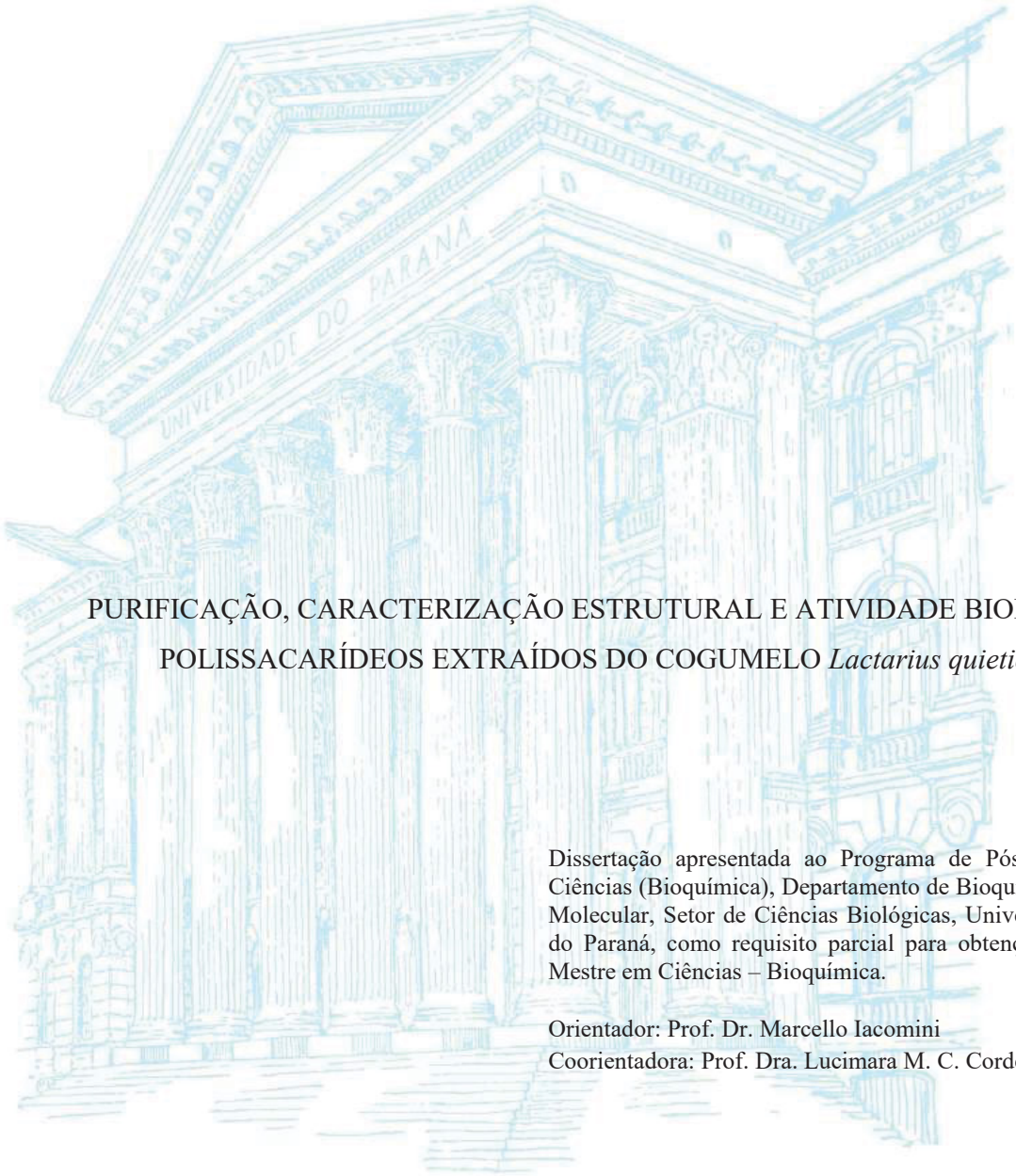

PURIFICAÇÃO, CARACTERIZAÇÃO ESTRUTURAL E ATIVIDADE BIOLÓGICA DE POLISSACARÍDEOS EXTRAÍDOS DO COGUMELO *Lactarius quieticolor*

Dissertação apresentada ao Programa de Pós-Graduação em Ciências (Bioquímica), Departamento de Bioquímica e Biologia Molecular, Setor de Ciências Biológicas, Universidade Federal do Paraná, como requisito parcial para obtenção do título de Mestre em Ciências – Bioquímica.

Orientador: Prof. Dr. Marcello Iacomini
Coorientadora: Prof. Dra. Lucimara M. C. Cordeiro

Curitiba-PR
2024

DADOS INTERNACIONAIS DE CATALOGAÇÃO NA PUBLICAÇÃO (CIP)
UNIVERSIDADE FEDERAL DO PARANÁ
SISTEMA DE BIBLIOTECAS – BIBLIOTECA DE CIÊNCIAS BIOLÓGICAS

De Lara, Eliane Leal.
Purificação, caracterização estrutural e atividade biológica de polissacarídeos extraídos do cogumelo *Lactarius quieticolor*. / Eliane Leal de Lara. – Curitiba, 2024.
1 recurso on-line : PDF.

Dissertação (Mestrado) – Universidade Federal do Paraná, Setor de Ciências Biológicas. Programa de Pós-Graduação em Ciências – Bioquímica.
Orientadora: Prof. Dr. Marcello Iacomini.
Coorientadora: Prof.ª Dra. Lucimara M. C. Cordeiro.

1. Cogumelos. 2. Polissacarídeos. 3. Câncer - Pesquisa. 4. Mamas - Câncer. 5. Mamas - Tumores. I. Iacomini, Marcello, 1947-. II. Cordeiro, Lucimara Mach C. III. Universidade Federal do Paraná. Setor de Ciências Biológicas. Programa de Pós-Graduação em Ciências - Bioquímica. IV. Título.

Bibliotecária: Rosilei Vilas Boas CRB-9/939

TERMO DE APROVAÇÃO

Os membros da Banca Examinadora designada pelo Colegiado do Programa de Pós-Graduação CIÊNCIAS (BIOQUÍMICA) da Universidade Federal do Paraná foram convocados para realizar a arguição da dissertação de Mestrado de **ELIANE LEAL DE LARA** intitulada: **Purificação, caracterização estrutural e atividade biológica de polissacarídeos extraídos do cogumelo *Lactarius quieticolor***, sob orientação do Prof. Dr. MARCELLO IACOMINI, que após terem inquirido a aluna e realizada a avaliação do trabalho, são de parecer pela sua APROVAÇÃO no rito de defesa.

A outorga do título de mestra está sujeita à homologação pelo colegiado, ao atendimento de todas as indicações e correções solicitadas pela banca e ao pleno atendimento das demandas regimentais do Programa de Pós-Graduação.

CURITIBA, 09 de Dezembro de 2024.

Assinatura Eletrônica
08/01/2025 12:59:25.0
MARCELLO IACOMINI
Presidente da Banca Examinadora

Assinatura Eletrônica
20/12/2024 10:06:27.0
THALES RICARDO CIPRIANI
Avaliador Interno (UNIVERSIDADE FEDERAL DO PARANÁ)

Assinatura Eletrônica
18/12/2024 15:14:11.0
FHERNANDA RIBEIRO SMIDERLE
Avaliador Externo (INSTITUTO PELÉ PEQUENO PRINCIPE)

NOTA EXPLICATIVA

Esta dissertação está estruturada no formato de artigo de acordo com as normas do Programa de Pós-Graduação em Ciências – Bioquímica e do Sistema de Bibliotecas (SiBi) da Universidade Federal do Paraná (UFPR). O conteúdo da dissertação é: introdução, revisão bibliográfica, justificativa, objetivos gerais e específicos, artigos científicos, conclusões e referências. Os artigos científicos possuem introdução, materiais e metodologias, resultados e discussão, agradecimentos e referências.

Agradecimentos

Ao Professor Dr. Marcello Iacomini, pela oportunidade e sua incessante dedicação à ciência e à Professora Dra. Lucimara Mach Cortes Cordeiro, pela coorientação e paciência durante a transição para uma nova área de estudo.

À Professora Dra. Giseli Klassen pela disponibilização do Laboratório de Epigenética (LabEpi) e auxílio nos experimentos biológicos e também aos alunos integrantes do laboratório: Karin, Bianca e João pela cordialidade e auxílio nos experimentos.

Aos colaboradores que foram essenciais para o desenvolvimento deste trabalho: Matheus Zavadinack, por auxiliar nas análises e práticas laboratoriais mais utilizadas. À Maria Paula Fernandes Bonaldi pela disponibilização do extrato alcalino e à Shayane da Silva Milhorini.

À minha mãe e irmão, Taina e Fagner, pelo amor e apoio que recebi ao longo de toda a vida.

Aos meus amigos e colegas dos laboratórios: Amanda, Dib, Wellington e Philippe, pelas conversas bem humoradas (na maioria das vezes), apoio,companheirismo e conhecimento compartilhado.

Às minhas professoras da graduação: Prof. Dra. Mariza Boscacci Marques pela inspiração para a bioquímica, Prof. Dra. Sandra Regina Masetto Antunes e Prof. Dra. Maria Elena Payret Arrúa que despertaram meu interesse para a pesquisa e pelo incentivo.

Aos técnicos Arquimedes, Keylla e Flávia pelas análises de RMN, HPSEC e GC-MS e ao coordenador do centro de RMN, Prof. Dr. Guilherme Lanzi Sassaki.

Ao Conselho Nacional de Desenvolvimento Científico e Tecnológico (CNPq) e à Coordenação de Aperfeiçoamento de Pessoal de Nível Superior (CAPES) pela bolsa e apoio financeiro à pesquisa (processos 403295/2021-1 e 310731/2021-6).

RESUMO

Cogumelos são importantes recursos alimentares com benefícios para a saúde, fontes de nutrientes essenciais e compostos de interesse medicinal, dentre os quais, destacam-se os polissacarídeos por suas diversas atividades biológicas, incluindo propriedades imunomodulatórias, antiinflamatórias e antitumorais – particularmente relevantes diante do desafio global do câncer. Com o câncer de mama entre os mais incidentes, o subtipo triplo-negativo destaca-se pela agressividade e mortalidade. Neste trabalho, exploramos a purificação, caracterização estrutural e avaliação biológica de polissacarídeos do cogumelo *Lactarius quieticolor*, a partir do extrato alcalino. Após tratamento com solução de Fehling, um heteropolissacarídeo (HTP – ramnogalactana) foi isolado do precipitado enquanto duas frações de glucanas com diferentes solubilidades foram obtidas do sobrenadante por subsequente precipitação etanólica fracionada. As análises estruturais, conduzidas por espectroscopia de ressonância magnética nuclear, RMN, (técnicas 1 e 2D: ^{1}H, HSQC-DEPT, COSY, TOCSY e HMBC), cromatografia gasosa acoplada à espectrometria de massas (GC-MS) e cromatografia por exclusão de tamanho de alta performance (HPSEC) revelaram que a fração HTP consiste em uma cadeia principal de (1→6)-α-D-galactopiranose com substituições em *O*-2 por ramnose, com massa molecular absoluta de 1.53×10^4 g/mol. Ensaios *in vitro* com células de câncer de mama da linhagem MDA-MB-231 demonstraram significativos efeitos antitumorais, com a ramnogalactana reduzindo a viabilidade celular em 50% a 1.200 μg/mL e aumentando a eficácia de paclitaxel, reduzindo a viabilidade em 42% quando coadministrados. Adicionalmente, as frações de glucanas GlcEt-Pp e GlcEtSn-300 apresentaram uma cadeia principal (1→3) com substituições em O-6, diferindo no grau de substituição, com valores de 21,4% e 70,6%, respectivamente. A GlcEtSn-300, sendo mais solúvel, demonstrou potencial antimetastático ao inibir a migração das células cancerígenas, efeito não observado na fração menos solúvel GlcEt-Pp, embora ambas tenham apresentado citotoxicidade seletiva, inibindo a viabilidade de células cancerígenas e poupando as células normais. Tais resultados ressaltam o potencial terapêutico dos polissacarídeos de *Lactarius quieticolor,* HTP e glucanas, possivelmente para o tratamento de câncer de mama, devido a sua citotoxicidade seletiva, sua sinergia na obtenção de resposta a um quimioterápico e potencialmente impedindo a migração das células tumorais.

Palavras- chave: *Lactarius quieticolor*; polissacarídeos; purificação; caracterização; ramnogalactana; β-D-glucanas

ABSTRACT

Mushrooms are important food resources with health benefits, providing essential nutrients and medicinal compounds, among which polysaccharides stand out for their diverse biological activities, including immunomodulatory, anti-inflammatory, and antitumor properties – particularly relevant given the global challenge of cancer. With breast cancer among the most common types, the triple-negative subtype stands out for its aggressiveness and mortality. In this study, we explored the purification, structural characterization, and biological evaluation of polysaccharides from the mushroom *Lactarius quieticolor*, starting from the alkaline extract. Following Fehling's treatment, a novel rhamnogalactan heteropolysaccharide (HTP) was isolated from the precipitate, while two glucan fractions with varying solubility were subsequently obtained from the supernatant through graded ethanol precipitation. Structural analysis, conducted with nuclear magnetic resonance (NMR) spectroscopy (1D and 2D techniques including ^{1}H, HSQC-DEPT, COSY, TOCSY, and HMBC), gas chromatography-mass spectrometry (GC-MS), and high-performance size exclusion chromatography (HPSEC), revealed that HTP consists of a (1→6)-linked α-D-galactopyranose main chain, substituted at *O*-2 by rhamnose, with an absolute molar mass of 1.53×10^4 g/mol. In vitro assays using MDA-MB-231 breast cancer cells demonstrated significant anticancer effects, with the rhamnogalactan reducing cell viability by 50% at 1.200 µg/mL and enhancing the efficacy of paclitaxel, reducing cell viability to 42% when co-administered. Additionally, the glucan fractions, GlcEt-Pp and GlcEtSn-300, possess a (1→3)-linked main chain with O-6 substitutions, differing in their degree of substitution at 21.4% and 70.6%, respectively. GlcEtSn-300, being more soluble, demonstrated antimetastatic potential by inhibiting cancer cell migration, an effect not observed with the less soluble GlcEt-Pp although both presented a selective cytotoxicity, inhibiting the viability of cancer cells while sparing normal ones. These results underscore the therapeutic promise of *Lactarius quieticolor* polysaccharides, HTP and glucans, for breast cancer treatment by promoting selective cytotoxicity, enhancing chemotherapeutic response, and potentially impeding cancer migration.

Keywords: *Lactarius quieticolor*; polysaccharides; purification; characterization; rhamnogalactan; β-D-glucans

LISTA DE FIGURAS

Revisão da literatura

Artigo I

Structural Characterization and Anticancer Properties of a Novel Mushroom-Derived Rhamnogalactan in Triple-Negative Breast Cancer in vitro model

Artigo II

Selective Cytotoxicity and Antimetastatic Effect on Breast Cancer Cell Model of a β-D-Glucan from Lactarius quieticolor mushroom

LISTA DE TABELAS

Revisão da literatura

Artigo I

Structural Characterization and Anticancer Properties of a Novel Mushroom-Derived Rhamnogalactan in Triple-Negative Breast Cancer in vitro model

Artigo II

Selective Cytotoxicity and Antimetastatic Effect on Breast Cancer Cell Model of a β-D-Glucan from Lactarius quieticolor mushroom

LISTA DE ABREVIATURAS, SIGLAS E SÍMBOLOS

Frações obtidas

EAS - Sobrenadante do Extrato alcalino após congelamento e descongelamento (Extrato alcalino bruto)

EAS-a / EAS-α - Extrato alcalino bruto após tratamento com α-amilase

EAS P / HTP - Fração obtida no precipitado de Fehling, heteropolissacarídeo (ramnogalactana)

Glc-Feh - Fração obtida no sobrenadante de Fehling

GlcEtSn-300 - Sobrenadante da precipitação etanólica fracionada realizada na fração EAS-Sn após eluição em membrana de 300 kDa.

GlcEt-Pp – Precipitado resultante da precipitação etanólica fracionada realizada na fração EAS-Sn

Análises instrumentais e termos associados

COSY - *Homonuclear correlation spectroscopy /* Espectroscopia de correlação homonuclear

DEPT - *Distortionless Enhancement by Polarization Transfer /* Intensificação sem distorção por transferência de polarização

GC - Cromatografia gasosa

GC-MS - *Gas chromatography–mass spectrometry /* Cromatografia gasosa-espectrometria de massas

HMBC - *Heteronuclear multiple bond coherence spectroscopy /* Correlação quântica múltipla heteronuclear

HPSEC-RI – *High-performance size exclusion chromatography – Refractive index/* Cromatografia por exclusão de tamanho de alta performance por índice de refração

HSQC - *Heteronuclear single quantum coherence spectroscopy /* Correlação quântica única heteronuclear

Mw – *Molecular weight /* Massa molecular ponderal média

RMN/NMR – Ressonância Magnética Nuclear / *Nuclear Magnetic Resonance*

Rt – *Retention time /* Tempo de retenção

SEC – *Size exclusion chromatography /* Cromatografia por exclusão de tamanho

TOCSY - *Total Correlation Spectroscopy /* Espectroscopia de correlação total

Reagentes gerais e termos associados

ATCC – *American type culture collection*

CH_3COOH – Ácido acético

CO_2 – Dióxido de carbono/gás carbônico

DMSO - Dimetilsulfóxido

KOH – Hidróxido de potássio

Me_2SO-*d_6* – Dimetilsulfóxido deuterado

MTT - 3-(4,5-dimetiltiazol-2yl)-2,5-difenil brometo de tetrazolina

$NaBD_4$ – Borohidreto de sódio deuterado

$NaBH_4$ - Borohidreto de sódio

NaN_3 – Azida sódica

$NaNO_3$ – Nitrato de sódio

NaOH – Hidróxido de sódio

PMAAs – *Partially (per)O-methylated alditol acetates* / Acetatos de alditol parcialmente metilados

RPMI – Meio *Gibco Roswell Park Memorial Institute*

TFA – Ácido trifluoroacético

Artigo I

$AgCO_3$ – Carbonato de prata

Ag_2O – Óxido de prata

$BaCO_3$ – Carbonato de bário

H_2SO_4 – Ácido sulfúrico

MeOH-HCl – Metanol:Ácido clorídrico

PCT – Paclitaxel (2α,4α,5β,7β,10β,13α)-4,10-bis(acetyloxy)-13-{[(2*R*,3*S*)-3-(benzoylamino)-2-hydroxy-3-phenylpropanoyl]oxy}-1,7-dihydroxy-9-oxo-5,20-epoxytax-11-en-2-yl benzoate

Outros

ANOVA – *Analysis of variance* / Análise de variância

BRM – *Biological response modifier* / Modificador de resposta biológica

SEM – *Standard error of the mean* / Erro padrão da média

Spp. – Espécies (todas espécies de um mesmo gênero)

TLR – *Toll-like Receptor* (Receptores tipo *toll*)

SUMÁRIO

ARTIGO II

Selective Cytotoxicity and Antimetastatic Effect on Breast Cancer Cell Model of a β-D-Glucan from *Lactarius quieticolor* mushroom

1. INTRODUÇÃO

No reino fungi há a predominância dos filos Ascomycota e Basidiomycota (Ruthes *et al.*, 2016) nos quais encontram-se os cogumelos: macro fungos heterotróficos e multicelulares, com corpos de frutificação e micélio característicos (Kour *et al.*, 2022; Zhong *et al.*, 2021). Atualmente estima-se a existência de mais de 40.000 espécies de macro fungos, com mais de 14.000 espécies de cogumelos catalogadas (Lu *et al.*, 2020; Mueller *et al.*, 2007), dentre as quais mais de 2.000 são comestíveis (Kour *et al.*, 2022; Lu *et al.*, 2020), incluindo cerca de 200 espécies silvestres (Shen *et al.*, 2023). O interesse alimentício nos cogumelos se deve ao seu valor nutricional, apresentando alto teor de fibras alimentares, carboidratos, proteínas, minerais e vitaminas, bem como baixo teor de calorias e gorduras (Kour *et al.*, 2022; Li *et al.*, 2022; Lu *et al.*, 2020; Pires *et al.*, 2013; Sulieman *et al.*, 2019).

Além dos valores nutricionais, os cogumelos também despertam interesse medicinal, devido ao fato de seus extratos apresentarem atividades biológicas anti-inflamatórias, antitumorais, neuroprotetoras, citoprotetoras, entre outras (Kono *et al.*, 2020; Kour *et al.*, 2022; Lu *et al.*, 2020; Mandal *et al.*, 2010; Pires *et al.*, 2013; Reddy Shetty *et al.*, 2021). Estes efeitos se devem à presença de compostos bioativos, tais como: lectina, ergotioneína, terpenos, esteróis, polifenóis e polissacarídeos (Kour *et al.*, 2022; Lu *et al.*, 2020; Reddy Shetty *et al.*, 2021).

Os polissacarídeos, macromoléculas de carboidratos compostas por monossacarídeos unidos por ligações glicosídicas (Sinnott, 2007; Zhong *et al.*, 2021), são encontrados majoritariamente na parede celular de fungos e desempenham funções como a manutenção da estrutura celular, reserva de energia e promoção de interações intercelulares (Reddy Shetty *et al.*, 2021; Ruthes *et al.*, 2016).

Além das atividades biológicas citadas anteriormente, os polissacarídeos de fungos também são considerados modificadores de resposta biológica (BRMs) de modo que otimizam a ação do sistema imune contra possíveis antígenos (Maity *et al.*, 2021; Ruthes *et al.*, 2013; Zhang, H. *et al.*, 2022). Outros fatores que destacam a aplicabilidade dos polissacarídeos são sua não toxicidade, biocompatibilidade e disponibilidade para extração (Maity *et al.*, 2021; Zhang, S. *et al.*, 2022).

O presente trabalho utilizou o cogumelo *Lactarius quieticolor* (Romagnesi, 1958) como fonte biológica de polissacarídeos, partindo-se do extrato alcalino, considerando-se a escassez de trabalhos científicos caracterizando estruturalmente os polissacarídeos obtidos desta espécie, de modo a identificar as moléculas obtidas.

2. REVISÃO DA LITERATURA

2.1 Fungos basidiomicetos

O reino fungi é composto por organismos eucariontes não fotossintetizantes, podendo ser uni ou multicelulares e de nutrição absortiva, podendo variar de células micrométricas a corpos de frutificação de até 1 m de diâmetro (Bridge *et al.*, 2005). Estima-se que globalmente existam mais de 1,5 milhões de espécies de fungos, com aproximadamente 150 mil capazes de produzir corpos de frutificação visíveis, denominados macrofungos. Dentre esses, em torno de 40 mil espécies pertencem aos filos Ascomycota e Basidiomycota, das quais apenas 14 mil são reconhecidas como cogumelos (Lu *et al.*, 2020; Webster; Weber, 2007).

Os cogumelos são organismos amplamente difundidos em diversos habitats e possuem papeis ecológicos vitais como saprótrofos, realizando a decomposição de matéria orgânica, e como simbiontes, formando relações mutualísticas com plantas e outros organismos (Hyde *et al.*, 2019; Webster; Weber, 2007).

Os basidiomicetos são notáveis por seus corpos de frutificação, que são formados por filamentos denominados hifas, os quais, ao se entrelaçarem, formam uma malha filamentosa chamado micélio, sendo a parte vegetativa do fungo. Sob condições ambientais adequadas o micélio desenvolve uma estrutura reprodutora conhecida como basidiocarpo, corpo de frutificação ou cogumelo, como mostrado na figura 1 (Webster; Weber, 2007).

Figura 1. Representação da estrutura de um basidiocarpo e seus principais componentes.

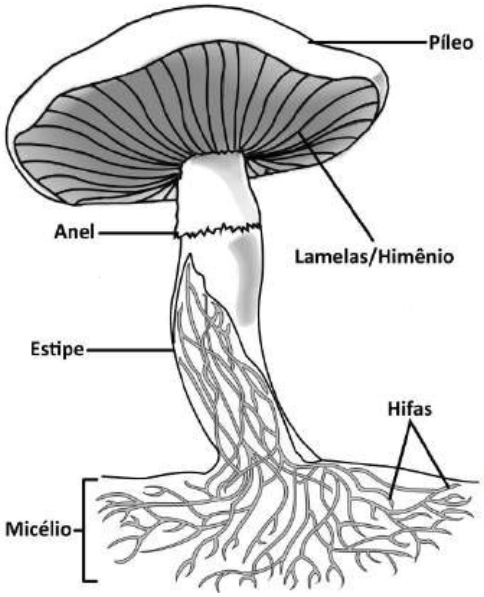

Fonte: Adaptado de Karakaya *et al.* (2023)

Os basidiomicetos possuem um importante subfilo, o Agaromycotina, que contém aproximadamente um terço de todas as espécies de fungos já identificadas, incluindo leveduras, fungos gelatinosos e cogumelos (Hibbett, 2006). Neste subfilo encontramos a classe Agaricomycetes, a qual possui alguns cogumelos lamelados, com uma de suas principais ordens sendo a Russulales, que inclui a família Russulaceae, cujos cogumelos apresentam píleo e himênio frágeis e quebradiços e frequentemente formam relações simbióticas ectomicrorrízicas com árvores coníferas, colonizando a superfície externa de suas raízes (Webster; Weber, 2007).

Um dos principais gêneros encontrados na família Russulaceae é o gênero *Lactarius,* recebendo esse nome devido ao exsudato de aspecto leitoso liberado quando o píleo ou lamelas são danificados (Buczacki *et al.*, 2012; Hall *et al.*, 1998; Webster; Weber, 2007). Dentre as várias espécies deste gênero, destaca-se o *Lactarius quieticolor.*

2.2 *Lactarius quieticolor*

O cogumelo *Lactarius quieticolor* foi inicialmente descrito pelo micologista francês Henri Romagnesi em 1958. A espécie possui o píleo medindo entre 2,5 e 11 cm de diâmetro, convexo e com o centro indentado, enquanto suas bordas são irregulares e enroladas, de coloração pálida e alaranjada, eventualmente marrom. Seu estipe possui aparência lisa e de coloração alaranjada podendo conter manchas verdes e marrons. As lamelas se apresentam com uma intensa coloração alaranjada ou amarelada, geralmente aglomeradas e se estendendo ao longo do estipe (decorrentes) (Romagnesi, 1958). Ao ser seccionado, apresenta um centro cavernoso e seu exsudato tem coloração pálida e amarelada, assim como sua superfície interna, a qual se torna azul-esverdeada após algum tempo (Buczacki *et al.*, 2012).

Geralmente o cogumelo é encontrado em pequenos grupos, formando ectomicorrizas com coníferas, sendo comumente distribuído pelo hemisfério norte. Entretanto, recentemente foi reportado a presença desta espécie no Brasil, possivelmente pela introdução de espécies de pinheiros norte americanos e europeus (*Pinus spp.*) na américa do sul (Silva-Filho *et al.*, 2020). As principais características do cogumelo em questão podem ser observadas na figura 2.

Figura 2. Cogumelo *Lactarius quieticolor* obtido numa plantação de *Pinus spp.*

Fonte: Adaptado de Silva-Filho *et al.* (2020)

Assim como a maioria dos cogumelos comestíveis, o *Lactarius quieticolor* tem sido consumido com mais frequência devido à sua palatabilidade e à sua composição rica em nutrientes (Li *et al.*, 2021) sendo os carboidratos presentes em maior quantidade, podendo chegar a 65% (Lu *et al.*, 2020). Além disso, os polissacarídeos de cogumelos são conhecidos por seus efeitos positivos para a saúde (Maity *et al.*, 2021), o que torna interessante a investigação desta espécie, especialmente considerando que até o momento encontram-se poucos relatos sobre os polissacarídeos de *Lactarius quieticolor*, com descrições de extratos polissacarídicos brutos e uma glucana (Zavadinack *et al.*, 2024), (Bonaldi, 2021).

2.3 Polissacarideos fúngicos

Como os cogumelos apresentam um alto teor de polissacarídeos, esses compostos exercem diversas funções essenciais para o organismo fúngico, dentre as principais funções, entre outras, destacam-se a reserva energética e manutenção da estrutura do cogumelo (Reddy Shetty *et al.*, 2021; Ruthes *et al.*, 2016). Entre as moléculas importantes presentes nos cogumelos estão as glucanas, que são polissacarídeos compostos exclusivamente por unidades de glucose (Ruthes *et al.*, 2016).

O armazenamento de energia em fungos, assim como em animais e bactérias, é realizado por meio do glicogênio, sendo este formado por α-D-glucanas (1→4), formando uma estrutura altamente ramificada (Reddy Shetty *et al.*, 2021).

Quanto à função estrutural, os polissacarídeos desempenham um papel essencial na composição e integridade da parede celular dos cogumelos. Embora nem todos os fungos possuam

parede celular, a maioria apresenta essa estrutura. No entanto, a composição e a estrutura da parede celular não são fixas, pois há uma grande variabilidade entre as espécies (Bueno; Silva, 2014). Tal diversidade estrutural reflete uma estrutura dinâmica que permite aos cogumelos ajustar a proporção e os tipos de polissacarídeos estruturais de acordo com suas necessidades específicas.

Mais de 90% da parede celular dos fungos é composta por polissacarídeos (Latgé, 2007), dos quais até 60% são glucanas (Bowman; Free, 2006). Embora a composição e a estrutura possam variar entre as espécies, há certas semelhanças estruturais comuns entre os fungos. A estrutura geral é organizada em camadas, com a quitina (formada por N-acetil-D-glucosamina) localizada na parte inferior, próxima à membrana celular do fungo. Em seguida, há uma matriz composta majoritariamente por β-D-glucanas (1→3), (1→6) – geralmente denominadas apenas de β-D-glucanas (1→3) (Ruthes *et al.*, 2015) – entrelaçadas com moléculas de β-D-glucanas (1→6) (Gow; Lenardon, 2023; Latgé, 2007), Nesta matriz, encontram-se proteínas que podem ou não estar ancoradas à membrana celular, além de outros polissacarídeos em menor quantidade, sendo comuns polissacarídeos que contêm manose e galactose, entre outros açúcares (Bowman; Free, 2006; Yugueros *et al.*, 2024). A figura 3 ilustra a composição e estruturação da parede celular fúngica.

Figura 3. Representação da estrutura geral da parede celular fúngica

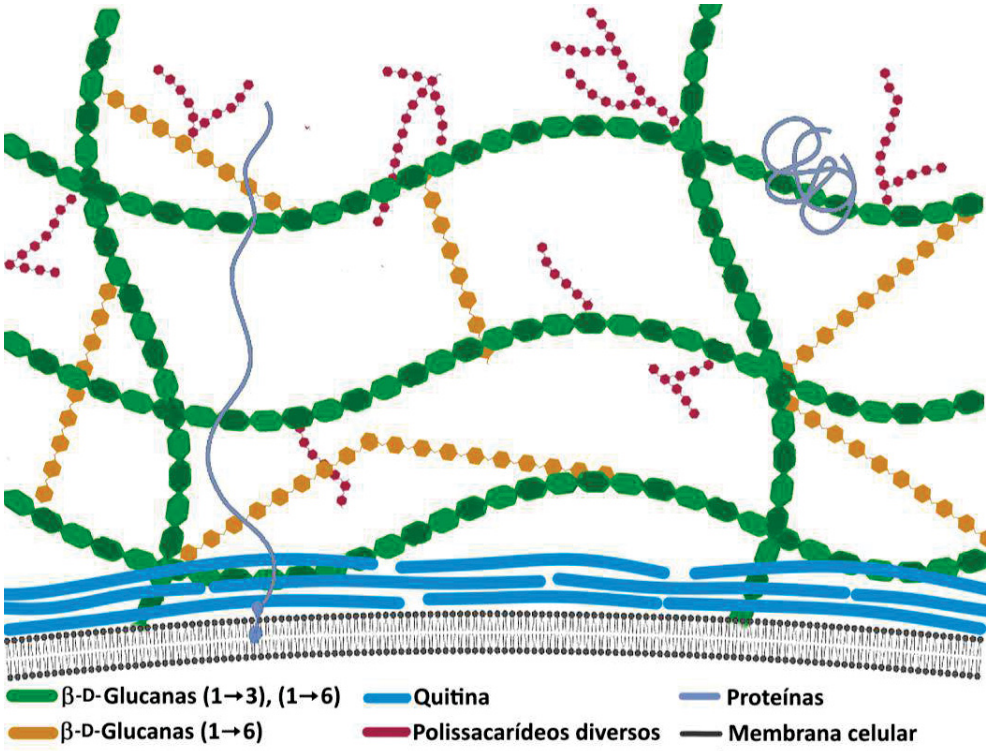

Fonte: Adaptado de Bowman e Free (2006)

Além das glucanas, a parede celular dos cogumelos e outras estruturas do organismo fúngico contêm diversos polissacarídeos que desempenham funções complementares, com destaque para os heteropolissacarídeos. Estes compostos são formados por uma combinação de diferentes monossacarídeos como galactose, manose, glucose, fucose, rhamnose, entre outros (Yu *et al.*, 2023), dando origem a heteropolissacarídeos com grande variedade em suas estruturas tais como:

- Fucoxilomananas com cadeia principal composta por α-D-Manose com ligações (1→4) e ramificadas em *O*-6 por um dissacarídeo composto por α-L-Fucose-(1→2)-β-D-Xilose (1→ extraídas do cogumelo *Ganoderma lucidum* (da Silva Milhorini *et al.*, 2022a). Também foram encontradas estruturas com cadeia principal composta por α-D-Man*p* (1→3) ramificadas em *O*-4 por um dissacarídeo similar ao anterior no cogumelo *Laricifomes officinales* (Golovchenko *et al.*, 2020);
- Manogalactanas do cogumelo *Sanghuangporus sanghuang* apresentando uma cadeia composta por α-D-Manose e α-D-Galactose, ambas com ligações (1→6), onde também foram observados resíduos de galactose naturalmente metilados em *O*-3 (Cheng *et al.*, 2022). Estruturas também naturalmente metiladas foram isoladas dos cogumelos *Pholiota nameko* e *Pleurotus eryngii*, ambas apresentando cadeia principal composta por α-D-galactose (1→6), com resíduos metilados em *O*-3 e ramificações de β-D-Manose em *O*-2 (Abreu *et al.*, 2021);
- Fucogalactanas do cogumelo *Macrolepiota dolichaula,* cuja cadeia principal era composta por α-D-Galactose (1→6) e 3-*O*-Metil-Galactose (1→6) com substituições em *O*-2 por um dissacarídeo de α-D-Galactose (1→2) e α-L-Fucose (1→ (Samanta *et al.*, 2015). Outro polissacarídeo também composto por uma cadeia de α-D-Galactose (1→6) com substituição em *O*-2 por α-L-Fucose (1→ foi isolado do cogumelo *Macrocybe titans* (Milhorini et al., 2018).

Esses são apenas alguns exemplos dos muitos heteropolissacarídeos que podem ser encontrados em cogumelos, ressaltando a diversidade e complexidade estrutural desses compostos. Polissacarídeos fúngicos apresentam diferentes tipos de ligações, graus de ramificação, peso molecular e solubilidade, bem como na localização destes compostos no corpo de frutificação. Essas diferenças tornam necessário o uso de abordagens distintas para a extração e purificação desses compostos de maneira eficiente.

2.4 Extração, purificação e caracterização de polissacarídeos fúngicos

2.4.1 EXTRAÇÃO DE POLISSACARÍDEOS

A extração de polissacarídeos de cogumelos geralmente começa com a secagem dos espécimes, processo que pode ser realizado por liofilização, seguida de trituração ou pulverização. Quanto menor o tamanho das partículas, maior será a superfície de contato com o solvente, favorecendo a eficiência da extração. Antes da extração propriamente dita, é comum realizar um tratamento preliminar com solventes orgânicos como etanol, metanol e clorofórmio para remover compostos apolares, como lipídios e fenóis de modo a evitar interferências no processo de extração dos polissacarídeos (Garcia *et al.*, 2022; Leong *et al.*, 2021).

Considerando a diversidade de solubilidades e a disposição em diferentes camadas estruturais dos polissacarídeos, frequentemente emprega-se uma sequência de extrações para maximizar o rendimento. Inicia-se com condições mais brandas, extraindo os polissacarídeos de solubilidade mais fácil, e, posteriormente, aplicam-se condições mais rigorosas de temperatura, pressão e pH para acessar polissacarídeos mais resistentes. Em alguns casos, enzimas específicas também são utilizadas para facilitar a degradação da matriz celular e liberar polissacarídeos de interesse (Leong *et al.*, 2021; Ruthes *et al.*, 2015). Dentre os principais métodos de extração utilizados, destacam-se as extrações aquosas em diferentes temperaturas e pressão, extração alcalina e a extração enzimática.

As extrações aquosas são amplamente utilizadas devido à elevada solubilidade dos polissacarídeos na mesma, tornando o processo mais seguro e facilitando os processos de purificação subsequentes. Geralmente, a primeira extração é realizada em temperatura ambiente, comumente referida como extração a frio (CW – *cold water)*, com duração de 1 a 6 horas sob agitação constante (Leong *et al.*, 2021; Ruthes *et al.*, 2015). Após esse período, o resíduo de cogumelo é separado por centrifugação e o processo pode ser repetido para aumentar o rendimento. Em seguida, realiza-se a extração com água quente (HW – *hot water)*, empregando temperaturas entre 90 e 100 °C, visando solubilizar polissacarídeos de menor solubilidade. Esse segundo processo segue os mesmos parâmetros de tempo, agitação, centrifugação e repetição (Garcia *et al.*, 2022; Ruthes *et al.*, 2015; Wang *et al.*, 2022).

Após as extrações aquosas, é comum aplicar extrações alcalinas com diferentes concentrações de hidróxidos de sódio ou potássio (NaOH ou KOH, respectivamente), geralmente de 2 a 10%, a temperaturas em torno de 100 °C ou inferiores. Esse procedimento é necessário para solubilizar certos polissacarídeos que não são extraídos em condições aquosas. Antes desse tipo de extração, é

fundamental proteger os polissacarídeos da oxidação, utilizando $NaBH_4$ como agente redutor (Leong *et al.*, 2021; Ruthes *et al.*, 2015; Wang *et al.*, 2015).

Após as extrações com diferentes temperaturas e pH, esses processos podem ser repetidos (com água quente e solução alcalina), mas sob pressões elevadas, variando de 1 a 22 MPa e temperaturas de 100 até mais de 300 °C. Esse método visa solubilizar uma quantidade maior de componentes e, possivelmente, hidrolisar o substrato do cogumelo (Leong *et al.*, 2021; Sakdasri *et al.*, 2022). Embora essas condições intensas geralmente resultem em maior rendimento em comparação às extrações aquosas e alcalinas convencionais, elas podem alterar a conformação e a estrutura das moléculas, impactando as propriedades dos polissacarídeos extraídos (Leong *et al.*, 2021).

2.4.2 PURIFICAÇÃO DE POLISSACARÍDEOS

Após a etapa de extração, a purificação dos polissacarídeos obtidos se torna essencial para remover impurezas e isolar frações específicas de interesse. As técnicas de purificação são escolhidas com base nas características esperadas dos polissacarídeos extraídos, como peso molecular, solubilidade, grau de ramificação e composição. Com isso, são aplicadas diferentes abordagens que variam conforme a natureza dos compostos presentes (Wang *et al.*, 2022).

Inicialmente, aplicam-se métodos mais gerais de purificação, como para remoção de proteínas. Entre as técnicas mais comuns estão o tratamento com hidróxido de sódio a 10-30% (p/v) (Tjahjaningsih *et al.*, 2023), precipitação com ácido tricloroacético a 20% (p/v) e o uso de solventes orgânicos, como clorofórmio e butanol, no método de Sevag, além de tratamentos enzimáticos com proteases (Leong *et al.*, 2021; Ruthes *et al.*, 2015).

Outro procedimento geralmente aplicado é o tratamento enzimático com α-amilase, visando remover glicogênio da amostra. Embora a α-amilase seja direcionada principalmente ao amido, ela também degrada o glicogênio, pois ambas as moléculas compartilham uma estrutura semelhante, com ligações glicosídicas α(1→4) entre unidades de glucose. Esse tratamento é geralmente repetido para garantir a completa remoção do glicogênio (da Silva Milhorini *et al.*, 2022b; Li *et al.*, 2024).

Em seguida, é comum realizar a precipitação com etanol, geralmente em uma proporção de 3:1 (v/v), onde ocorre a precipitação dos polissacarídeos de maior peso molecular, devido à sua insolubilidade em solventes orgânicos (Ruthes *et al.*, 2015). Essa precipitação também pode ser feita de maneira gradual, aumentando progressivamente a concentração de etanol para fracionar diferentes

tipos de polissacarídeos. Posteriormente, as frações precipitadas são recuperadas por centrifugação (Hu; Goff, 2018; Peng *et al.*, 2009).

Outro método empregado é o de congelamento e descongelamento, no qual o extrato é totalmente solubilizado em água destilada, congelado e, em seguida, descongelado lentamente em temperatura ambiente. Após esse processo, precipitado e sobrenadante são separados por centrifugação, repetindo-se o procedimento até que não haja mais formação de precipitado (Gorin; Iacomini, 1984; Ruthes *et al.*, 2015). Geralmente, as moléculas mais lineares precipitam, enquanto moléculas com maior grau de ramificação permanecem solúveis no sobrenadante (Ruthes *et al.*, 2015).

A separação de polissacarídeos com base em sua composição pode ser realizada por meio do tratamento com solução de Fehling (Jones; Stoodley, 1965). Inicialmente, o polissacarídeo é solubilizado em uma solução alcalina contendo hidróxido de potássio a 25% (p/v) e tartarato de sódio e potássio a aproximadamente 35% (p/v). Em seguida, adiciona-se uma solução de sulfato de cobre II penta hidratado a cerca de 11% (p/v). Esse processo permite que monossacarídeos com grupos reativos (COOH, OH) em posições mais favoráveis complexem-se mais eficientemente com os íons Cu^{2+}, formando um precipitado (Ruthes *et al.*, 2015). Assim, polissacarídeos compostos por outros monossacarídeos permanecem no sobrenadante. Normalmente, as glucanas, devido à sua estrutura, permanecem no sobrenadante após tal tratamento (Kruppa *et al.*, 2009; Milhorini *et al.*, 2024).

Após o tratamento com a solução de Fehling, o polissacarídeo geralmente passa por diálise, um processo que utiliza uma membrana semipermeável permitindo a passagem de impurezas e retendo o polissacarídeo, no caso do tratamento de Fehling a diálise é utilizada para retirar íons de cobre e sais de potássio em excesso. A diálise também permite a remoção de outras impurezas, solventes e até mesmo o fracionamento de polissacarídeos. No entanto, o corte de peso molecular pode não ser exato em todas as circunstâncias, uma vez que a conformação da molécula do polissacarídeo, como se é ramificada ou linear, ou forma aglomerados, pode fazer com que moléculas de maior peso molecular passem pela membrana ou que moléculas menores fiquem retidas (Ruthes *et al.*, 2015; Shi, 2016).

2.4.3 CARACTERIZAÇÃO ESTRUTURAL DE POLISSACARÍDEOS

Após as etapas de extração e purificação, é fundamental realizar a caracterização estrutural dos polissacarídeos isolados. Essa etapa permite uma compreensão detalhada de suas estruturas, por meio da identificação de ligações específicas, composição de monossacarídeos, anomericidade, entre outras características estruturais que podem influenciar diretamente suas propriedades.

A composição monossacarídica é frequentemente determinada após a hidrólise ácida das ligações glicosídicas (Adams, 1965; Wang *et al.*, 2022). Para essa análise, técnicas como cromatografia em camada delgada (TLC) e cromatografia líquida de alta eficiência (HPLC) podem ser utilizadas. No entanto, o método geralmente empregado é a cromatografia gasosa, isolada (GC) ou acoplada à espectrometria de massas (GC-MS), que requerem uma etapa adicional de derivatização. Essa derivatização é feita normalmente pela acetilação dos grupos OH livres nos monossacarídeos, facilitando sua vaporização para análise (Albersheim *et al.*, 1967; Ruthes *et al.*, 2015).

A análise das ligações entre os monossacarídeos pode ser realizada por meio de metilação, que é aplicada antes da hidrólise ácida. Nesse processo, adicionam-se grupos metila a todas as hidroxilas livres, permitindo a identificação dos pontos de ligação entre as unidades monossacarídicas. O método utilizado normalmente baseia-se na técnica descrita por (Ciucanu; Kerek, 1984), com algumas modificações. Após a hidrólise ácida, realiza-se uma nova etapa de derivatização para viabilizar a análise por GC-MS, onde o tempo de retenção e o perfil de fragmentação fornecem informações sobre as posições das ligações glicosídicas (Han *et al.*, 2024; Ruthes *et al.*, 2015).

A determinação do peso molecular é um parâmetro importante, pois este é diretamente ligado à atividade biológica dos polissacarídeos, que podem apresentar uma ampla faixa de tamanhos moleculares (Wang *et al.*, 2023). Dessa forma, um dos métodos mais comuns para essa análise é a cromatografia por exclusão de tamanho de alta pressão (HPSEC) ou, em alguns casos, a cromatografia por exclusão de tamanho convencional (SEC), que separa os solutos em ordem decrescente de tamanho molecular (Han *et al.*, 2024; Wang *et al.*, 2023).

A ressonância magnética nuclear (RMN) mono e bidimensional é utilizada para obter informações como as configurações anoméricas α/β, análise de alguns padrões de ligação e a identificação de extremidades não redutoras, além da conformação do anel dos monossacarídeos, permitindo a confirmação de outras análises, como a metilação (Ruthes *et al.*, 2015). Como alguns polissacarídeos possuem estruturas extensas e complexas, pode haver sobreposição de sinais, tornando interessante o uso combinado de técnicas 1D e 2D para uma caracterização mais completa (Han *et al.*, 2024).

As análises mais comuns em RMN para polissacarídeos incluem as técnicas unidimensionais de ^{1}H e ^{13}C, identificando os tipos de prótons e carbonos presentes na estrutura, fornecendo informações iniciais sobre o ambiente químico das ligações e algumas proporções (Yao *et al.*, 2021). Já nas técnicas bidimensionais, destacam-se:

- HSQC (*Heteronuclear Single Quantum Coherence*), que mostra correlações entre prótons e outros heteroátomos, principalmente carbono, ajudando a estabelecer a ligação entre hidrogênios e carbonos adjacentes (Han *et al.*, 2024).
- COSY (*Correlation Spectroscopy*), que indica interações entre prótons vizinhos, facilitando a identificação de cadeias laterais e sequências de ligação próximas (Kim; Prestegard, 1989; Yao *et al.*, 2021).
- TOCSY (*Total Correlation Spectroscopy*), que revela acoplamentos entre hidrogênios dentro de um mesmo sistema de spin, abrangendo interações além das três ligações típicas do COSY, permitindo a análise de agrupamentos mais distantes no polissacarídeo (Han *et al.*, 2024; Yao *et al.*, 2021).

Essas técnicas, entre outras, fornecem uma visão detalhada das interações e conexões moleculares, sendo essenciais para a elucidação estrutural dos polissacarídeos. A caracterização estrutural é necessária, pois a estrutura do polissacarídeo é determinante para definir suas possíveis atividades biológicas e, consequentemente, suas potenciais aplicações.

2.5 Atividade biológica de polissacarídeos fúngicos

Os cogumelos têm sido amplamente consumidos e utilizados na medicina popular em diversas culturas, baseando-se principalmente em conhecimento empírico (Araújo-Rodrigues *et al.*, 2024; Yin *et al.*, 2020; Zhang, S. *et al.*, 2022). Tais efeitos benéficos para a saúde são atribuídos a uma rica variedade de compostos bioativos presentes nos cogumelos, como proteínas, terpenoides, esteróis, polifenóis e, sobretudo, polissacarídeos (Araújo-Rodrigues *et al.*, 2024; Kour *et al.*, 2022; Navarro-Simarro *et al.*, 2024).

Como mencionado, a estrutura específica dos polissacarídeos — incluindo ramificações, tipos de ligações glicosídicas, peso molecular e composição monossacarídica — desempenha um papel crítico em determinar suas atividades biológicas (Maity *et al.*, 2021). Estudos têm demonstrado esses efeitos em pesquisas *in vivo* e *in vitro*, mostrando que os polissacarídeos são agentes ativos com uma ampla gama de bioatividades (Lu *et al.*, 2020).

Os polissacarídeos de cogumelos têm se mostrado promissores em várias aplicações terapêuticas. Eles podem ter efeitos antidiabéticos, reduzindo a resistência à insulina e os níveis de glicose no sangue e também efeitos anti-inflamatórios, inibindo enzimas como a ciclooxigenase (COX-2) e a óxido nítrico sintase (NOS) (Araújo-Rodrigues *et al.*, 2024). Adicionalmente, polissacarídeos influenciam positivamente a saúde intestinal, pois promovem o crescimento de

bactérias benéficas, o que leva à produção de ácidos graxos de cadeia curta (SCFAs) como subproduto metabólico (Araújo-Rodrigues *et al.*, 2024; Yu *et al.*, 2023). Além disso, os polissacarídeos de cogumelos são reconhecidos por suas atividades neuroprotetoras e antioxidantes. Contudo, entre suas várias bioatividades, os efeitos imunomoduladores se destacam de forma notável (Garcia *et al.*, 2022; Zhang, S. *et al.*, 2022).

Os polissacarídeos, especialmente as glucanas, são excelentes estimuladores do sistema imunológico, sendo comumente referidos como modificadores de resposta biológica (BRMs - *biological response modifiers*), possuindo vários métodos de ação. Por exemplo, as glucanas podem interagir com receptores do tipo *toll* (TLRs – *toll-like receptors*) em células, promovendo a liberação de citocinas e também na ativação de células dendríticas (Garcia *et al.*, 2022; Yu *et al.*, 2023). Tais efeitos justificam a aplicação de algumas glucanas, principalmente a lentinana, como adjuvantes em terapias contra o câncer (Araújo-Rodrigues *et al.*, 2024; Cognigni *et al.*, 2021; Lin *et al.*, 2020; Park *et al.*, 2024; Steimbach *et al.*, 2021).

Além dos efeitos imunomoduladores, os polissacarídeos de cogumelos apresentam atividades antitumorais diretas. Podendo induzir a apoptose em células cancerosas ou inibir o crescimento tumoral (Garcia *et al.*, 2022; Zhang, S. *et al.*, 2022). Alguns polissacarídeos também demonstram potencial em prevenir metástases, interferindo na adesão de células cancerosas (Milhorini *et al.*, 2018; Zhang, S. *et al.*, 2022). Esses efeitos, combinados com as ações imunomoduladoras mencionadas acima, indicam o potencial apresentado pelos polissacarídeos fúngicos.

O câncer é uma doença complexa, que demanda abordagens terapêuticas variadas e está entre as principais causas de morte em todo o mundo, responsável por quase 10 milhões de mortes em 2020 (World Health Organization , 2022). Entre os tipos mais comuns estão os cânceres de mama, pulmão, cólon e reto, e próstata. O câncer de mama, especificamente foi o tipo de câncer mais comum entre mulheres em 84,5% dos 185 países avaliados em 2022 (World Health Organization , 2024). Trata-se, portanto, de uma preocupação de saúde mundial significativa, que demanda a busca por opções de tratamento complementares eficazes. Os polissacarídeos de cogumelos, com seus diversos mecanismos de ação, incluindo o fortalecimento do sistema imunológico e efeitos antitumorais diretos, oferecem alternativas para o desenvolvimento de terapias adjuvantes ao tratamento do câncer. Esse potencial destaca a importância da investigação contínua sobre como os polissacarídeos podem complementar ou potencializar as estratégias terapêuticas atuais.

Considerando-se a grande diversidade de espécies e polissacarídeos que podem ser obtidos de cogumelos a partir de diferentes metodologias de extração e estes apresentarem propriedades

biológicas diversas, a Tabela 1 contém alguns dos polissacarídeos já isolados a partir de corpos de frutificação, bem como o tipo de extração empregado e suas propriedades observadas.

Tabela 1. Propriedades e métodos de extração de polissacarídeos de cogumelos.

Espécie	Polissacarídeo	Extração	Propriedades	Autor
Ganoderma lucidum	Fucoxilomanana	HW; Alk.	Antimelanoma; antiproliferativa	(da Silva Milhorini *et al.*, 2022a)
Amanita muscaria	α-D-galactana β-D-glucana	CW	Antimelanoma; antitumoral	(Zavadinack *et al.*, 2021)
Lactarius rufus	β -D-glucana	CW; HW	Antinociceptiva; Antiinflamatória	(Ruthes *et al.*, 2013)
			Antitumoral	(Pires *et al.*, 2013)
Lactarius deliciosus	Glucogalactomanana	HW	Citoprotetora	(Li *et al.*, 2022)
Agaricus bisporus	β -D-glucana	HW	Antitumoral; imunomodulatória	(Rutckeviski *et al.*, 2022)
			Imunomodulatória	(Smiderle *et al.*, 2013)
		CW; HW	Antitumoral	(Pires *et al.*, 2013)
Macrocybe titans	Fucogalactana	CW	Antiproliferativa	(Milhorini *et al.*, 2018)
	β -D-glucana	CW; HW; Alk	Espessante	(da Silva Milhorini *et al.*, 2022b)
Tremella fuciformis	Glucuronoxilomanana β -glucana	HW; EAE	Espessante; Hipoglicêmica	(Tu *et al.*, 2023)
Lactarius volemus	Manogalactoglucana	HW	Imunomodulatória; antiproliferativa	(Zhong *et al.*, 2021)
Lactarius hatsudake	β -D-glucana	HW	Antitumoral; antioxidante	(Yang *et al.*, 2024)

HW: extração aquosa quente; CW: extração aquosa fria; Alk: extração aquosa alcalina; EAE: extração aquosa assistida por enzimas.

Fonte: A autora (2024)

Considerando a ampla variedade de metodologias e moléculas extraídas, observa-se na Tabela 1 uma predominância de β-glucanas, mas também a presença de diversos polissacarídeos isolados do gênero *Lactarius*, ao qual pertence o *Lactarius quieticolor*, foco deste trabalho. Esses achados ressaltam o potencial promissor do gênero *Lactarius* para a obtenção de moléculas bioativas, sugerindo que ele pode conter outros polissacarídeos com importantes propriedades biológicas.

3. JUSTIFICATIVA

Os polissacarídeos de cogumelos possuem ampla utilização e aplicabilidade, abrangendo propriedades medicinais e atividades biológicas frequentemente relatadas na literatura. Tais propriedades são intimamente relacionadas à estrutura química destes polissacarídeos, sendo importantes os estudos referentes à identificação e caracterização de possíveis novas moléculas, bem como a avaliação de suas propriedades físico-químicas e biológicas. Atualmente, existem poucos relatos científicos identificando e caracterizando polissacarídeos provenientes do cogumelo *Lactarius quieticolor,* sendo este a fonte biológica de polissacarídeos escolhida para o presente estudo de modo a buscar estruturas de polissacarídeos ainda não reportadas.

4. OBJETIVOS

4.1 Objetivo Geral

- Purificar e caracterizar química e estruturalmente os polissacarídeos provenientes do extrato alcalino dos corpos de frutificação desidratados do basidiomiceto *Lactarius quieticolor* e avaliar suas possíveis atividades biológicas e aplicabilidade.

4.2 Objetivos Específicos

- Purificar polissacarídeos provenientes do extrato alcalino do cogumelo *Lactarius quieticolor*;
- Caracterizar estruturalmente os polissacarídeos das frações obtidas, utilizando técnicas analíticas de RMN, GC-MS e HPSEC.
- Avaliar a bioatividade dos polissacarídeos isolados
  - Verificar se frações obtidas possuem efeito citotóxico em células normais e células cancerosas
  - Verificar se as frações obtidas interferem na migração de células cancerosas

Artigo I

Anticancer Effects of a Rhamnogalactan Isolated from the *Lactarius quieticolor* Mushroom in a Triple-Negative Breast Cancer Cell Model

Anticancer Effects of a Rhamnogalactan Isolated from the *Lactarius quieticolor* Mushroom in a Triple-Negative Breast Cancer Cell Model

Eliane Leal de Lara[a1]; Matheus Zavadinack[a1], Shayane da Silva Milhorini[a], Karin Macial Wurzer[b], Giseli Klassen[b] Lucimara M.C. Cordeiro[a], Marcello Iacomini[a]*

[a] Department of Biochemistry and Molecular Biology, Federal University of Paraná, Curitiba- PR, CEP 81531-980, Brazil.

[b] Department of Basic Pathology, Federal University of Parana, Curitiba-PR, CEP 81531-980, Brazil

[1]Equal contribution

*Corresponding author: Department of Biochemistry and Molecular Biology, Federal University of Paraná, Mailbox (Caixa Postal) 19046, Curitiba- PR, CEP 81531-980, Brazil. Tel.: +55 (41) 3361-1655; Fax: +55 (41) 3266-2042; e-mail: iacomini@ufpr.br

Research supported by Universal Project (Process 403295/2021-1 and 307314/2018-9) provided by CNPq foundation (Brazil).

Abstract

Mushroom-derived polysaccharides are well-known for their diverse biological activities, including immunomodulatory and anticancer properties. Breast cancer, the leading cause of cancer-related deaths among women globally, is considered one of the most aggressive forms, largely due to the lack of targeted molecular therapies. In this study, we report the extraction, purification, and chemical characterization of a novel heteropolysaccharide, a rhamnogalactan, composed of galactose (72.6%) and rhamnose (27.4%), isolated from the edible mushroom *Lactarius quieticolor*. This molecule (HTP) was extracted using an alkaline extraction method followed by treatment with Fehling's solution. Comprehensive structural analysis was conducted using nuclear magnetic resonance (NMR) spectroscopy, including both one-dimensional and two-dimensional techniques (1H, HSQC-DEPT, COSY, TOCSY and HMBC), gas chromatography-mass spectrometry (GC-MS), and high-pressure size exclusion chromatography (HPSEC). The analyses revealed that HTP consists of a (1 → 6)-linked α-D-galactopyranose main chain, heavily substituted at O-2 by non-reducing end units of rhamnose, with a relative molar mass of 1.53×10^{4} g.mol^{-1}.In vitro studies using a triple-negative breast cancer cell model showed a significantly reduction in cell viability (50%, at 1.200 µg. mL^{-1}). Furthermore, a synergistic effect was observed when co-administrated with the chemotherapy drug paclitaxel, reducing the cell viability to 42 %. These findings suggest potential therapeutic applications of the purified mushroom heteropolysaccharide reported in this study.

Keywords: *Lactarius quieticolor*; Polysaccharides; Heteropolysaccharides; Breast cancer

Graphical abstract

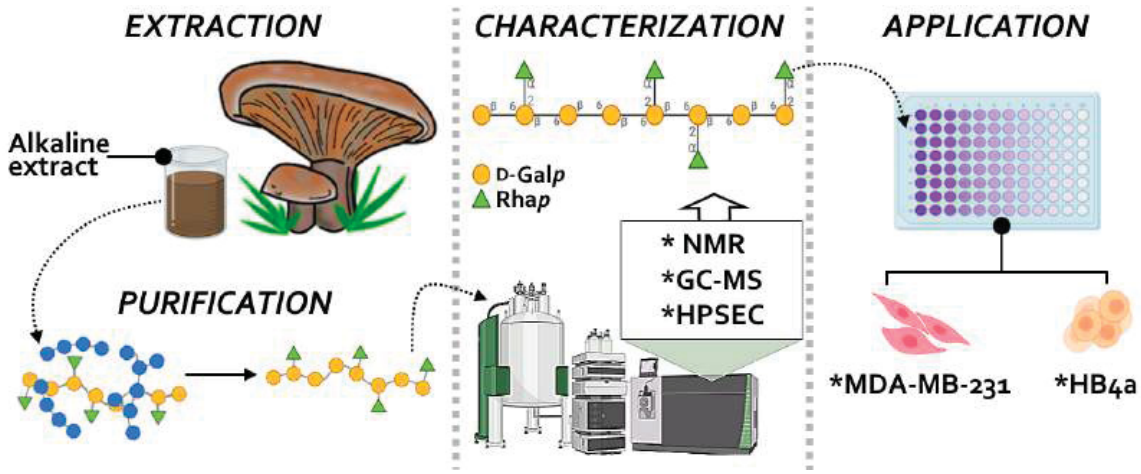

1. Introduction

Lactarius, a genus of ectomycorrhizal fungi, includes several edible species known as milk-caps. Among these, *Lactarius quieticolor* is primarily found in the Northern Hemisphere but has recently been reported in South America as well (Niedzielski et al., 2023; Silva-Filho et al., 2020). *Lactarius* mushrooms are nutritionally rich in fiber, carbohydrates, proteins, minerals, and vitamins, while being low in calories and fat (Dawadi et al., 2022; Li et al., 2022). Mushrooms have long been valued medically for their anti-inflammatory, antitumor, neuroprotective, and cytoprotective properties (Navarro-Simarro et al., 2024). Growing interest in their consumption and medicinal potential has spurred extensive research into identifying the compounds responsible for their bioactivity. Among the various compounds studied, such as phenols, fatty acids, and others, polysaccharides have been highlighted for their significant role (Araújo-Rodrigues et al., 2024).

Mushroom polysaccharides display an array of functions, primarily serving as an energy storage and maintaining structural integrity, being predominantly found in the cell walls of mushrooms (Dedousi et al., 2024; Panda et al., 2024) and are composed by several monossacharides including glucose in high concentrations, mannose, galactose, fucose, uronic acids in lower concentrations as well as rhamnose and xylose rarely (Elnahas et al., 2024; Yang et al., 2024). These monosaccharides form complex molecules such as glucans, galactans and other homo- or heteropolysaccharides (Araújo-Rodrigues et al., 2024; Yu et al., 2023).

Mushroom polysaccharides have gained attention for their wide range of biological activities, including immunomodulatory, anti-tumor, and anti-inflammatory effects. These compounds are not only biodegradable but also biocompatible and highly available (Araújo-Rodrigues et al., 2024; Navarro-Simarro et al., 2024). Their health benefits include stimulating the immune system by activating toll-like receptors (TLRs), dendritic cells, and macrophages (Yu et al., 2023). This immune activation helps clear pathogens, regulate inflammation, and modulate immune responses, contributing to their prebiotic, anticancer, and antimicrobial properties.

Mushrooms from the *Lactarius* genus have already been the subject of research, demonstrating promising results. Among the polysaccharides identified are β-glucans from *Lactarius rufus* and *Lactarius hatsudake* (Ruthes et al., 2013; Yang et al., 2024); glucomannans from *Lactarius deliciosus* (Li et al., 2022) and glucogalactomannans from *Lactarius volemus* (Zhong et al., 2021), among others. Currently, there are no reports specifically identifying the polysaccharides from the *Lactarius quieticolor* species, with further research being needed to determine the presence and potential bioactivity of these compounds.

Polysaccharides derived from mushrooms have demonstrated various effects on cancer cells. A galactan from *Amanita muscaria* and a fucogalactan from *Macrocybe titans* have been shown to inhibit the migration and reduce the clonogenic capabilities of melanoma cells (B16-F10 line) (Milhorini et al., 2018; Zavadinack et al., 2021). Additionally, polysaccharides from the *Lactarius* genus such as glucans from *Lactarius rufus*, have induced apoptosis in hepatocellular carcinoma HepG2 cells (Pires et al., 2013). Based on these results, the polysaccharide demonstrated low or no toxicity and showed excellent biocompatibility, making it a promising candidate for therapeutic applications. (Elnahas et al., 2024; Kour et al., 2022).

With such effects, seeking mushroom polysaccharides for said therapies is accounted for, considering that cancer is a prominent cause of death worldwide, with the most common types of cancer being lung, colorectal, prostate, and breast cancer (World Health Organization 2022b). Breast cancer, in particular, is the most frequently diagnosed cancer among women globally, with treatment options including surgery and radiation followed by hormone or targeted therapy for luminal A/B and HER2 subtype respectively, and only chemotherapy to the most aggressive, the triple negative subtype (Patel & Adrada, 2024; Regua et al., 2024; World Health Organization 2022a).

On that account, the present work aimed to obtain and purify polysaccharides from *Lactarius quieticolor* whose polysaccharides have not been previously reported and test their potential adjuvant capability against the triple negative human breast cancer MDA-MB-231 cell line. Our study identified a polysaccharide predominantly composed of galactose and rhamnose, which demonstrated significant inhibition of cancer cell viability, contributing valuable insights into the bioactivity and therapeutic potential of these unreported mushroom-derived compounds.

2. Material and methods

2.1. Biological material

The fruiting bodies of *L. quieticolor* were collected at the Federal University of Paraná's Botanic Garden Campus (25º26'49.1" S; 49º.14'16.4" W) in Curitiba, Paraná – Brazil. After cleaning and freeze-drying, the mushrooms were ground until powdered.

2.2. Extraction procedures

The powdered mushrooms were defatted with chloroform-methanol (2:1, v/v) in a Soxhlet extractor at 60 °C for 3h. The resulting material was submitted to aqueous extractions followed by reduction with $NaBH_4$ before undergoing alkaline extractions with 5% NaOH (m/v) for 6 h (96 °C).

The insoluble residue was filtered, and the liquid extract was neutralized (CH_3COOH) and dialyzed for 2 days against tap water. The flowchart in Figure 1 depicts the overall extraction and purification procedures.

2.3. Purification procedures

The initial purification of the alkaline extract employed freeze-thawing cycles (Gorin & Iacomini, 1984) with removal of the precipitate through centrifugation (10 min, 8.000 rpm). Further purification of the cold-water soluble fraction was achieved by removing glycogen through enzymatic treatment with α-amylase for 48 h followed by ethanol precipitation (3:1 v/v), dialysis (48 h, 6-8 kDa membrane) and freeze-drying. Subsequently, the sample was treated with the Fehling solution (Jones & Stoodley, 1965) yielding a soluble, Cu^{2+}-uncomplexed fraction and an insoluble precipitate of Cu^{2+}-complexed polysaccharides recovered through centrifugation (15 min, 8.000 rpm). After neutralization with CH_3COOH and deionization with ion exchange resin the precipitate was dialyzed (48 h, 6-8 kDa membrane) and lyophilized ensuing a second Fehling treatment. During the dialysis (48h, 6-8 kDa membrane) of the Cu^{2+}-complexed phase originated from the second Fehling treatment the formation of a precipitate was observed. This precipitate was removed through centrifugation (15 min, 8.000 rpm) leaving only the soluble heteropolysaccharide, which was then freeze-dried.

2.4. Monosaccharide composition of *L. quieticolor*'s fractions

The procedure for hydrolyzing the samples (2 mg) involved incubation with 2 M trifluoroacetic acid (TFA, 100 °C, 8 h.). After evaporation of the acid, the resulting material was dissolved in water and subjected to reduction with $NaBH_4$ treatment. Subsequently, the reduced material underwent acetylation using a mixture of pyridine-acetic anhydride (1:1 v/v) at 100 °C (30 min.). The alditol acetate derivatives obtained were subjected to analysis using a Varian® CP3800 gas chromatograph with a VF-5ms capillary column. Helium was used as the carrier gas at a flow rate of 1 mL/min. Identification of monosaccharides was based on their retention times compared to standards (Fig. 2A and D).

2.5. Nuclear Magnetic Resonance Spectroscopy (NMR)

Nuclear magnetic resonance (NMR) analyses were performed using Bruker™ Avance III HD 400 MHz and Bruker™ Avance III 600 MHz spectrometers. For each analysis, samples weighing between 15 to 30 mg were dissolved in 500 µL of deuterated dimethyl sulfoxide (Me_2SO-d_6) and transferred to 5 mm NMR tubes. The analyses were conducted at a temperature of 70 °C. Chemical

shifts were recorded and expressed in δ (ppm) relative to signals from Me_2SO-d_6, which were set at δ 39.7 ppm and δ 2.5 ppm for ^{13}C and ^{1}H, respectively.

2.6. Analysis of methylated derivatives by GC-MS

The polysaccharides were submitted to methylation analysis using an adapted method from Ciucanu and Kerek (1984) and Zavadinack et al. (2024). An aliquot of each fraction (10 mg) was dissolved, separately, in DMSO, followed by the addition of powdered NaOH and methyl iodide (1 mL). The mixture was stirred for 30 minutes at room temperature, then left overnight. Subsequently, the reaction was neutralized with acetic acid, dialyzed (6-8 kDa cut-off membranes, 24h), and freeze-dried. This methylation process was repeated twice for each sample, followed by extraction with chloroform. The per-*O*-methylated derivatives were hydrolyzed using 45% formic acid (100 °C, 16 h.), followed by treatment with 2 M TFA (100 °C, 8 h.), As previously described by Zavadinack et al. (2024). The samples were then reduced using deuterated sodium borohydride then acetylated as described in section 2.4. and subjected to GC-MS analysis following the same procedure described above for monosaccharide composition. Identification of the partially *O*-methylated alditol acetates derivatives was based on their ion *m/z* values compared to standards, and the results were expressed as the relative percentage of each component (Sassaki et al., 2005).

2.7. Preparation of methylated rhamnose standard

The methylated standard was prepared as described by Sassaki et al. (2005) initially through the glycosylation of the *L*-Rha standard (50 mg) in 5 mL of 3% MeOH-HCl under reflux for 2 hours. The glycoside was neutralized with $AgCO_3$ and filtered. After drying, 10 mg of the sample was added to 1.5 mL of methyl iodide and stirred with 250 mg of Ag_2O for 12 h at room temperature. After decantation of the oxide, the methylated supernatant was removed and dried, then hydrolyzed with 1 M H_2SO_4 (8 h, 100 °C), neutralized with $BaCO_3$ and reduced with $NaBD_4$. The standard's acetylation and analysis were carried out as described in section 2.4.3.

2.8. Determination of homogeneity and relative molecular weight

Relative molecular weight and homogeneity assessments were conducted using high-performance size exclusion chromatography (HPSEC) with a Waters™ 2410 differential refractometer, equipped with a refractive index detector and a series of four Waters™ Ultrahydrogel columns (2000, 500, 250, and 120 Å). The eluent used was composed of 0.1 M sodium nitrite ($NaNO_3$) with 0.5 g/L sodium azide (NaN_3). The samples were dissolved in the eluent at a concentration of 1 mg. mL^{-1} and filtered

through a 0.22 μm Millipore® membrane before injection. A curve generated from dextran standards (487, 266, 124, 72.2, 40.2, 17.2, and 9.40 kDa) was employed to determine the relative molecular weight of the samples.

2.9. Cell culture and treatments

Normal-like breast cell line, HB4a (Stamps et al., 1994) and breast cancer cell line MDA-MB-231 (triple negative-like) used were acquired by American Type Culture Collection (ATCC). The cells were cultivated in RPMI 1640 medium (Gibco), supplemented with 10% fetal bovine serum and incubated at 5% of CO_2 at 37 °C in a humidified atmosphere.

Cells were plated at 100 μL per well in a 96-well plate, achieving a density of 5,000 cells per well, and incubated at 37 °C with 5% CO_2 for 2 hours to allow adhesion. Afterward, 100 μL of the HTP fraction at 200, 400, 600, and 1.200 μg. mL^{-1} were added, while the control solvent (distilled water/DMSO 1:1), without the presence of the polysaccharide, was also added to designated wells, with the treatment lasting for 24 hours. After incubation, the supernatant was removed, and 0.5 mg/mL of MTT (3-(4,5-dimethylthiazol-2-yl)-2,5-diphenyltetrazolium bromide) was added, and 100 μL of DMSO was later used to solubilize formazan crystals. Absorbance at 570 nm was measured using a Synergy HT microplate reader, and cell viability was calculated relative to controls.

To evaluate the synergistic effect of HTP with paclitaxel, a common chemotherapeutic agent, the cells were treated with the dose that both were cytotoxic for close to 50% of cells, with 1.200 μg. mL^{-1} for HTP and 0.0850 μg. mL^{-1} for paclitaxel (Habibi et al., 2024).

2.10 Statistical analysis

The results are presented as mean ± standard error of mean (SEM). Statistical analysis was conducted using GraphPad Prism (v. 5.0), with significance set at $p < 0.05$. Comparisons between groups were performed using ordinary one-way ANOVA, followed by Tukey's multiple comparisons test for post-hoc analysis.

3. Results and discussion

3.1. Chemical structure of the heteropolysaccharide from *L. quieticolor*

The crude extract obtained from alkaline extraction (NaOH 5% m/v, 96 °C, 6 h, 3x) underwent the initial purification step through freeze-thawing with subsequent centrifugation (9.000 rpm, 15 min), yielding 15.03 g of the soluble fraction (EAS). After acid hydrolysis and acetylation, the EAS

fraction was found to consist of mannose (3.30%), rhamnose (6.54%), galactose (17.5%), and glucose (72.6%) Given that the fruiting body typically contains glycogen as a reserve polysaccharide (as confirmed by NMR analysis, shown in Suppl. Figure 1 A and B) the fraction was submitted to enzymatic treatment with α-amylase (48 h, 40 °C, ethanolic precipitation 3:1 v/v and dialysis, 2x), obtaining a new treated fraction (EAS-α) composed of rhamnose (9.1%), mannose (5.0%), galactose (24.3%) and glucose (61.5%) (Fig 2B). A decrease in glucose content, as shown in Table 1, indicates the success of the α-amylase treatment.

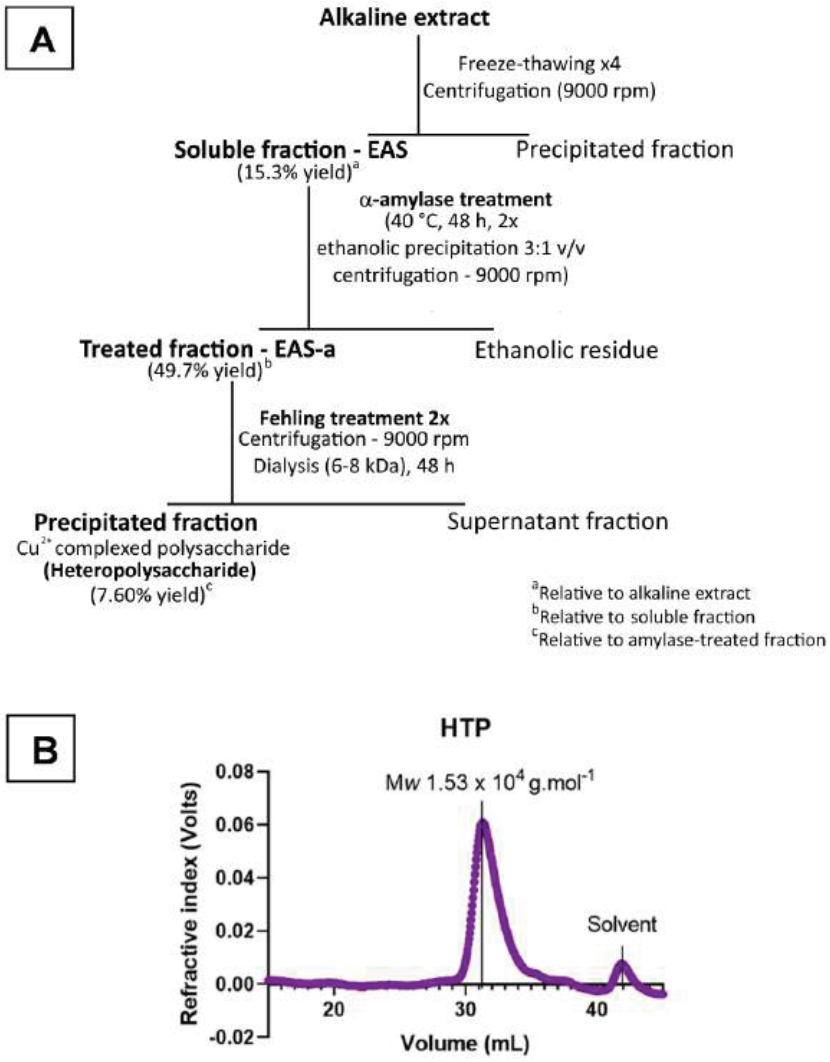

Figure. 1. Extraction and purification scheme of the *Lactarius quieticolor*'s heteropolysaccharide rhamnogalactan (HTP) and its elution profile in HPSEC coupled to a Refractive Index (RI) detector. (A) Flowchart of the extraction processes performed on the *Lactarius quieticolor* mushroom; **(B)** HPSEC-RI

elution profile of the HTP fraction. The relative molecular weight was determined using dextran standards (487, 266, 124, 72.2, 40.2, 17.2, and 9.40 kDa).

Following the removal of glycogen, an additional purification step was required to further fractionate the polysaccharides. For this purpose, a treatment with Fehling Solution was employed twice. The complexation of Cu^{2+} with the polymer resulted in a precipitate, which, upon decomplexation, was found to consist of rhamnose (27.4%) and galactose (72.6%) (Fig 2C and Table 1). Given that fucose is typically the monosaccharide found in mushrooms (Wang et al., 2018; Yang et al., 2024), we conducted a monosaccharide composition experiment using only fucose, rhamnose, and galactose standards (Fig. 2D). The retention time (Rt), observed at 26.2 minutes, confirmed the presence of rhamnose in the purified fraction (HTP), indicating that the applied method effectively isolated the desired monosaccharides. In fact, HPSEC revealed a homogeneous elution profile (Fig. 1B), indicating a uniform molecular weight distribution, with a M*w* of 1.53×10^4 $g.mol^{-1}$. These results demonstrate that the complexation of the polysaccharide with Fehling's solution is an effective method for polysaccharide purification, as described by Zavadinack et al. (2024). Additionally, sugar and protein analyses revealed that this fraction consists solely of carbohydrates, with no protein detected (Table 1). This heteropolymer (HTP), identified as rhamnogalactan, represents a molecule that is rarely observed in mushrooms (Elnahas et al., 2024; Yu et al., 2023).

Table 1. Monosaccharide composition of fractions obtained from *L. quieticolor.*

Fractions	Monosaccharides (%)[a]				Sugar content (%)	Protein Content (%)
	Rha	Man	Glc	Gal		
Crude extract	6.54	3.30	72.6	17.5	nd[b]	nd[b]
Amylase treatment	9.10	5.00	61.5	24.3	nd[b]	nd[b]
Heteropolysaccharide	27.4	-	-	72.6	99.6	-

[a] Relative to peak area
[b] Not determined

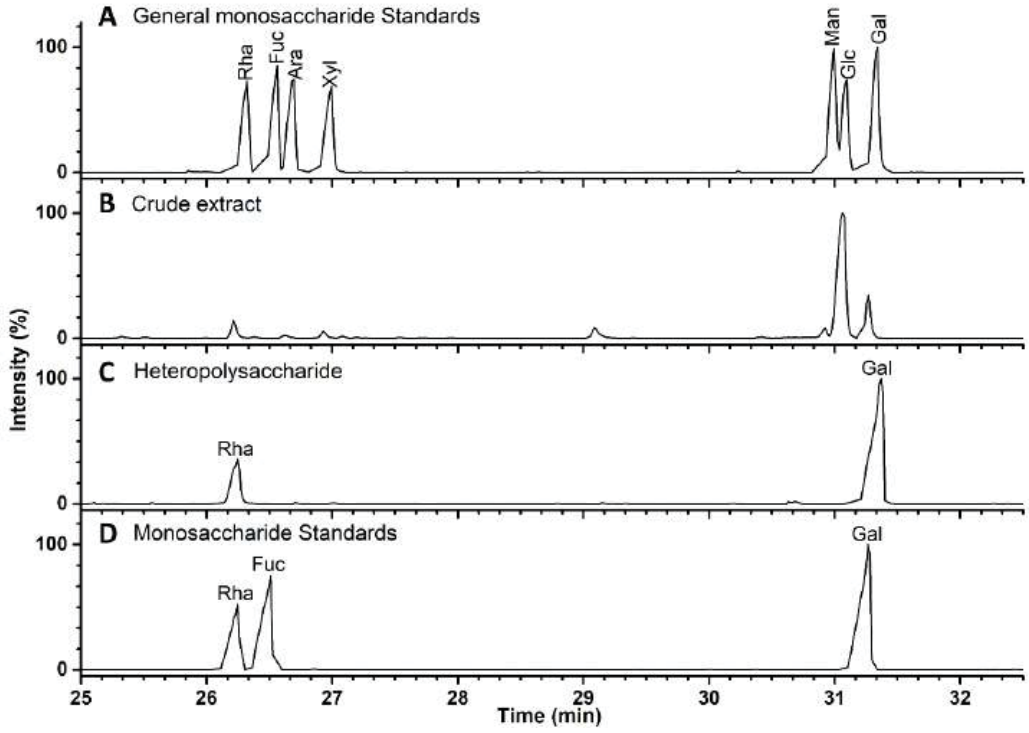

Figure 2. Monosaccharide composition determination of the HTP fraction obtained from the *Lactarius quieticolor* mushroom. (A) Monosaccharide standards; **(B)** the crude extract obtained after alkaline extraction and α-amylase treatment; **(C)** the purified HTP fraction; **(D)** monosaccharide chromatogram using rhamnose, fucose and galactose standards. The analyses were conducted using a Varian® CP3800 gas chromatograph, equipped with a VF-5ms capillary column and helium as the carrier gas at a flow rate of 1 mL/min. Monosaccharides were identified by comparing their retention times to reference standards.

To gain further insights into the molecular structure, methylation analyzes were performed (Fig. 4 and Table 2), which provide a more detailed understanding of the units, and the glycosidic linkages present in the HTP fraction. The results showed the presence of three distinct partially *O*-methyl alditol acetate (PMAAs) derivatives, the 2,3,4-Me_3-Galactitol (44.0%), indicating a (1→6)-Gal*p*-linked main chain highly 2-*O* substituted, as indicated by the presence of the 3,4-Me_2-Galactitol (28.4%) derivative. The 2,3,4-Me_3-Rhamnitol (27.6%) fragments indicate the presence of non-reducing end units of rhamnose. To confirm the presence of the 2,3,4-Me_3-Rhamnitol derivatives, we synthesize PMAAS derivatives standards of Rhamnose, as described by Sassaki et al. (2005). As shown in Figure 4A, the peaks corresponding to 2,3,4-Me_3-Rhamnitol derivatives are overlapped (21.8 minutes), confirming the presence of non-reducing terminal rhamnose units in the HTP fraction. Additionally, no other rhamnose units overlap with the heteropolymer peaks, further confirming that

these units present in the heteropolymer are exclusively non-reducing terminals. All derivatives observed for HTP fraction and Rhamnose standard PMAAs are represented in the Figure 3 and table 2.

Table 2. Partially *O*-methylated alditol acetates derivatives (PMAAs)[a] obtained upon the methylation of the HTP fraction[b] and the Rhamnose standard[c].

Partially *O*-methyl alditol acetates (PMAAs)[a]	**RT[d]**	**Relative Peak Area (%)[e]**	**Linkage types**
HTP fraction PMAAs			
2,3,4-Me_3-Rha	21.8	27.6	Rha*p*-(1→
2,3,4-Me_3-Gal	27.2	44.0	→6)-Gal*p*-(1→
3,4-Me_2-Gal	28.8	28.4	→2,6)-Gal*p*-(1→
Rhamnose standard PMAAs			
2,3,4-Me_3-Rha	21.8	Nd	Rha*p*-(1→
3,4-Me_2-Rha	22.7	Nd	2→)-Rha*p*-(1→
2,3-Me_2-Rha	23.9	Nd	4→)-Rha*p*-(1→
2,4-Me_2-Rha	25.5	Nd	3→)-Rha*p*-(1→

[a] PMAAs obtained through methylation process, as described in sections 2.6 and 2.7, and analyzed by GC-MS on a Varian® CP3800 chromatograph with a VF-5ms capillary column;
[b] Heteropolysaccharide rhamnogalactan obtained from the *L. quieticolor* mushroom;
[c] *L*-Rhamnose standard was purchased from Sigma-Aldrich®
[d] Retention time (minutes);
[e] Based on standard derived PMAAs derivatives.

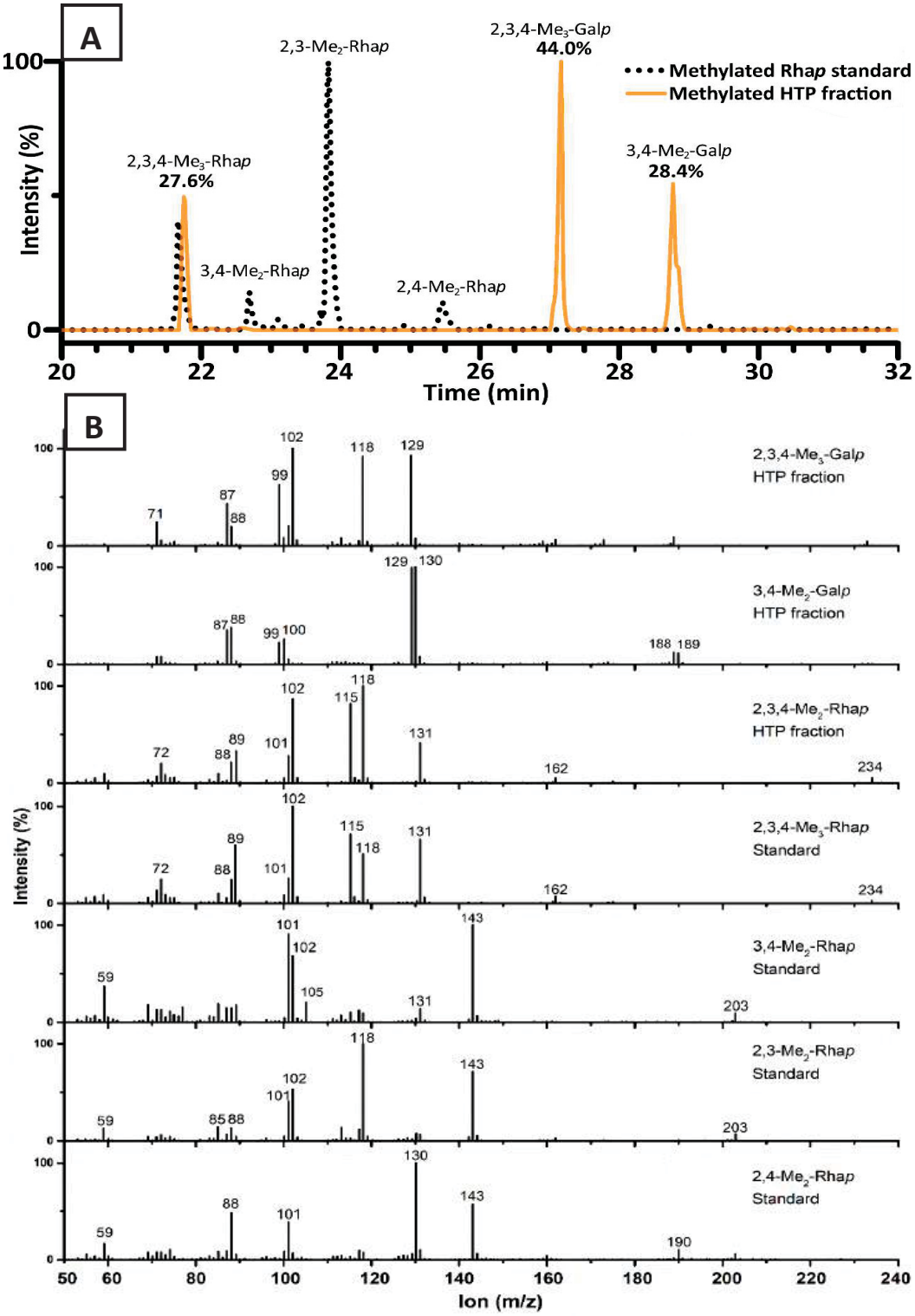

Figure 3. GC-MS chromatogram and fragmentation profiles of the HTP fraction and rhamnose standard after permethylation, acid hydrolysis and acetylation. (A) GC-MS chromatogram with the partially *O*-methyl alditol acetate (PMAAs) derivatives from the HTP fraction superimposed on the methylated rhamnose standard; **(B)** Fragmentation profile of the 2,3,4-Me_3-Rha, 2,3,4-Me_3-Gal and 3,4-Me_2-Gal from HTP fraction

PMAAs and 2,3,4-Me_3-Rha, 3,4-Me_2-Rha, 2,3-Me_2-Rha and 2,4-Me_2-Rha from Rhamnose standard PMAAs. The analyses were performed using a Varian® CP3800 gas chromatograph equipped with a VF-5ms capillary column, with helium as the carrier gas at a flow rate of 1 mL/min. Identification of the partially methylated alditol acetate (PMAA) derivatives was based on their ion *m/z* values.

The HSQC-DEPT NMR spectra of the crude soluble fraction (EAS) (Suppl. Fig. 1A) confirm the presence of glycogen, evidenced by characteristic signals at δ 100.4/5.04 ppm (C1/H1) and δ 79.9/3.33 ppm (C4/H4) (da Silva Milhorini et al., 2022b). Additionally, six other distinct anomeric signals at δ 99.4/4.81, δ 98.7/4.83, δ 98.5/4.73, δ 102.7/4.52, δ 102.7/4.35, and δ 102.7/4.25 were observed. Even after treatment with α-amylase, these five signals persisted in the resulting EAS-α fraction (Supp. Fig. 1B), suggesting the presence of a mixture of polysaccharides. In fact, both EAS and EAS-α presented heterogenous elution profiles in HPSEC-RI analyses (Suppl. Fig. 2A and B) further reinforcing the need to purify this fraction. Therefore, a treatment with Fehling´s solution was performed, resulting in the homogeneous fraction HTP (Fig. 1B), which present only three distinct anomeric signals at δ 98.5/4.73, δ 98.7/4.83 and δ 99.4/4.81, corresponding to →6)-Gal*p*-(1→, →2,6)-Gal*p*-(1→, and Rha*p*-(1→ units, respectively. The anomericities were confirmed through a coupled-HSQC-NMR experiment (Suppl. Fig. 3), which showed that the Gal*p* units present α anomericity, as the $J_{C1\text{-}H1}$ values observed were >170.0 Hz (Cordeiro et al., 2012), while for the Rha*p* units the β configuration was observed ($J_{C1\text{-}H1}$ = 160.6 Hz) (Amaral et al., 2008).

To confirm the attributed units, further NMR studies were conducted (^{1}H, COSY, TOCSY, HMBC). As demonstrated in Figure 4 and Table 3, several correlations were observed, as expected. In COSY experiment (Fig. 5A), it was possible to observe the H-1 coupling with H-2 for the three anomeric signals at δ 4.83/3.70, δ4.73/3.60 and δ 4.81/3.72. Additionally, the -CH_3/H-5 correlation for Rha*p* units was identified at δ 1.18/3.61 (^{1}H/^{1}H). Distant correlations from the TOCSY experiment (Fig. 5B) were observed for Rha*p* units at δ 1.18/3.33 for -CH_3/H-4 (^{1}H/^{1}H), further confirmed by HMBC analysis (Fig. 5C and D) through the -CH_3/H-4 (^{13}C/^{1}H) coupling at δ 17.8/3.33. Additionally, a H-1/C-3 coupled signal at δ 4.81/70.4 was observed for this unit. As the observed Rha*p* units were assigned to non-reducing end units (*t*-β-Rha*p*-(1→) linked to Gal*p* main chain at the *O*-2 position through methylation analyzes (Fig. 4 and Table 2), we attributed the ^{13}C/^{1}H correlation at δ 4.83/73.7 to the *t*-Rha*p*β1→2Gal*p* linkage. The HSQC-DEPT signal at δ 73.7/3.70 was attributed to the C-2/H-2 of the →2,6)-α-D-Gal*p*-(1→ units, as confirmed by the COSY and TOCSY spectra, which show the H-1/H-2 correlation at δ 4.83/3.70. Moreover, the equivalent values between these units were confirmed by similar percentages in the methylation analysis (27.6% and 28.4%), as well as by the integration of the ^{1}H signals at δ 4.83, δ 4.81, δ 4.73, and δ 1.18, with ratios of 1:1.1:1.5:3.2,

respectively (Fig. 5). The -CH_3 (δ 1.18 ppm) integrated value obtained agrees with and supports the proposed chemical structure. Theoretically, the relationship between H-1 and -CH_3 values should be 1:3, as each Rha*p*-(1→ unit contains only one methyl group. This consistency reinforces the accuracy of the structural assignments made in the study.

Substitution at C-6 can be observed at δ 66.4/3.68 and δ 66.4/3.53 as inverted signals (in blue, Fig. 4C, D and E), indicating the presence of -CH_2 groups (Abreu et al., 2021). As described by Ascêncio et al. (2006), Distortionless Enhancement by Polarization Transfer-135 (DEPT-135) experiments differentiate methylene (-CH_2) peaks from methyl (-CH_3) and methine (-CH) peaks. The -CH_2 groups appears in the negative phase, while -CH and -CH_3 appear in the positive phase. For Gal*p*, the C-6 non-substituted is usually observed at δ 60.5 to δ 61.5 ppm (Ruthes et al., 2010; Zavadinack et al., 2021), and no signal was observed in this region. Additionally, HMBC H-1/C-6 correlations were observed for both Gal*p* units at δ 4.73/66.4 and δ 4.83/66.4 (Fig. 5C), confirming that this polysaccharide has a (1→6)-linked backbone, as indicated by the methylation analysis. Therefore, we conclude that the heteropolysaccharide rhamnogalactan (HTP) presents a main chain (1→6)-α-D-Gal*p* linked substituted at *O*-2 by *t*-β-Rha*p*-(1→ units, as represented in Figure 4F. The complete attribution of the signals and all observed correlations are summarized in Figure 4E and Table 3.

Mushroom-derived polysaccharides are a complex group of molecules, and a variety of different chemical structures have already been reported (Ren et al., 2012; Ruthes et al., 2016). Moreover, the existence of a relationship between the structure and function of these molecules is well-established (Huang & Nie, 2015; Villares et al., 2012), making precise chemical characterization essential before conducting biological analyses. Among the biological activities observed, anticancer effects have been demonstrated by several authors (Khan et al., 2019; Ma et al., 2014; Zavadinack et al., 2021). According to Zhang et al. (2019), these molecules can exert their effects either by modulating the immune system - enhancing immune responses against cancer cells - or through direct cytotoxicity, reducing cell viability by activating pathways that induce cell death, which is mediated by its interaction with specific cellular receptors (Li et al., 2023; Zhang et al., 2017). In addition, studies on these molecules have demonstrated their low or absent cytotoxicity in normal cells and no side effects (Zhang et al., 2022), even when administered at high concentrations (Mao et al., 2015; Wang et al., 2014).

Given the discoveries about the chemical structure of the HTP fraction, we aim to investigate its cytotoxic effects on cancer cells. Specifically, we seek to elucidate the effects of HTP on normal breast

cells and triple-negative breast cancer cells, comparing the cytotoxic effects observed in each. Additionally, studies have been conducted to explore the potential synergistic effects of HTP when combined with the antitumor drug paclitaxel.

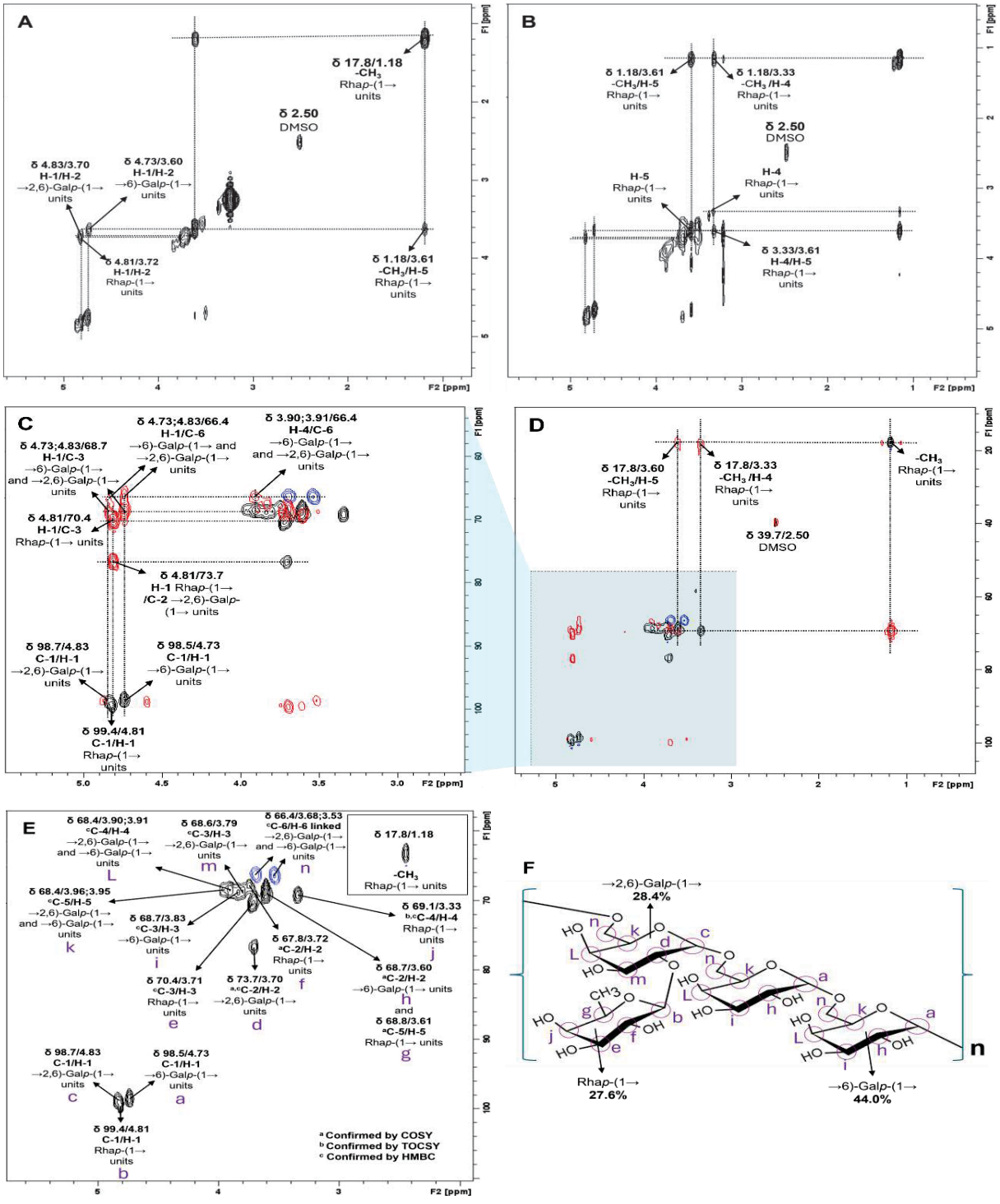

Figure 4. 2D-NMR studies of the heteropolysaccharide rhamnogalactan (HTP) obtained from the *Lactarius quieticolor* mushroom. (A) COSY, **(B)** TOCSY, **(C and D)** HSQC-DEPT (in black and blue) with superimposed HMBC (in red) spectrum. The selected area (^{1}H 1.90 to 5.80 ppm and ^{13}C 57.0 to 110.0 ppm) is represented in **C**, while the full spectrum is represented in **D**. **(E)** HSQC-DEPT spectrum. The inverted signals (negative phase) are in blue. **(F)** The presumed HTP chemical structure. The sample was analyzed in Me_2SO-d_6 (calibration parameters: δ 39.7/ 2.50 for C/H) at 70°C and the results are expressed in ppm (δ).

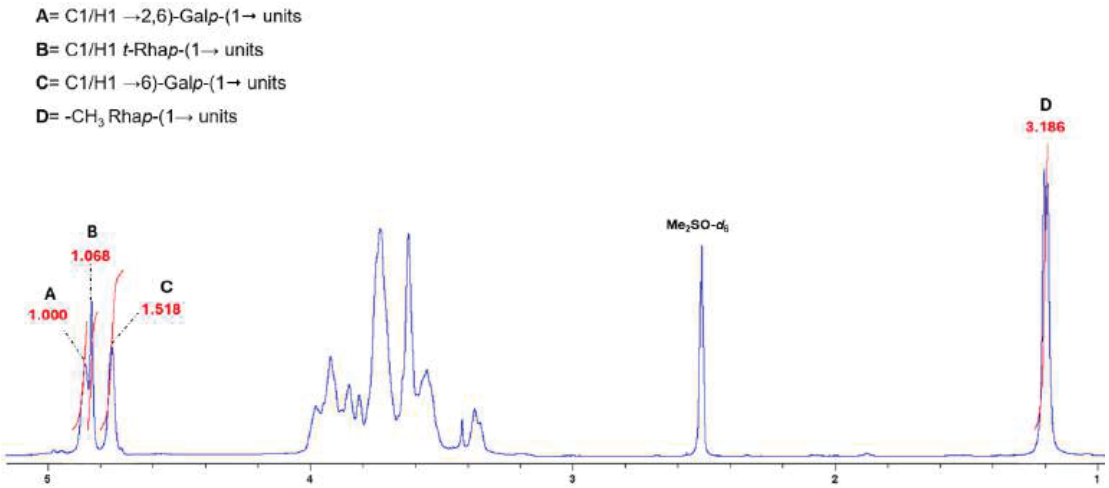

Figure 5. 1H-NMR of the heteropolysaccharide rhamnogalactan (HTP) obtained from the Lactarius quieticolor mushroom. Integrated values (in red) obtained through ^{1}H-NMR spectra.The sample was analyzed in Me_2SO-d_6 (calibration parameters: δ 2.50) at 70°C and the results are expressed in ppm (δ). The analysis and peak assignments were performed using TopSpin software, version 3.6.5.

Table 3. Chemical shifts[a] and the correlations observed ($^{1}H/^{1}H$ and $^{13}C/^{1}H$) through NMR experiments for each unit observed in HTP fraction.

Units	Signal (δ C/H)	Correlations
→6)-α-D-Gal*p*-(1→ **C-1/H-1**	98.5/4.73	H-1/C-6 (δ 4.73/66.4)[d] ; H-1/H-2 (δ 4.73/3.60)[b,c]
→6)-α-D-Gal*p*-(1→ **C-2/H-2**	68.7/3.60	H-1/H-2 (δ 4.73/3.60)[b,c]
→6)-α-D-Gal*p*-(1→ **C-3/H-3**	68.7/3.83	H-1/C-3 (δ 4.73/68.7)[d]
→6)-α-D-Gal*p*-(1→ **C-4/H-4**	68.4/3.91	H-4/C-6 (δ 3.91/66.4)[d]
→6)-α-D-Gal*p*-(1→ **C-5/H-5**	68.4/3.95	-
→6)-α-D-Gal*p*-(1→ **C-6/H-6[a]**	66.4/3.68	H-1/C-6 (δ 4.73/66.4)[d]
→6)-α-D-Gal*p*-(1→ **C-6/H-6b**	66.4/3.53	H-1/C-6 (δ 4.73/66.4)[d]
→2,6)-α-D-Gal*p*-(1→ **C-1/H-1**	98.7/4.83	H-1/C-6 (δ 4.83/66.4)[d] ; H-1/H-2 (δ 4.83/3.70)[b,c]
→2,6)-α-D-Gal*p*-(1 **C-2/H-2**	73.7/3.70	H-1/H-2 (δ 4.83/3.70)[b,c] ; H-1/C-2 (δ 4.81/73.7)[d]
→2,6)-α-D-Gal*p*-(1→ **C-3/H-3**	68.6/3.79	H-1/C-3 (δ 4.83/68.7)[d]
→2,6)-α-D-Gal*p*-(1→ **C-4/H-4**	68.4/3.90	H-4/C-6 (δ 3.90/66.4)[d]
→2,6)-α-D-Gal*p*-(1→ **C-5/H-5**	68.4/3.96	-
→2,6)-α-D-Gal*p*-(1→ **C-6/H-6**	66.4/3.69	H-1/C-6 (δ 4.83/66.6)[d]
→2,6)-α-D-Gal*p*-(1→ **C-6/H-6**	66.4/3.52	H-1/C-6 (δ 4.83/66.6)[d]
β-L-Rha*p*-(1→ **C-1/H-1**	99.4/4.81	H-1/H-2 (δ 4.81/3.72)[b,c] ; H-1/C-2 (δ 4.81/73.7)[d] H-1/C-3 (δ 4.81/70.4)[d]
β-L-Rha*p*-(1→ **C-2/H-2**	67.8/3.72	H-1/H-2 (δ 4.81/3.72)[b,c]
β-L-Rha*p*-(1→ **C-3/H-3**	70.4/3.71	H-1/C-3 (δ 4.81/70.4)[d]
β-L-Rha*p*-(1→ **C-4/H-4**	69.1/3.33	H-1/H-2 (δ 3.33/3.61)[b,c] ; -CH_3/H-4 (δ 1.18/3.31)[c,d]
β-L-Rha*p*-(1→ **C-5/H-5**	68.8/3.61	H-1/H-2 (δ 3.33/3.61)[b,c] ; -CH_3/H-5 (δ 1.18/3.61)[b,c]
β-L-Rha*p*-(1→ **-CH_3**	17.8/1.18	-CH_3/H-5 (δ 1.18/3.61)[b,c]

[a] Assignments are based on HSQC-DEPT analysis and are expressed as ppm (δ). [b] Signals in COSY spectrum. [c] Signals in TOCSY spectrum. [d] Signals in HMBC spectrum.

3.2. HTP fraction exhibited a high cytotoxic dose-dependent effect only in MDA-MB-231 cells

The triple-negative breast cancer cell model was used to evaluate the cytotoxic effects of the HTP fraction. As the HTP fraction was fully soluble only with the addition of 50% DMSO, the maximum dosage applied was 1.200 µg. mL^{-1}, as higher concentrations of either DMSO or the initial solution negatively impacted cell viability (data not shown) (Krajnak et al., 2023). Initially, we conducted the assay using the normal breast-derived HB4a cell line. The results showed that the HTP fraction had low cytotoxic effects in MTT assay (Quadrado et al., 2024; van de Loosdrecht et al., 1994) even at the highest dosage (1.200 µg. mL^{-1}), with less than 20% of cells affected (Fig. 6A), showing that the HTP heteropolysaccharide does not present acute toxicity in normal breast-derived HB4a cell line. In contrast, in MDA-MB-231 cells, a triple-negative breast cancer cell line, the HTP fraction exhibited a dose-dependent cytotoxic effect, reducing cell viability by 50% at the highest concentration tested (1.200 µg. mL^{-1}) (Figure 6B), suggesting a potential mechanism involving interactions with cellular receptors that are minimally or not expressed in normal cells (Ferreira et al., 2021). In fact, it has already been demonstrated that certain cell surface membrane receptors are overexpressed in tumor cells (Kischel et al., 2008; Panjehpour et al., 2005)

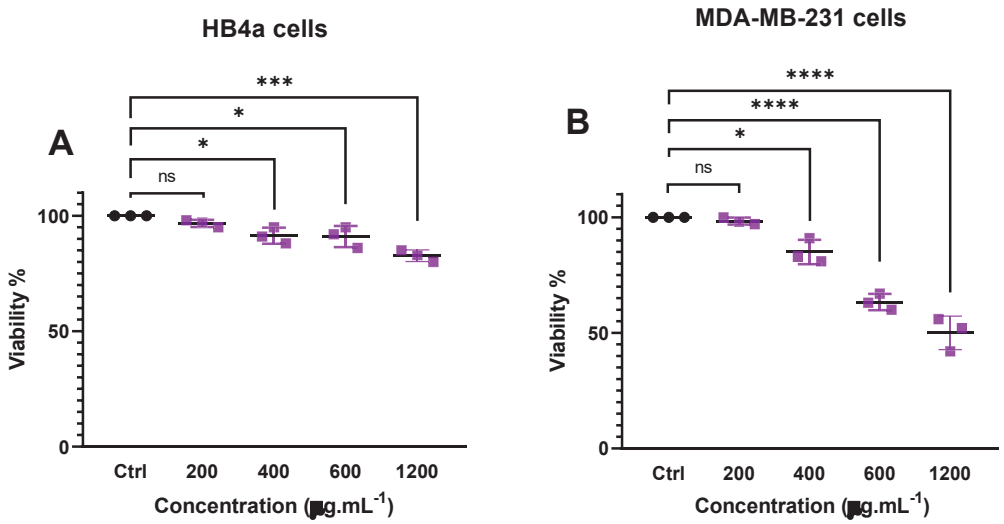

Figure 6. Cytotoxic effects of the HTP fraction. (A) Normal breast-derived HB4a cell line treated with different concentration of HTP. **(B)** Triple-negative breast cancer MDA-MB-231 cell line treated with

different concentrations of HTP. Distilled water/DMSO (1:1; v/v) was used alone as a control (Ctrl). ns = non significative * *p< 0,05 ***<0,01 ****<0,0001.*

3.3 The HTP fraction presented a synergetic cytotoxic effect in MDA-MB-231 cells when treated with paclitaxel

The HTP concentration with higher cytotoxic effect (1.200 µg. mL^{-1}), resulting in 50% of cell viability reduction in MDA-MB-231 cells was now co-administrated with paclitaxel, a well-known drug used in cancer treatments (Kaveh Zenjanab et al., 2024; Sledge et al., 2003). Their isolated effects at a concentration of 0.1 µM presented a reduction in cell viability to 64% in MDA-MB-231 cells (Fig. 7, in green). In combination (Fig. 7, in blue) it was observed a synergistic cytotoxic effect, which leads to a reduction off cell viability to 42%.

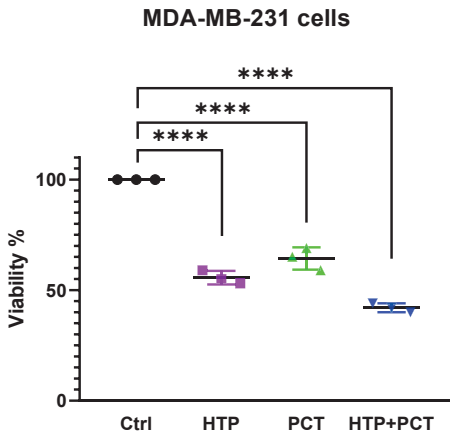

Figure 7. Synergistic cytotoxic effect of HTP (1.200 mg. mL-1) in combination with paclitaxel (PCT) (0.1 µM) in MDA-MB-231 cells. Cytotoxic effect of the HTP fraction at 1.200 µg. mL^{-1} (in purple); Cytotoxic effect of the paclitaxel (PCT) 0.1 µM (in green); Synergistic cytotoxic effect (in blue) when co-administrated at previously tested doses (1.200 µg. mL for HTP and 0.1 µM for PCT). Distilled water/DMSO (1:1; v/v) was used alone as a control (Ctrl). * *p< 0,05 ***<0,01 ****<0,0001.*

Triple-negative breast cancer is a less common, heterogeneous subtype of breast cancer, accounting for 15-20% of cases. It is characterized by moderate to high-grade, highly proliferative cancer cells (Zagami & Carey, 2022). The absence of approved targeted therapies and the limited treatment options result in the poorest prognosis among all breast cancer subtypes (Ferreira et al., 2021; Simu et al., 2021). Traditional chemotherapy frequently associated with side effects like cardiomyopathy, nephrotoxicity and many others (Schirrmacher, 2019). In this context the use of natural compounds is trend in cancer therapy research (Lin et al., 2020). There are many natural compounds in combination with chemotherapeutic drugs with the goal to enhance efficacy, reduce chemoresistance or relieve adverse effects (Lin et al., 2020). Notably, the herbal compound TLBZT has shown promising results

in combination with chemotherapeutic drugs against colon carcinoma (Wei et al., 2017). Curcumin, extracted from *Curcuma longa*, enhances the anticancer effects of carboplatin and doxorubicin in gastric and lung cancers (Lin et al., 2020). Silibinin, derived from *Silybum marianum*, has been found to potentiate the efficacy of paclitaxel. Similarly, several natural phenolic acids, including caffeic, rosmarinic, and ursolic acid, have demonstrated synergistic effects when paired with paclitaxel, further improving its anticancer activity (Kaveh Zenjanab et al., 2024; Lin et al., 2020).

The reduction in viability and density of cancer cells due to the action of mushroom polysaccharides has been previously reported for various authors. For instance, a fucoxylomannan isolated from *Ganoderma lucidum* was tested against B16-F10 murine melanoma cells by Milhorini et al. (2022a). The study demonstrated a significant reduction in cell proliferation and colony formation capabilities, achieving an 80% decrease in the observed colony area at a concentration of 500 μg. mL^{-1} compared to untreated cells. A similar effect on the B16-F10 cell line was observed for the homopolysaccharide (1→6), (1→2)-α-D-galactan isolated from *Amanita muscaria*, as noted by Zavadinack et al. (2021). Although its chemical structure is similar to that of the polysaccharide evaluated in this study, the latter is composed exclusively of galactose units.

Some studies involving polysaccharides from the *Lactarius* genus also demonstrate their antitumoral effects. A polysaccharide primarily composed of glucose and galactose, isolated from the *Lactarius volemus* species, showed antiproliferative effects against human lung (H1299) and breast (MCF-7) cancer cell lines (Zhong et al., 2021). The polysaccharide has M*w* 1.28×10^4 g. mol^{-1} and was able to inhibit H1299 and MCF-7 cell proliferation at concentrations ranging from 250 μg. mL^{-1} to 1000 μg. mL^{-1}. Additionally, Ding et al. (2012) isolated a heteropolysaccharide from the mushroom *Lactarius deliciosus* composed of L-mannose and D-xylose with M*w* 1.1×10^4 g.mol^{-1}. This heteropolysaccharide exhibited significant antitumoral activity *in vivo*, achieving a 68.4% inhibition rate at a concentration of 80 mg.kg^{-1}. These findings indicate that polysaccharides, including those derived from mushrooms of the *Lactarius* genus, possess significant potential as therapeutic agents.

4. Conclusion

A novel heteropolysaccharide was obtained from the *Lactarius quieticolor* mushroom through alkaline extraction followed by purification. Chemical characterization analyses revealed its precise composition and structure, consisting of β-rhamnose (27.4%) and α-galactose (72.6%) units, with a molecular weight of 1.53×10^4 g.mol^{-1}. The main chain is composed of (1→6)-linked galactopyranose

(Gal*p*) units, which are heavily substituted at the *O*-2 position by non-reducing end units of rhamnose. This polysaccharide demonstrated selective cytotoxicity, being minimally toxic to normal cells while exhibiting significant cytotoxic effects against triple-negative-like breast cancer cells. Furthermore, its synergistic interaction with paclitaxel highlights its potential to enhance the efficacy of chemotherapy, presenting not only a promising avenue for the development of novel cancer therapeutics as well as a new polysaccharide structure isolated from an edible mushroom, candidate as a new adjuvant in the therapy for triple-negative breast cancer.

Acknowledgments

This work was supported by the Brazilian funding agencies: Conselho Nacional de Desenvolvimento Científico e Tecnológico (CNPq, Process 403295/2021-1 and 310731/2021-6) and Coordenação de Aperfeiçoamento de Pessoal de Nível Superior (CAPES, Finance Code 001). The authors are also grateful to the NMR Center of UFPR for recording the NMR spectra.

References

Amaral, A. E., Carbonero, E. R., Simão, R. d. C. G., Kadowaki, M. K., Sassaki, G. L., Osaku, C. A., Gorin, P. A. J., & Iacomini, M. (2008). An unusual water-soluble β-glucan from the basidiocarp of the fungus *Ganoderma resinaceum*. *Carbohydrate Polymers*, *72*(3), 473-478. https://doi.org/10.1016/j.carbpol.2007.09.016

Araújo-Rodrigues, H., Sousa, A. S., Relvas, J. B., Tavaria, F. K., & Pintado, M. (2024). An Overview on Mushroom Polysaccharides: Health-promoting Properties, Prebiotic and Gut Microbiota Modulation Effects and Structure-function Correlation. *Carbohydrate Polymers*, *333*, 121978. https://doi.org/10.1016/j.carbpol.2024.121978

Ascêncio, S. D., Orsato, A., França, R. A., Duarte, M. E. R., & Noseda, M. D. (2006). Complete 1H and 13C NMR assignment of digeneaside, a low-molecular-mass carbohydrate produced by red seaweeds. *Carbohydrate Research*, *341*(5), 677-682. https://doi.org/10.1016/j.carres.2006.01.002

Ciucanu, I., & Kerek, F. (1984). A simple and rapid method for the permethylation of carbohydrates. *Carbohydrate Research*, *131*(2), 209-217. https://doi.org/10.1016/0008-6215(84)85242-8

Cordeiro, L. M. C., Reinhardt, V. d. F., & Iacomini, M. (2012). Glucomannan and branched (1→3)(1→6) β-glucan from the aposymbiotically grown Physcia kalbii mycobiont. *Phytochemistry*, *84*, 88-93. https://doi.org/10.1016/j.phytochem.2012.08.010

da Silva Milhorini, S., Simas, F. F., Smiderle, F. R., Inara de Jesus, L., Rosado, F. R., Longoria, E. L., & Iacomini, M. (2022b). β-Glucans from the giant mushroom Macrocybe titans: Chemical characterization and rheological properties. *Food Hydrocolloids*, *125*, 107392. https://doi.org/10.1016/j.foodhyd.2021.107392

Dawadi, E., Magar, P. B., Bhandari, S., Subedi, S., Shrestha, S., & Shrestha, J. (2022). Nutritional and post-harvest quality preservation of mushrooms: A review. *Heliyon*, *8*(12), e12093. https://doi.org/10.1016/j.heliyon.2022.e12093

Dedousi, M., Melanouri, E. M., Diamantis, I., Papanikolaou, S., & Diamantopoulou, P. (2024). Biochemical, functional and antioxidant potential of higher fungi cultivated on agro-industrial residues. Part II: Cultures on mixtures of spent mushroom substrates and mushroom cropping by-products. *Resources Chemicals and Materials*. https://doi.org/10.1016/j.recm.2024.04.001

Ding, X., Hou, Y., & Hou, W. (2012). Structure feature and antitumor activity of a novel polysaccharide isolated from Lactarius deliciosus Gray. *Carbohydrate Polymers*, *89*(2), 397-402. https://doi.org/10.1016/j.carbpol.2012.03.020

Elnahas, M. O., Elkhateeb, W. A., & Daba, G. M. (2024). Nutritive profile, pharmaceutical potentials, and structural analysis of multifunctional bioactive fungal polysaccharides—A review. *International Journal of Biological Macromolecules*, *266*, 130893. https://doi.org/10.1016/j.ijbiomac.2024.130893

Ferreira, S., Saraiva, N., Rijo, P., & Fernandes, A. S. (2021). LOXL2 Inhibitors and Breast Cancer Progression. *Antioxidants*, *10*(2).

Gorin, P. A. J., & Iacomini, M. (1984). Polysaccharides of the lichens Cetraria islandica and Ramalina usnea. *Carbohydrate Research*, *128*(1), 119-132. https://doi.org/10.1016/0008-6215(84)85090-9

Habibi, E., Sepehrara, A., Arabnozari, H., Sharifianjazi, F., Enderami, S. E., Sarker, S. D., Hassannia, H., & Nahar, L. (2024). Alkaloid-rich extract of jujube seed regenerate the antiproliferative effect of paclitaxel on paclitaxel-resistant MDA-MB-231 breast cancer cell line in 2D and 3D cultures. *Journal of Agriculture and Food Research*, *18*, 101438. https://doi.org/10.1016/j.jafr.2024.101438

Huang, X., & Nie, S. (2015). The structure of mushroom polysaccharides and their beneficial role in health [10.1039/C5FO00678C]. *Food & Function*, *6*(10), 3205-3217. 10.1039/C5FO00678C

Jones, J. K. N., & Stoodley, R. J. (1965). Fractionation using copper complexes. *Methods in carbohydrate chemistry*, *5*, 36-38.

Kaveh Zenjanab, M., Alimohammadvand, S., Doustmihan, A., Kianian, S., Sadeghzadeh Oskouei, B., Mazloomi, M., Akbari, M., & Jahanban-Esfahlan, R. (2024). Paclitaxel for breast cancer therapy: A review on effective drug combination modalities and nano drug delivery platforms. *Journal of Drug Delivery Science and Technology*, *95*, 105567. https://doi.org/10.1016/j.jddst.2024.105567

Khan, T., Date, A., Chawda, H., & Patel, K. (2019). Polysaccharides as potential anticancer agents—A review of their progress. *Carbohydrate Polymers*, *210*, 412-428. https://doi.org/10.1016/j.carbpol.2019.01.064

Kischel, P., Guillonneau, F., Dumont, B., Bellahcène, A., Stresing, V., Clézardin, P., Pauw, E. A. D., & Castronovo, V. (2008). Cell Membrane Proteomic Analysis Identifies Proteins Differentially Expressed in Osteotropic Human Breast Cancer Cells. *Neoplasia*, *10*(9), 1014-IN1011. https://doi.org/10.1593/neo.08570

Kour, H., Kour, D., Kour, S., Singh, S., Jawad Hashmi, S. A., Yadav, A. N., Kumar, K., Sharma, Y. P., & Ahluwalia, A. S. (2022). Bioactive compounds from mushrooms: Emerging bioresources of food and nutraceuticals. *Food Bioscience*, *50*, 102124. https://doi.org/10.1016/j.fbio.2022.102124

Krajnak, S., Trier, J., Heinzmann, P., Anic, K., Heimes, A.-S., Loewe, A., Schmidt, M., Battista, M., Hasenburg, A., & Brenner, W. (2023). Anti-tumor effects of low-dose metronomic vinorelbine in combination with alpelisib in breast cancer cells. *EXCLI journal*, *22*, 114-130. 10.17179/excli2022-5064

Li, K., Wang, L., Hu, Y., & Zhu, Z. (2022). Structural characterization and protective effect on PC12 cells against H2O2-induced oxidative damage of a polysaccharide extracted from mycelia of Lactarius deliciosus Gray. *International Journal of Biological Macromolecules*, *209*, 1815-1825. https://doi.org/10.1016/j.ijbiomac.2022.04.154

Li, M., Huang, X., Wen, J., Chen, S., Wu, X., Ma, W., Cui, S. W., Xie, M., & Nie, S. (2023). Innate immune receptors co-recognition of polysaccharides initiates multi-pathway synergistic immune response. *Carbohydrate Polymers*, *305*, 120533. https://doi.org/10.1016/j.carbpol.2022.120533

Lin, S.-R., Chang, C.-H., Hsu, C.-F., Tsai, M.-J., Cheng, H., Leong, M. K., Sung, P.-J., Chen, J.-C., & Weng, C.-F. (2020). Natural compounds as potential adjuvants to cancer therapy: Preclinical evidence. *British Journal of Pharmacology*, *177*(6), 1409-1423. https://doi.org/10.1111/bph.14816

Ma, G., Yang, W., Mariga, A. M., Fang, Y., Ma, N., Pei, F., & Hu, Q. (2014). Purification, characterization and antitumor activity of polysaccharides from Pleurotus eryngii residue. *Carbohydrate Polymers*, *114*, 297-305. https://doi.org/10.1016/j.carbpol.2014.07.069

Mao, G.-H., Ren, Y., Feng, W.-W., Li, Q., Wu, H.-Y., jin, D., Zhao, T., Xu, C.-Q., Yang, L.-Q., & Wu, X.-Y. (2015). Antitumor and immunomodulatory activity of a water-soluble polysaccharide from Grifola frondosa. *Carbohydrate Polymers*, *134*, 406-412. https://doi.org/10.1016/j.carbpol.2015.08.020

Milhorini, S. d. S., Smiderle, F. R., Biscaia, S. M. P., Rosado, F. R., Trindade, E. S., & Iacomini, M. (2018). Fucogalactan from the giant mushroom Macrocybe titans inhibits melanoma cells migration. *Carbohydrate Polymers*, *190*, 50-56. https://doi.org/10.1016/j.carbpol.2018.02.063

Navarro-Simarro, P., Gómez-Gómez, L., Ahrazem, O., & Rubio-Moraga, Á. (2024). Food and human health applications of edible mushroom by-products. *New Biotechnology*, *81*, 43-56. https://doi.org/10.1016/j.nbt.2024.03.003

Niedzielski, P., Szostek, M., Budka, A., Budzyńska, S., Siwulski, M., Proch, J., Kalač, P., & Mleczek, M. (2023). Lactarius and Russula mushroom genera – Similarities/differences in mineral composition within the Russulaceae family. *Journal of Food Composition and Analysis*, *115*, 104970. https://doi.org/10.1016/j.jfca.2022.104970

Panda, J., Mishra, A. K., Nath, P. C., Mahanta, S., Sharma, M., Nayak, P. K., Mohanta, Y. K., & Sridhar, K. (2024). Wild edible mushrooms to achieve sustainable development goals: Novel sources for food security, health, and well-being. *Food Bioscience*, *60*, 104277. https://doi.org/10.1016/j.fbio.2024.104277

Panjehpour, M., Castro, M., & Klotz, K.-N. (2005). Human breast cancer cell line MDA-MB-231 expresses endogenous A2B adenosine receptors mediating a Ca2+ signal. *British Journal of Pharmacology*, *145*(2), 211-218. https://doi.org/10.1038/sj.bjp.0706180

Patel, M. M., & Adrada, B. E. (2024). Hereditary Breast Cancer: BRCA Mutations and Beyond. *Radiologic Clinics of North America*, *62*(4), 627-642. https://doi.org/10.1016/j.rcl.2023.12.014

Pires, A. d. R. A., Ruthes, A. C., Cadena, S. M. S. C., Acco, A., Gorin, P. A. J., & Iacomini, M. (2013). Cytotoxic effect of Agaricus bisporus and Lactarius rufus β-d-glucans on HepG2 cells. *International Journal of Biological Macromolecules*, *58*, 95-103. https://doi.org/10.1016/j.ijbiomac.2013.03.040

Quadrado, R. F. N., Zhai, Z., Zavadinack, M., Klassen, G., Iacomini, M., Edgar, K. J., & Fajardo, A. R. (2024). All-polysaccharide, self-healing, pH-sensitive, in situ-forming hydrogel of carboxymethyl chitosan and aldehyde-functionalized hydroxyethyl cellulose. *Carbohydrate Polymers*, *336*, 122105. https://doi.org/10.1016/j.carbpol.2024.122105

Regua, A. T., Bindal, S., Najjar, M. K., Zhuang, C., Khan, M., Arrigo, A. B. J., Gonzalez, A. O., Zhang, X. R., Zhu, J.-J., Watabe, K., & Lo, H.-W. (2024). Dual inhibition of the TrkA and JAK2 pathways using entrectinib and pacritinib suppresses the growth and metastasis of HER2-positive and triple-negative breast cancers. *Cancer Letters*, *597*, 217023. https://doi.org/10.1016/j.canlet.2024.217023

Ren, L., Perera, C., & Hemar, Y. (2012). Antitumor activity of mushroom polysaccharides: a review [10.1039/C2FO10279J]. *Food & Function*, *3*(11), 1118-1130. 10.1039/C2FO10279J

Ruthes, A. C., Carbonero, E. R., Córdova, M. M., Baggio, C. H., Santos, A. R. S., Sassaki, G. L., Cipriani, T. R., Gorin, P. A. J., & Iacomini, M. (2013). Lactarius rufus (1→3),(1→6)-β-d-glucans: Structure, antinociceptive and anti-inflammatory effects. *Carbohydrate Polymers*, *94*(1), 129-136. https://doi.org/10.1016/j.carbpol.2013.01.026

Ruthes, A. C., Komura, D. L., Carbonero, E. R., Sassaki, G. L., Gorin, P. A. J., & Iacomini, M. (2010). Structural characterization of the uncommon polysaccharides obtained from Peltigera canina photobiont Nostoc muscorum. *Carbohydrate Polymers*, *81*(1), 29-34. https://doi.org/10.1016/j.carbpol.2010.01.050

Ruthes, A. C., Smiderle, F. R., & Iacomini, M. (2016). Mushroom heteropolysaccharides: A review on their sources, structure and biological effects. *Carbohydrate Polymers*, *136*, 358-375. https://doi.org/10.1016/j.carbpol.2015.08.061

Sassaki, G. L., Gorin, P. A. J., Souza, L. M., Czelusniak, P. A., & Iacomini, M. (2005). Rapid synthesis of partially O-methylated alditol acetate standards for GC-MS: Some relative activities of hydroxyl groups of methyl glycopyranosides on Purdie methylation [Article]. *Carbohydrate Research*, *340*(4), 731-739. 10.1016/j.carres.2005.01.020

Schirrmacher, V. (2019). From chemotherapy to biological therapy: A review of novel concepts to reduce the side effects of systemic cancer treatment (Review). *Int J Oncol*, *54*(2), 407-419. 10.3892/ijo.2018.4661

Silva-Filho, A., Sulzbacher, M., Grebenc, T., & Wartchow, F. (2020). Not every edible orange milkcap is Lactarius deliciosus: first record of *Lactarius quieticolor* (sect. Deliciosi) from Brazil. *Journal of Applied Botany and Food Quality*, *93*, 289-299. https://doi.org/10.5073/JABFQ.2020.093.036

Simu, S., Marcovici, I., Dobrescu, A., Malita, D., Dehelean, C. A., Coricovac, D., Olaru, F., Draghici, G. A., & Navolan, D. (2021). Insights into the Behavior of Triple-Negative MDA-MB-231 Breast Carcinoma Cells Following the Treatment with 17β-Ethinylestradiol and Levonorgestrel. *Molecules*, *26*(9). 10.3390/molecules26092776

Sledge, G. W., Neuberg, D., Bernardo, P., Ingle, J. N., Martino, S., Rowinsky, E. K., & Wood, W. C. (2003). Phase III Trial of Doxorubicin, Paclitaxel, and the Combination of Doxorubicin and Paclitaxel

as Front-Line Chemotherapy for Metastatic Breast Cancer: An Intergroup Trial (E1193). *Journal of Clinical Oncology*, *21*(4), 588-592. 10.1200/JCO.2003.08.013

Stamps, A. C., Davies, S. C., Burman, J., & O'Hare, M. J. (1994). Analysis of proviral integration in human mammary epithelial cell lines immortalized by retroviral infection with a temperature-sensitive SV40 T-antigen construct. *International Journal of Cancer*, *57*(6), 865-874. https://doi.org/10.1002/ijc.2910570616

van de Loosdrecht, A. A., Beelen, R. H. J., Ossenkoppele, G. J., Broekhoven, M. G., & Langenhuijsen, M. M. A. C. (1994). A tetrazolium-based colorimetric MTT assay to quantitate human monocyte mediated cytotoxicity against leukemic cells from cell lines and patients with acute myeloid leukemia. *Journal of Immunological Methods*, *174*(1), 311-320. https://doi.org/10.1016/0022-1759(94)90034-5

Villares, A., Mateo-Vivaracho, L., & Guillamón, E. (2012). Structural Features and Healthy Properties of Polysaccharides Occurring in Mushrooms. *Agriculture*, *2*(4), 452-471.

Wang, D., Sun, S.-Q., Wu, W.-Z., Yang, S.-L., & Tan, J.-M. (2014). Characterization of a water-soluble polysaccharide from Boletus edulis and its antitumor and immunomodulatory activities on renal cancer in mice. *Carbohydrate Polymers*, *105*, 127-134. https://doi.org/10.1016/j.carbpol.2013.12.085

Wang, H.-T., Yang, L.-C., Yu, H.-C., Chen, M.-L., Wang, H.-J., & Lu, T.-J. (2018). Characteristics of fucose-containing polysaccharides from submerged fermentation of Agaricus blazei Murill. *Journal of Food and Drug Analysis*, *26*(2), 678-687. https://doi.org/10.1016/j.jfda.2017.07.006

Wei, M. M., Wang, S. S., Zheng, J. L., Chen, J. J., Yan, X., An, H. M., & Hu, B. (2017). Herbal compound Teng-Long-Bu-Zhong-Tang inhibits metastasis in human RKO colon carcinoma. *Oncol Lett*, *14*(6), 7767-7772. 10.3892/ol.2017.7206

World Health Organization (2022a). *Breast Cancer*. [WHO]. Retrieved 06/2024 from https://www.who.int/news-room/fact-sheets/detail/breast-cancer

World Health Organization (2022b). *Cancer*. [WHO]. Retrieved 06/2024 from https://www.who.int/news-room/fact-sheets/detail/cancer

Yang, Q., Chang, S.-L., Tian, Y.-M., Li, W., & Ren, J.-L. (2024). Glucan polysaccharides isolated from Lactarius hatsudake Tanaka mushroom: Structural characterization and in vitro bioactivities. *Carbohydrate Polymers*, *337*, 122171. https://doi.org/10.1016/j.carbpol.2024.122171

Yu, Y., Liu, Z., Song, K., Li, L., & Chen, M. (2023). Medicinal value of edible mushroom polysaccharides: a review. *Journal of Future Foods*, *3*(1), 16-23. https://doi.org/10.1016/j.jfutfo.2022.09.003

Zagami, P., & Carey, L. A. (2022). Triple negative breast cancer: Pitfalls and progress. *npj Breast Cancer*, *8*(1), 95. 10.1038/s41523-022-00468-0

Zavadinack, M., Cantu-Jungles, T. M., Abreu, H., Ozturk, O. K., Cordeiro, L. M. C., de Freitas, R. A., Hamaker, B. R., & Iacomini, M. (2024). (1 → 3),(1 → 6) and (1 → 3)-β-D-glucan physico-chemical features drive their fermentation profile by the human gut microbiota. *Carbohydrate Polymers*, *327*, 121678. https://doi.org/10.1016/j.carbpol.2023.121678

Zavadinack, M., de Lima Bellan, D., da Rocha Bertage, J. L., da Silva Milhorini, S., da Silva Trindade, E., Simas, F. F., Sassaki, G. L., Cordeiro, L. M. C., & Iacomini, M. (2021). An α-D-galactan and a β-D-glucan from the mushroom Amanita muscaria: Structural characterization and antitumor activity

against melanoma. *Carbohydrate Polymers*, *274*, 118647. https://doi.org/10.1016/j.carbpol.2021.118647

Zhang, F., Shi, J.-J., Thakur, K., Hu, F., Zhang, J.-G., & Wei, Z.-J. (2017). Anti-Cancerous Potential of Polysaccharide Fractions Extracted from Peony Seed Dreg on Various Human Cancer Cell Lines Via Cell Cycle Arrest and Apoptosis [Original Research]. *Frontiers in Pharmacology*, *8*. https://www.frontiersin.org/journals/pharmacology/articles/10.3389/fphar.2017.00102

Zhang, J., Wen, C., Zhang, H., & Duan, Y. (2019). Review of isolation, structural properties, chain conformation, and bioactivities of psyllium polysaccharides. *International Journal of Biological Macromolecules*, *139*, 409-420. https://doi.org/10.1016/j.ijbiomac.2019.08.014

Zhang, S., Lei, L., Zhou, Y., Ye, F.-y., & Zhao, G.-h. (2022). Roles of mushroom polysaccharides in chronic disease management. *Journal of Integrative Agriculture*, *21*(7), 1839-1866. https://doi.org/10.1016/S2095-3119(21)63871-6

Zhong, R.-F., Yang, J.-J., Geng, J.-H., & Chen, J. (2021). Structural characteristics, anti-proliferative and immunomodulatory activities of a purified polysaccharide from Lactarius volemus Fr. *International Journal of Biological Macromolecules*, *192*, 967-977. https://doi.org/10.1016/j.ijbiomac.2021.10.049

Supplementary material

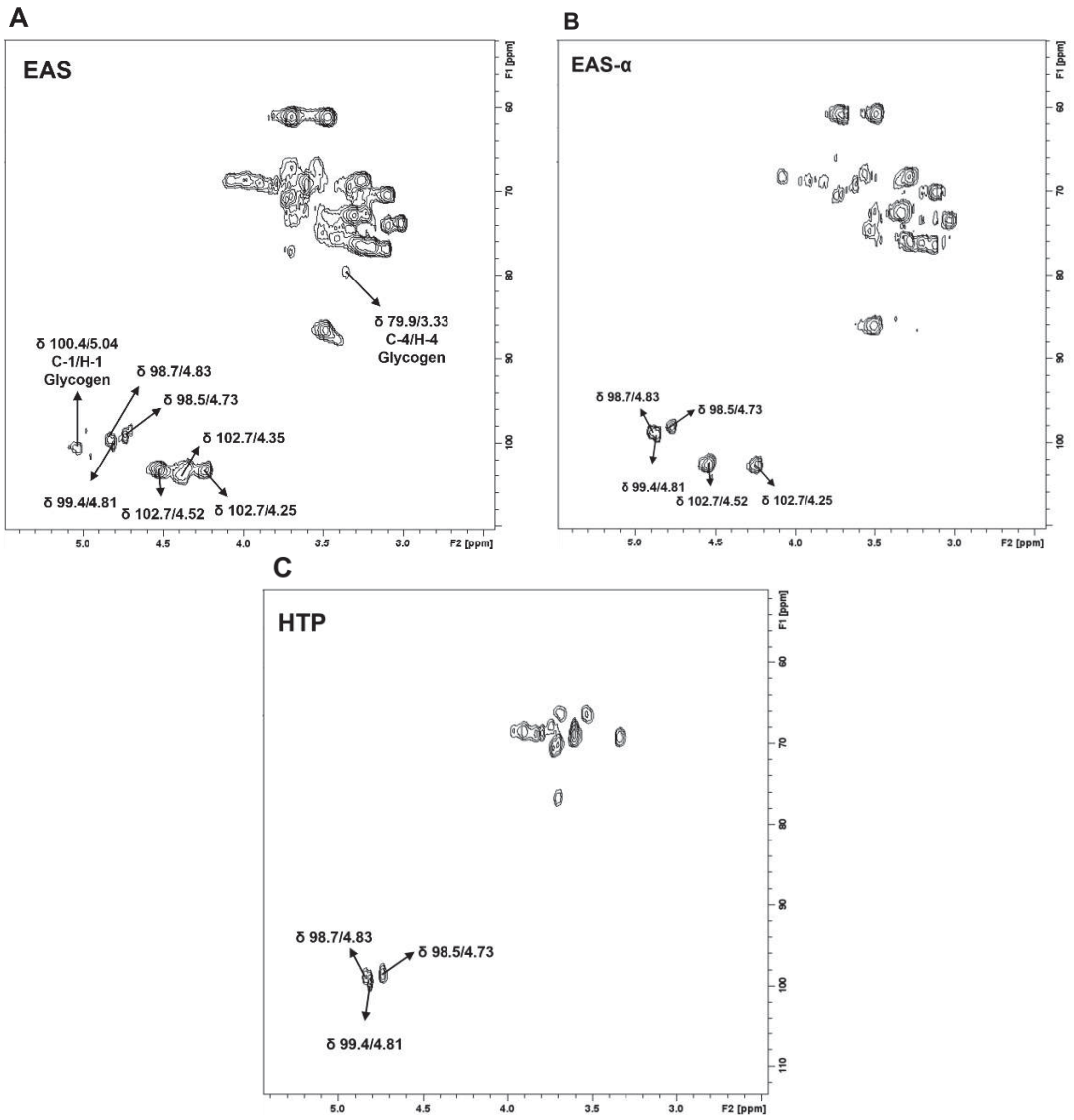

Supplementary Figure 1. HSQC-NMR studies of the fractions obtained from L. quieticolor during the purification process. (A) Crude extract (EAS) obtained from alkaline extraction; **(B)** Fraction obtained after α-amylase treatment of the EAS extract (EAS-α); **(C)** Heteropolysaccharide rhamnogalactan (HTP) obtained after treatment with Fehling´s solution (Cu^{2+} precipitate fraction). Samples were analyzed in Me_2SO-d_6, at 70 °C (calibration parameters: δ 39.7/ 2.50 for C/H), and the chemical shifts are expressed in δ ppm.

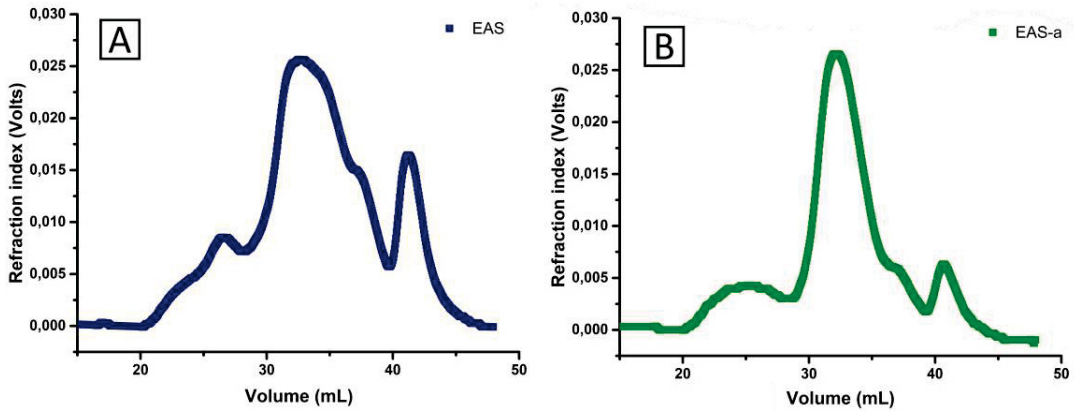

Supplementary Figure 2. EAS and EAS-a elution profile in HPSEC coupled to a Refractive Index (RI) detector. (A) HPSEC-RI elution profile of the EAS fraction; **(B)** HPSEC-RI elution profile of the EAS-a fraction. The relative molecular weight was determined using dextran standards (487, 266, 124, 72.2, 40.2, 17.2, and 9.40 kDa).

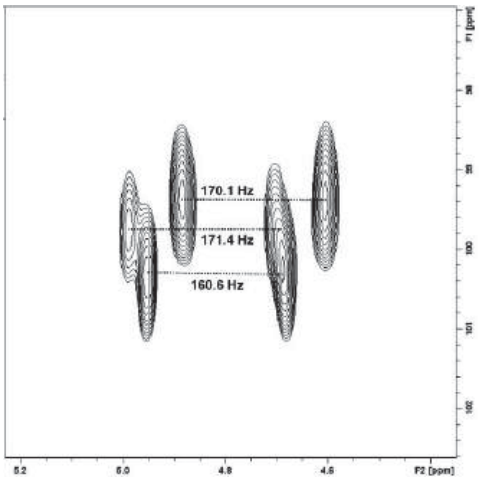

Supplementary Figure 3. Coupled-HSQC NMR experiments were performed on the HTP fraction. Coupling constant values ($J_{C1\text{-}H1}$) were calculated using TopSpin software, version 3.6.5, by measuring the distance between each anomeric signal observed in the selected region (δ 4.35 to δ 5.22 ppm for ^{1}H and δ 97.0 to δ 102.6 ppm for ^{13}C). The sample was analyzed in $Me_2SO\text{-}d_6$ at 70 °C (calibration parameters: δ 39.7/2.50 for C/H), with chemical shifts expressed in δ ppm.

Artigo II

Selective Cytotoxicity and Antimetastatic Effect on Breast Cancer Cell Model of a β-D-Glucan from *Lactarius quieticolor* mushroom

Selective Cytotoxicity and Antimetastatic Effect on Breast Cancer Cell Model of a β-D-Glucan from *Lactarius quieticolor* mushroom

Eliane Leal de Lara[a1]; Matheus Zavadinack[a1], Shayane da Silva Milhorini[a], Karin Maciel Wurzer[b], Giseli Klassen[b], Lucimara M.C. Cordeiro[a], Marcello Iacomini[a]*

[a] Department of Biochemistry and Molecular Biology, Federal University of Paraná, Curitiba- PR, CEP 81531-980, Brazil.

[b] Department of Basic Pathology, Federal University of Paraná, Curitiba- PR, CEP 81531-980, Brazil.

[1] Equal contribution

*Corresponding author: Department of Biochemistry and Molecular Biology, Federal University of Paraná, Mailbox (Caixa Postal) 19046, Curitiba- PR, CEP 81531-980, Brazil. Tel.: +55 (41) 3361-1655; Fax: +55 (41) 3266-2042; e-mail: iacomini@ufpr.br

Abstract

(1→3), (1→6)-β-D-glucans derived from mushrooms are widely recognized for their biological properties, with their physicochemical characteristics playing a crucial role in determining the biological responses. In this study, two different (1→3),(1→6)-β-D-glucans were purified (graded ethanolic precipitation and dialysis) from an alkaline extract of the *Lactarius quieticolor* mushroom and presented distinct chemical structures. Chemical characterization through NMR, GC-MS, and HPSEC-RI revealed that both fractions, Glc-EtPp and GlcEtSn-300, possess a main chain (1→3)-linked, substituted at the *O*-6 position. However, they differ in their degree of substitution, with values of 21.4% and 70.6%, respectively, and side chain composition. The GlcEtSn-300 fraction has extensive (1→6)-linked side chains, whereas GlcEt-Pp is solely substituted by terminal *t*-Glc*p*-(→ units. Notably, the GlcEtSn-300 fraction was identified as a previously unreported polysaccharide, adding novelty to the study. Given the significant differences between both fractions, we sought to investigate and compare their anticancer activities. Remarkably, both glucans reduced the viability of MDA-MB-231 breast cancer cells, but only the GlcEtSn-300 fraction exhibited a selective effect, showing low toxicity in HB4a cells even at high concentrations (1.200 µg. mL^{-1}). In addition, the highly substituted glucan effectively inhibited cancer cell migration, suggesting potential antimetastatic properties. These findings highlight a combination of selective cytotoxicity and the ability to prevent cancer progression, underscoring the therapeutic potential of GlcEtSn-300.

Keywords: *Lactarius quieticolor*; (1→3),(1→6)-β-D-glucan; Breast cancer.

Graphical Abstract

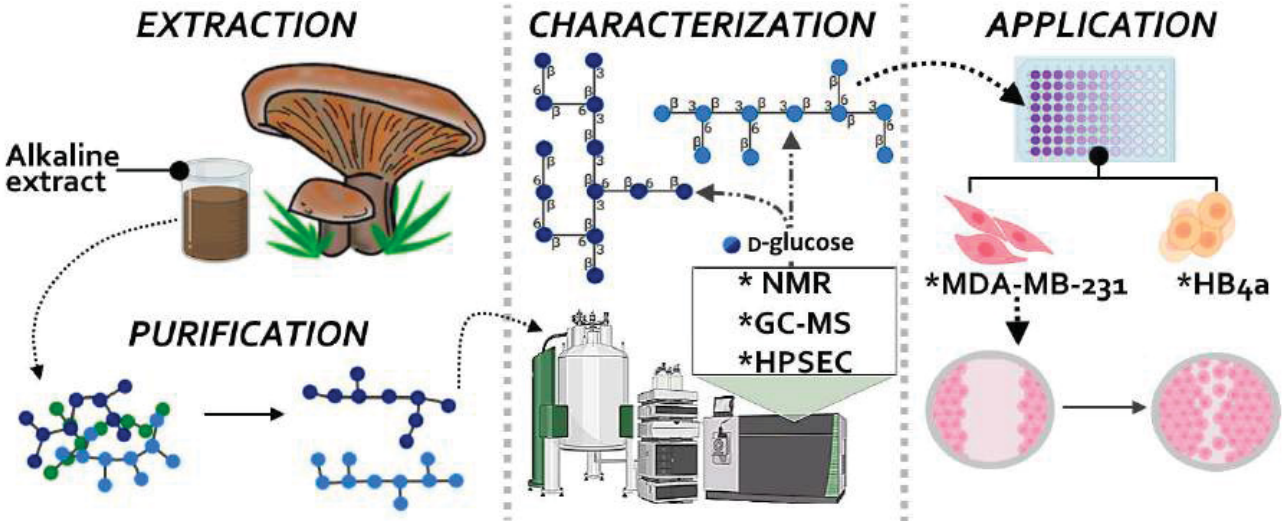

1. Introduction

Mushrooms, particularly those from the Ascomycota and Basidiomycota phyla, play a significant role in both diet and medicine. Nutritionally, they are valued for their high fiber, carbohydrate, protein, mineral, and vitamin content, coupled with low calories and fat (Lu et al., 2020; Ruthes et al., 2016; Sulieman et al., 2019). Medically, mushroom extracts are prized for their diverse biological activities, including anti-inflammatory, antitumor, neuroprotective, and cytoprotective properties (Mizuno & Minato, 2024; S. Zhang et al., 2022). This combination of nutritional and medicinal benefits underscores the importance of mushrooms, where said properties are attributed to their content of amino acids, fatty acids, phenols, and polysaccharides.

The extraction of said polysaccharides employs various methodologies, commonly starting with the use of organic solvents to remove nonpolar compounds, followed by aqueous extraction, both at low and elevated temperatures. Alkaline extraction using varying amounts of KOH or NaOH is also utilized (Leong et al., 2021; Rodrigues Barbosa et al., 2020). The purification of these polysaccharides is achieved through methods such as ethanol precipitation, dialysis with semipermeable membranes, ultrafiltration, freezing and thawing, and reaction with Fehling's solution, among others. Less conventional methods, like graded ethanol precipitation, are also employed (Ruthes et al., 2015).

Mushroom polysaccharides, particularly glucans, are notable for their significant health benefits and diverse biological activities. Glucans, primarily β-glucans, are complex carbohydrates found in the cell walls of mushrooms and are distinguished by their β-(1→3) and β-(1→6) glycosidic bonds (Pérez-Bassart et al., 2023; Reddy Shetty et al., 2021). These natural compounds have garnered attention for displaying effects such as anti-clonogenic effect on B16-F10 melanoma cells (Zavadinack et al., 2021); cytotoxicity against HepG2 hepatocellular and colorectal (HT-29 and SW-480) carcinoma cells (Liu et al., 2023; Pires et al., 2013). Additionally, β-glucans can complement conventional cancer treatments like chemotherapy and radiation therapy by reducing their side effects and enhancing their efficacy, as observed with mushroom glucans from *A. bisporus* glucans synergizing with doxorubicin against breast cancer (Rutckeviski et al., 2022), allowing mushroom polysaccharides to be employed in adjunct therapies for cancer treatment (Cognigni et al., 2021; Steimbach et al., 2021).

Moreover, glucans exhibit antioxidant, antinociceptive and anti-inflammatory effects, making them valuable in both traditional and modern medical applications (da Silva Milhorini et al., 2022b; Ruthes et al., 2013). Therefore, this study aimed to extract and purify glucans from *Lactarius quieticolor* mushrooms, a species recently reported in South America whose polysaccharides remain uncharacterized. The research also assessed the potential effects of these glucans against the triple

116 negative subtype MDA-MB-231 human breast cancer cell line, as cancer remains the second leading
117 cause of death globally (World Health Organization, 2024), with breast cancer being among the most
118 frequently diagnosed types. Of all breast cancer cases, approximately 10-15% are classified as the
119 triple-negative subtype, which is typically associated with poorly differentiated tumor cells, meaning
120 the cancer cells appear more abnormal and tend to grow faster (Grosse et al., 2024). Furthermore,
121 triple-negative breast cancer (TNBC) is recognized as the most aggressive of all breast cancer
122 subtypes (Mazzeo et al., 2024). Given the growing interest in natural compounds from mushrooms
123 for their therapeutic properties, particularly in cancer treatment, this investigation fills a critical gap
124 in understanding the bioactive components of *L. quieticolor.*
125

126 **2. Material and methods**

127 **2.1. Biological material and general extraction**

128 The crude alkaline extract was obtained, and the mushroom was identified by Zavadinack, de Lima
129 Bellan, et al. (2024). Based on morphological and molecular aspects, the mushroom was classified as
130 *Lactarius quieticolor*. After extraction, the crude alkaline extract was neutralized with acetic acid,
131 dialyzed using 6-8 kDa membranes for 48 hours, and then freeze-dried, resulting in the fraction AE.

132 **2.2. Purification procedures**

133 The alkaline extract underwent freeze-thaw cycles (Gorin & Iacomini, 1984) followed by
134 centrifugation (10 min, 8,000 rpm), yielding the cold-water soluble fraction, named EAS. This fraction
135 was treated enzymatically with α-amylase (48 h, 40 °C) to remove glycogen, then precipitated with
136 ethanol (3:1, v/v) and dialyzed (48 h, using 6-8 kDa membranes). After freeze-drying, the sample
137 underwent Fehling solution treatment (Jones & Stoodley, 1965), resulting in two fractions. The Cu^{2+}-
138 complexed polysaccharide precipitate was recovered by centrifugation (15 min, 8,000 rpm), while the
139 Cu^{2+}-uncomplexed polysaccharides remained in the supernatant. Both fractions were neutralized with
140 acetic acid, deionized with ion exchange resin, dialyzed (48 h, 6-8 kDa membranes), and freeze-dried.
141 The soluble fraction underwent a second Fehling treatment, yielding the Glc-Feh fraction and a
142 negligible amount of precipitated. After freeze-drying, the Glc-Feh fraction was further purified
143 through graded ethanol precipitation (Peng et al., 2009). The dried sample was dissolved in water at
144 approx. 5.70 mg. mL^{-1} and ethanol was gradually added until a final concentration of 41% was
145 reached. The resulting precipitate, named GlcEt-Pp, and the supernatant were separated by
146 centrifugation (15 min, 8,000 rpm) and freeze-dried. Subsequently, the supernatant was further

147 purified by dialysis (300 kDa membrane, 6 hours), and the eluted fraction was recovered and freeze-
148 dried, yielding the GlcEtSn-300 fraction.

149 **2.3. Characterization**

150 **2.3.1. Monosaccharide composition**

151 The samples (2 mg) were hydrolyzed using 2 M trifluoroacetic acid (TFA) for 8 h at 100 °C. The
152 acid was evaporated, and the material was dissolved in water and treated with $NaBH_4$. The resulting
153 hydrolysates were acetylated with pyridine-acetic anhydride (1:1 v/v; 30 min, 100 °C). Then, the
154 resulting alditol acetates formed were extracted with chloroform and analyzed using a Varian®
155 CP3800 gas chromatograph coupled to an Ion-Trap 4000 mass spectrometer with a VF-5ms capillary
156 column held at 90 to 320 °C with Helium as carrier gas (1 mL/min). The monosaccharides were
157 identified by their retention times and their electron impact breakdown profiles were compared to
158 standards.

159 **2.3.2. Nuclear Magnetic Resonance Spectroscopy (NMR)**

160 NMR analyses were carried out on a Bruker™ Avance III HD 400 MHz and Bruker™ Avance III
161 600 MHz spectrometers. The samples (15-30 mg) were dissolved in 500 mL of deuterated dimethyl
162 sulfoxide (Me_2SO-d_6) and transferred to 5 mm NMR tubes and the analyses conducted at 70 °C. The
163 chemical shifts are expressed in δ (ppm) relative to signals from Me_2SO-d_6 at δ 39.7 and δ 2.5 for ^{13}C
164 and ^{1}H, respectively.

165 **2.3.3. Determination of homogeneity and relative molecular weight**

166 Relative M_w and homogeneity were performed by high performance steric exclusion
167 chromatography (HPSEC, Waters™ 2410 differential refractometer) employing a refractive index
168 detector and a series of four Waters™ Ultrahydrogel columns (2000, 500, 250 and 120 Å). The eluent
169 was sodium nitrite ($NaNO_3$, 0.1 M) with sodium azide (NaN_3, 0.5 g/L). The samples were dissolved
170 in the eluent (1 mg/mL) and filtered through a 0.22 mm Millipore® membrane prior to the injection).
171 A curve of dextran standards (487, 266, 124, 72.2, 40.2, 17.2 and 9.40 kDa) was utilized for the
172 determination of the samples' relative M_w.

173

174

175 **2.4. Biological activity**

176 **2.4.1. Cell cultures**

177 Normal-like breast cell line, HB4a (Stamps et al., 1994) and triple-negative breast cancer cell line
178 MDA-MB-231 were acquired by American Type Culture Collection (ATCC). The cells were
179 cultivated in RPMI 1640 medium (Gibco), supplemented with 10% fetal bovine serum and incubated
180 at 5% of CO_2 at 37 °C in a humidified atmosphere (85-95%).

181 **2.4.2. Cell viability assays**

182 Both cell lines were retrieved from the stock and detached using trypsin-EDTA. Following
183 detachment, the cells were resuspended and counted, being then plated at 100 µL per well in a 96-
184 well plate, achieving a density of 5,000 cells per well. The plate was incubated at 37 °C in a humidified
185 atmosphere with 5% CO_2 for 2 hours to allow for cell adhesion. Following this incubation, in the
186 control wells, 100 µL of medium containing the same DMSO volume used in different glucans
187 concentrations, was added. For glucans treatment 100 µL of glucan solutions (solved in water and
188 DMSO 1:1) at concentrations of 200, 400, 600, and 1200 µg. mL^{-1} were added for treatment. After a
189 24-hour incubation, the supernatant was removed, and 0.5 mg/mL of MTT (3-(4,5-dimethylthiazol-2-
190 yl)-2,5-diphenyltetrazolium bromide) was added to each well. Following further incubation, 100 µL
191 of DMSO was then added to solubilize any formazan crystals formed. Finally, the absorbance at 570
192 nm was measured using a spectrophotometer (Synergy HT, Biotek microplate reader), and cell
193 viability was calculated as a percentage relative to the control wells.

194 **2.4.3. Cell migration assays (Scratch wound healing)**

195 MDA-MB-231 cancer cells were cultured in 6-well plates until they reached full confluence. A
196 straight scratch was made in the monolayer of each well using a sterile pipette tip, creating an artificial
197 wound. The wells were then treated with glucan samples, while control wells were left untreated.
198 Images of the wound area were captured at a 10x magnification at the beginning of the experiment
199 and after 24 hours of incubation. The extent of cell migration into the wound area was measured and
200 quantified by ImageJ software and wound healing expressed as a percentage of the area closed relative
201 to the control wells.
202

203 **3. Results and discussion**

204 **3.1. Purification and structural characterization of the β-D-Glucans**

The alkaline extract from the *Lactarius quieticolor* mushroom was submitted to purification processes, as demonstrated in Figure 1.

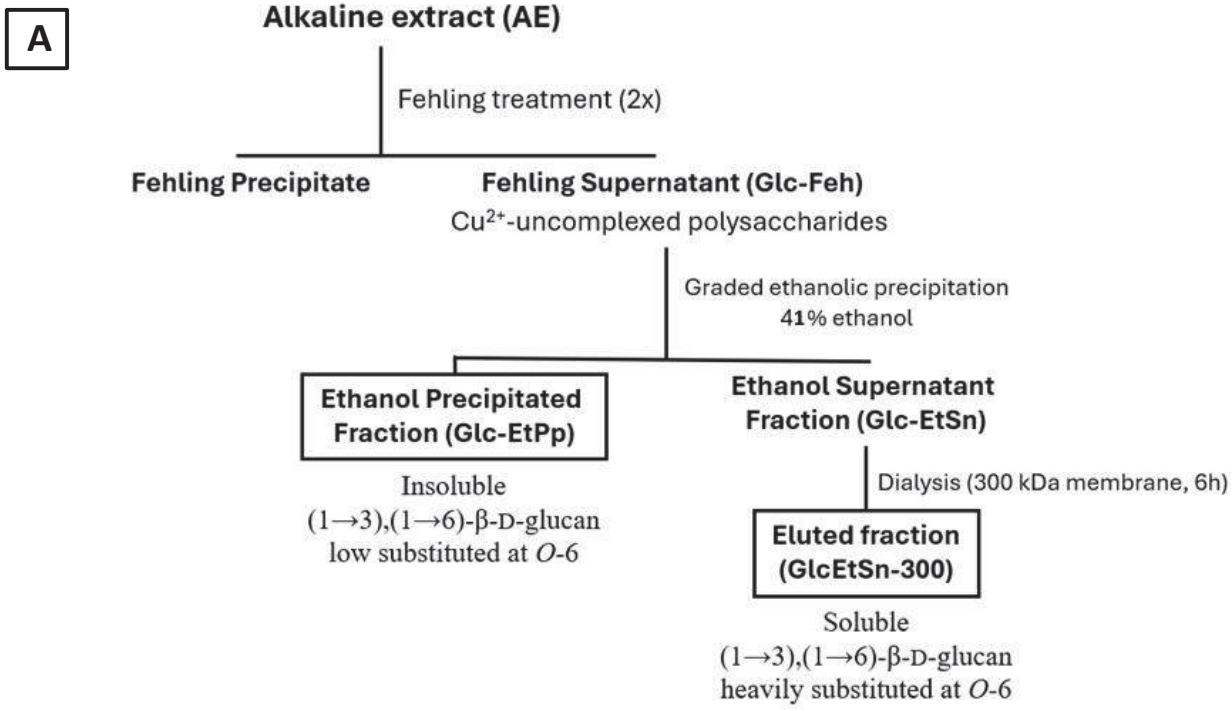

Figure 1. Flowchart summarizing the purification procedures applied in the *Lactarius quieticolor* mushroom crude alkaline extract in order to obtain the insoluble and low substituted (1→3), (1→6)-β-D-glucan Glc-EtPp and the soluble and heavily substituted (1→3), (1→6)-β-D-glucan GlcEtSn-300.

The alkaline extract was analyzed through HSQC-NMR (Suppl. Fig. 1) and exhibited various anomeric signals, indicating the presence of different polysaccharides. Additionally, monosaccharide composition analysis showed the presence of glucose and galactose, and small amounts mannose and fucose (Glc*p*>Gal*p*>Fuc*p*>Man*p*), as represented in the Suppl. Fig. 2. As the signals observed in HSQC spectrum was characteristics from β-D-Glucans, the sample was submitted to purification through Fehling Solution treatments two times to obtain total purification, as described by Jones and Stoodley (1965) and adapted by Zavadinack et al. (2021). D-Glucans, common mushroom-derived polysaccharides, are expected to remain in the Fehling supernatant because the copper ions (Cu^{2+}) in the copper sulfate solution do not complex with the hydroxyl groups present in these molecules, which occur especially with heteropolysaccharides (da Silva Milhorini et al., 2022a; Vaz da Luz et al., 2024). This lack of interaction allows D-Glucans to stay soluble, separating them from other polysaccharides that may precipitate during the Fehling treatment. In fact, after Fehling treatments, the supernatant fraction Glc-Feh (Cu^{2+}-uncomplexed polysaccharides, Figure 2A), presented only glucose in its

composition (Suppl. Fig. 2), and displays only anomeric signals characteristics from β-D-Glucans at δ 102.6/4.56, δ 102.7/4.36, δ 103.5/4.40, and δ102.6/4.26, usually described as the →3)-Glc*p*-(1→, →3,6)-Glc*p*-(1→, *t*-)-Glc*p*-(1→, and →6)-Glc*p*-(1→ units, respectively (Zavadinack, de Lima Bellan, et al., 2024).

Despite the similarities with (1→3), (1→6)-β-D-glucans previously described, the lack of homogeneity observed in the HPSEC analysis (Suppl. Fig. 3), and the presence of a signal at δ 86.7/3.45 and duplicated C-6 linked (-CH_2) signals at δ 68.0/4.08, δ 68.0/4.01, δ 68.0/3.62, and δ 68.0/4.56, prompted us to continue the purification process. Normally, the β1→3 linkage is observed as an intense signal at δ 86.0/3.50, accompanied by a low-intensity signal at the same carbon (δ 86.0/3.33), as described by (Zavadinack, Cantu-Jungles, et al., 2024), corresponding to the C-3/H-3 linked in →3)-Glc*p*-(1→ and →3,6)-Glc*p*-(1→ units, respectively. However, this signal is not always detected, as the degree of substitution can vary among molecules (H. Zhang et al., 2022), and the sensitivity of the NMR experiment is limited (Webb, 2012). For C6-linked units, it is expected to observe distinct signals for the same carbon at δ 68.0/4.00 and δ 68.0/3.55, rather than four signals. This is because the signals for →3,6)-Glc*p*-(1→ and →6)-Glc*p*-(1→ units typically overlap, and are usually detected as two distinct peaks – one for each hydrogen in the -CH_2 group - corresponding to the C6-linked carbon (Gao et al., 2023; Lowman et al., 2011). The presence of four signals suggests either structural complexity or a mixture of molecules with different conformational states. Hence, we performed a new purification step on the Glc-Feh fraction through graded ethanol precipitation, as reported by Yang et al. (2024) and Ruthes et al. (2015). This approach resulted in two new fractions, the supernatant ethanolic fraction, named Glc-EtSn, and the precipitated ethanolic fraction, named Glc-EtPp. As the β-D-glucan in the ethanolic supernatant theoretically has a low molecular weight, we further purified this fraction using dialysis with a 300 kDa membrane to ensure that no high-mass molecules remained in this fraction. The eluted fraction, named GlcEtSn-300, as well as the ethanolic precipitated fraction, Glc-EtPp, were subjected to chemical characterization.

3.2 Chemical characterization of the GlcEtSn-300 and Glc-EtPp fractions

Both samples were submitted to chemical characterization by NMR (^{1}H, ^{13}C and HSQC-DEPT, and COSY), GC-MS, and HPSEC-RI analyzes. Additionally, sugar and protein content were evaluated, which shows exclusively carbohydrates in both fractions. The distinct HPSEC peak patterns in each fraction allowed for molecular mass estimation, with GlcEtSn-300 presenting an estimated mass of 8.85 x 10^3 g.mol^{-1} while the GlcEt-Pp presented a mass of 2.92 x 10^3 g.mol^{-1}. The

NMR spectrum of the GlcEt-Pp fraction, shown in Figure 2B, revealed two distinct anomeric signals at δ 102.6/4.56 and δ 102.6/4.26, belonging to 3-*O*-substituted glucose and 6-*O*-substituted units, respectively. These findings are further supported by the presence of signals indicating Glc*p*β1→3Glc*p* linkages at δ 86.0/3.50 (C-3/H-3) and Glc*p*β1→6Glc*p* linkages at δ 68.0/4.10; 3.55 (C-6/H-6) (Ruthes et al., 2013) suggesting that the GlcEt-Pp fraction has a main chain predominantly composed of (1→3)-glycosidic linkages, with branches at *O*-6. The absence of signals around δ 102.5/4.36 and δ 103.5/4.40 in the HSQC-DEPT spectrum may indicate a (1→3), (1→6)-β-D-glucan with low branching, substituted by non-reducing end terminals of Glc*p* units. These signals are typically attributed to →3,6)-Glc*p*-(1→ and *t*-Glc*p*-(1→ units, respectively, in (1→3), (1→6)-β-D-glucans with (1→6)-linked side chains (Lowman et al., 2011; Tondolo et al., 2017). However, there are several assignments that seem inconsistent for these units (Abreu et al., 2021; Cantu-Jungles et al., 2018; Lowman et al., 2011; Oliveira et al., 2015), which, based on our experience, can be attributed to the presence or absence of (1→6)-linked side chains. This variability often leads to uncertainties during the chemical characterization process of (1→3), (1→6)-β-D-glucans, causing authors to assign the signals of each unit present in glucans to regions that may not always correspond accurately. Another hypothesis for the absence of these signals in certain HSQC spectrum is the sensitivity of the NMR equipment used. Therefore, to ensure more accurate assignments, it is essential to verify the presence or absence of signals in the region between δ 4.56 and δ 4.26 ppm in the ^{1}H spectra. In fact, the GlcEt-Pp (1→3), (1→6)-β-D-Glucan does not present signals in these regions (Suppl. Fig 4), suggesting that variations in chemical structure and branching type can induce significant chemical shifts. These shifts may cause the overlapping of signals corresponding to the *t*-Glc*p*-(1→ and →3,6)-Glc*p*-(1→ units, complicating their precise identification. This highlights the importance of considering branching patterns and chemical structure differences when interpreting NMR spectra for accurate characterization of glucans.

In contrast, the GlcEtSn-300 fraction exhibited significant differences in HSQC-DEPT NMR experiment (Fig. 2C). It is possible to observe intense signals at δ 102.7/4.36 and δ 103.5/4.40, indicating the presence of 3,6-di-*O*-substituted units as well as non-reducing end terminals of β-D-Glucose, respectively (Lowman et al., 2011; Zavadinack, de Lima Bellan, et al., 2024). Additionally, the signals at δ 102.6/4.56 and δ 102.6/4.26, also present in GlcEt-Pp fraction, indicate the presence of →3)-Glc*p*-(1→ and →6)-Glc*p*-(1→ units, respectively (Zavadinack, Cantu-Jungles, et al., 2024). Despite some similarities in the observed anomeric signals, it is evident that the analyzed fractions possess distinct molecular arrangement. This becomes particularly clear when examining the

superimposed spectrum of the GlcEt-Pp and GlcEtSn-300 samples (Fig. 2D), where subtle differences in chemical shifts and intensities can be observed. The signals at δ 86.0/3.50 and δ 86.7/3.45, previously observed at the same spectrum (Fig. 2A), can now be observed as signals belonging to different molecules. Additionally, the four C-6 linked signals (Fig. 2A) were also separated (Fig. 2B and C). Other signals, such as δ 74.5/3.52, δ 75.0/3.41, and δ 73.5/3.10, marked in the Figure 2D, emphasize the differences between the spectra.

Correlational spectroscopy studies were also performed (COSY, Fig. 3). For the GlcEt-Pp fraction (Fig. 3A), only two distinct H-1/H-2 correlations were observed for the anomeric signals at δ 4.56/3.34 and δ 4.26/3.03, which indicate that the H-2 of →3,6)-Glc*p*-(1→ and →3)-Glc*p*-(1→ are overlapping. According to Smiderle et al. (2008), only H-5 and H-6 differ significantly for these units. Furthermore, NMR studies conducted by H. Zhang et al. (2022) showed similar results to those observed for the GlcEt-Pp fraction. For the GlcEtSn-300 fraction (Fig. 3B), four distinct H-1/H-2 correlations were observed at δ 4.56/3.34, δ 4.40/3.14, δ 4.36/3.26 and δ 4.26/3.05 for the →3)-Glc*p*-(1→ and t-Glc*p*-(1→ →3,6)-Glc*p*-(1→ and →6)-Glc*p*-(1→ units, respectively. These signals agree with the assignments indicated by Lowman et al. (2011) and Tondolo et al. (2017).

To confirm the results described above and gain further insights into the chemical structures of GlcEt-Pp and GlcEtSn-300, we integrated the anomeric peaks (Fig. 4). The values obtained (Table 1) indicate that the GlcEt-Pp fraction (Fig. 4A) has a (1→3)-linked main chain, with half of its main-chain units substituted at *O*-6 by non-reducing terminal units. Through HSQC-NMR, however, only two signals (δ 102.6/4.56 and δ 102.6/4.26, representing 66.0% and 34.0%, respectively) could be integrated due to the overlap of the →3)-Glc*p*-(1→ and →3,6)-Glc*p*-(1→ signals. Since the →3,6)-Glc*p*-(1→ and *t*-Glc*p*-(1→ should theoretically have an equivalent ratio, we hypothesized that the measured value for *t*-Glc*p*-(1→ (34.0%) should correspond to that of the →3,6)-Glc*p*-(1→ units (Table 1). To confirm these values, we performed anomeric ^{1}H-NMR integration (Suppl. Fig. 4). The results were very similar to those observed in the HSQC-NMR analysis described above (Table 1).

For the GlcEtSn-300 the HSQC-integrated values (Fig. 4B) show that this molecule has a main chain (1→3)-linked highly substituted at the C-6 position by *t*-Glc*p*-(1→ and →6)-Glc*p*-(1→ units. This is due to the high and equal area values obtained for the →3,6)-Glc*p*-(1→ and *t*-Glc*p*-(1→ units (29.6% and 28.9%, respectively), while a notably low value was observed for the →3)-Glc*p*-(1→ unit (12.3%). The presence of long (1→6)-linked side chains was also confirmed by the high percentage of →6)-Glc*p*-(1→ units (29.2%). Additionally, an equivalent relationship (1:1) was identified between the values obtained for the sum of the →3,6)-Glc*p*-(1→ and →3)-Glc*p*-(1→ with the signal

at δ 86.7/3.45, which corresponds to the C-3/H-3 linked. This relationship reinforces the hypothesis regarding their chemical arrangement (Suppl. Fig. 5).

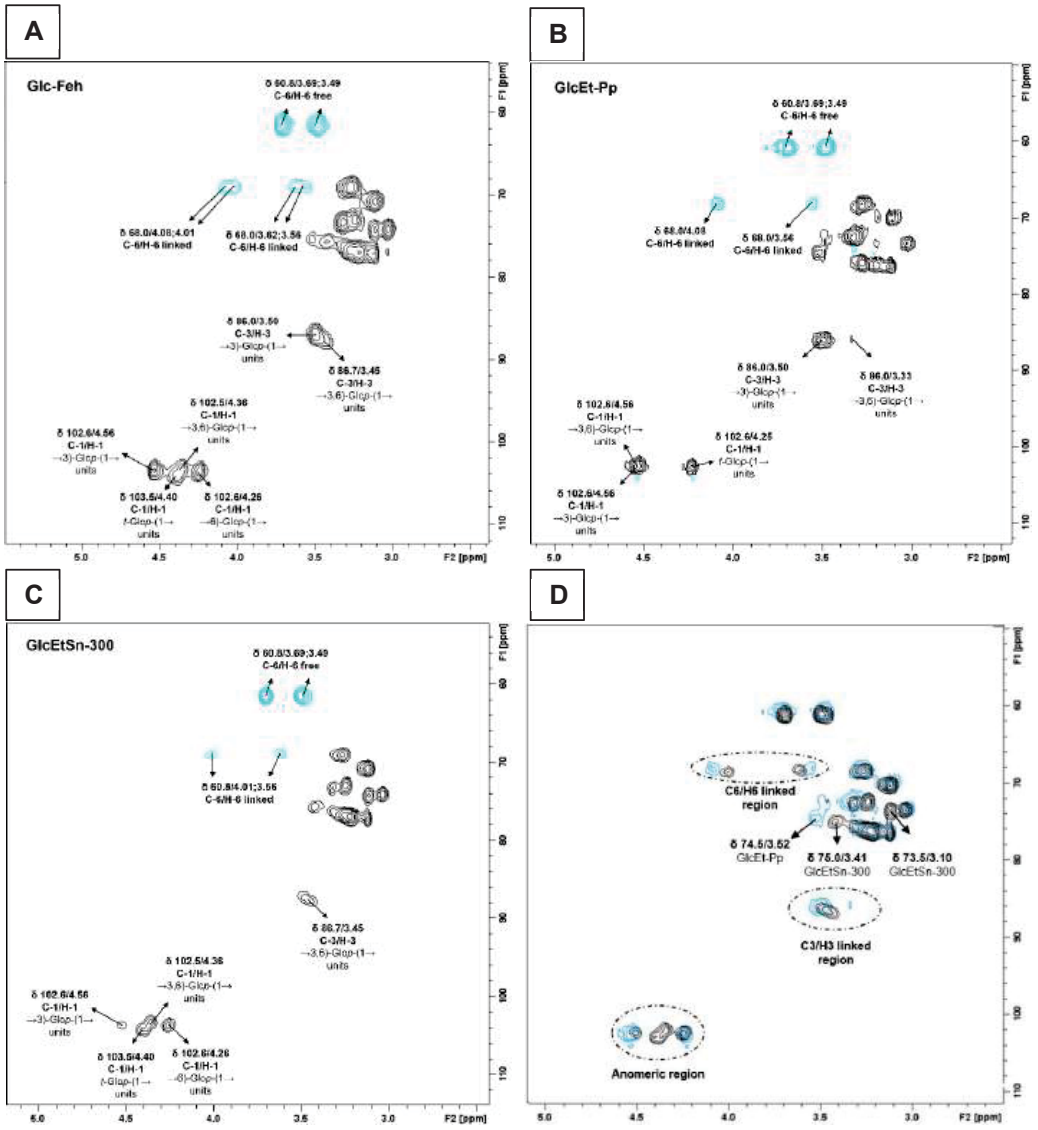

Figure 2. HSQC-NMR studies of the Glc-Feh, GlcEt-Pp and the GlcEtSn-300 fractions. (A); HSQC-DEPT spectrum of the Glc-Feh fraction; **(B)** HSQC-DEPT spectrum of the GlcEt-Pp fraction; **(C)** HSQC-DEPT spectrum of the GlcEtSn-300 fraction; **(D)** Superimposed HSQC spectrum of the GlcEt-Pp (in blue) and GlcEtSn-300 (in black) fractions. The samples were analyzed in Me_2SO-d_6 (calibration parameters: δ 2.50) at 70°C and the results are expressed in ppm (δ).

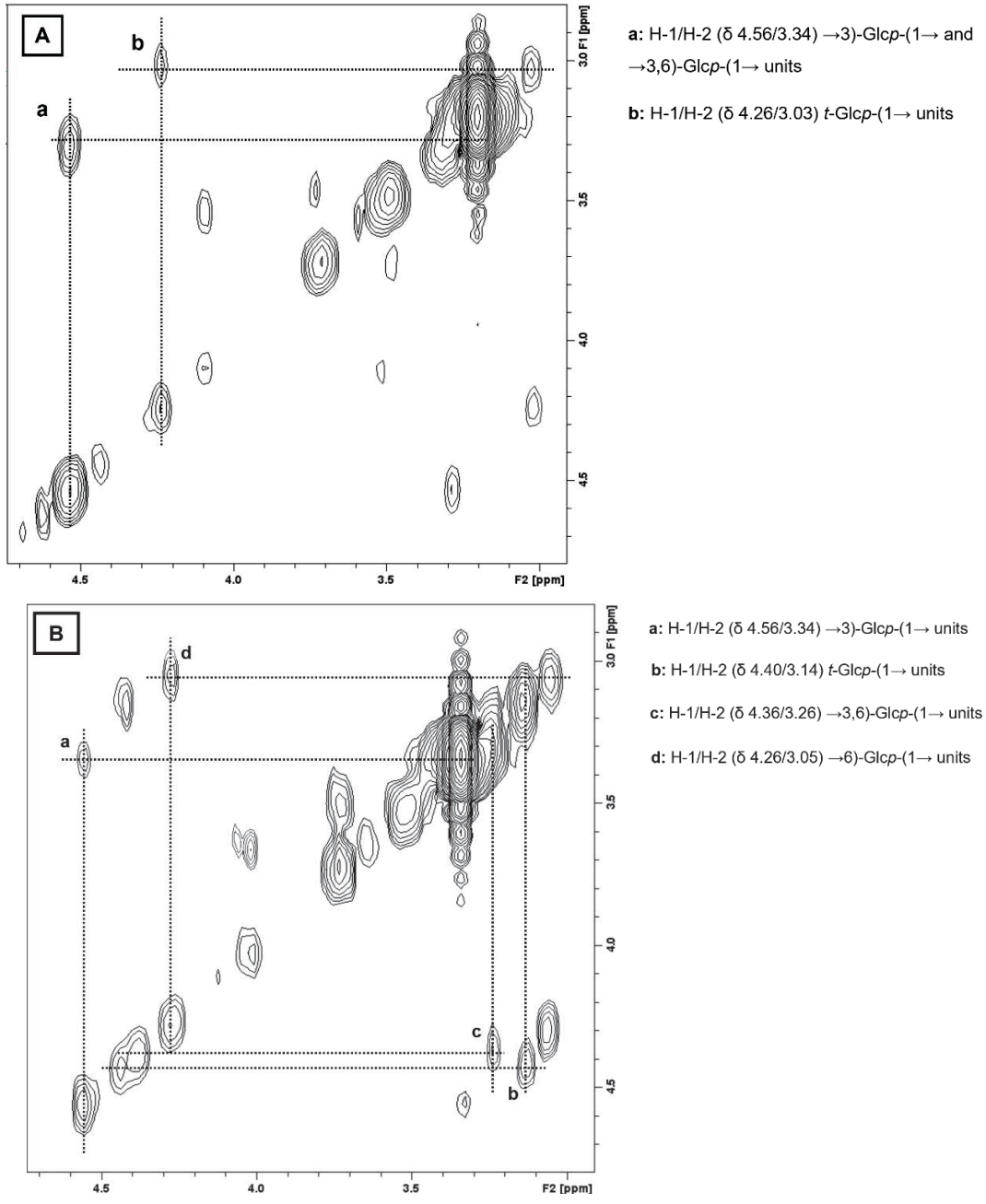

Figure 3. 2D-NMR studies of the GlcEt-Pp and GlcEtSn-300 fractions. (A) COSY spectrum from GlcEt-Pp fractions; **(B)** COSY spectrum from GlcEtSn-300 fraction. The sample was analyzed in Me_2SO-d_6 (calibration parameters: δ 2.50) at 70°C and the results are expressed in ppm (δ).

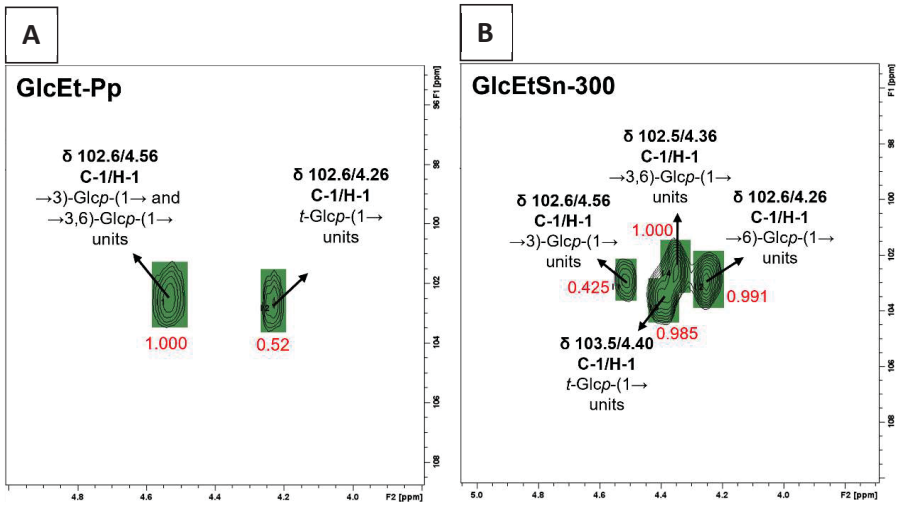

332

333 **Figure 4. HSQC-NMR of the GlcEt-Pp and the GlcEtSn-300 fractions. (A)** GlcEt-Pp fraction; **(B)** GlcEtSn-
334 300 fraction. The integrated values (highlighted in red) correspond to the areas marked in green on the anomeric
335 signals obtained through the HSQC-NMR spectra. The samples were analyzed in Me_2SO-d_6 (calibration
336 parameters: δ 2.50) at 70°C and the results are expressed in ppm (δ). The analysis and peak assignments were
337 performed using TopSpin software, version 3.6.5.

338 **Table 1. Integrated values[a] obtained through HSQC-spectra from GlcEt-Pp and GlcEtSn-300 fractions.**

Unit	C/H and signal (δ)	Integrated area[a]		Relative Area (%)		References[b]
GlcEtSn-300		HSQC		HSQC		
→3)-Glc*p*-(1→	C1/H1 102.6/4.56	0.425		12.3%		c, d, e,
→6)-Glc*p*-(1→	C1/H1 102.6/4.26	0.991		29.2%		e, f
t-Glc*p*-(1→	C1/H1 103.5/4.40	0.985		28.9%		e, f, g
→3,6)-Glc*p*-(1→	C1/H1 102.5/4.36	1.000		29.6%		e, f
GlcEt-Pp		^{1}H	HSQC	^{1}H	HSQC	
→3)-Glc*p*-(1→	C1/H1 102.6/4.56	1.000	1.000	33.3%	30.0%	c, d
t-Glc*p*-(1→	C1/H1 102.6/4.25	0.247		33.4%	35.0%	c, d
→3,6)-Glc*p*-(1→	C1/H1 102.6/4.27	0.273	0.541	33.3%	35.0%	c, d

339 [a]The analysis and peak assignments were performed using TopSpin software, version 3.6.5;
340 [b]References support signal/unit relationship assignments; [c](Ruthes et al., 2013); [d](Carbonero et al., 2012);
341 [e](Zavadinack, de Lima Bellan, et al., 2024); [f](Lowman et al., 2011); [g](Cantu-Jungles et al., 2018).

342 (1→3), (1→6)-β-D-glucans are widely recognized for their positive biological effects, including
343 immunomodulatory, anti-inflammatory, and anticancer activities (Ruthes et al., 2015). However, their
344 efficacy is closely linked to their physicochemical and chemical characteristics, such as molecular
345 weight, branching pattern, and solubility (Meng et al., 2016). These structural features can influence
346 their interaction with biological systems. Furthermore, the site of action plays a crucial role, as the
347 presence or absence of specific cellular receptors, such as Dectin-1, Toll-like Receptors, or CR3, will
348 guide the type of immune or therapeutic response observed (Meng et al., 2016). This receptor-
349 mediated interaction largely determines how β-D-glucans act as a biological response modifier.

Depending on the receptor engaged, β-D-glucans can trigger pathways that lead to immunostimulant effects (Sahasrabudhe et al., 2016), or direct tumor cell cytotoxicity (Pires et al., 2013). In fact, several studies have explored the interactions between immune cell receptors and β-glucans (Gantner et al., 2003; Goodridge et al., 2011). According to (Zavadinack, Cantu-Jungles, et al., 2024), the presence of 3,6-di-*O*-substituted units is a crucial factor in determining the biological responses, which can lead to immunostimulant or even cytotoxic effects (Pires et al., 2013). However, few studies have attempted to compare (1→3), (1→6)-β-D-glucans with distinct chemical structures simultaneously, aiming to establish a clear structure-function relationship related to their cytotoxic effects on cells.

Due to the presence of distinct physicochemical and chemical characteristics in the GlcEtSn-300 and GlcEt-Pp fractions, particularly the significant difference in the percentages of 3,6-di-*O*-substituted units and (1→6)-linked side chains, we sought to investigate their different antitumor properties *in vitro*. These structural variations could lead to distinct biological responses, influencing their potential therapeutic applications. Therefore, a comparative analysis of their biological activity is crucial to understanding the relationship between structure and function in these β-D-Glucans fractions.

3.2 Biological activity

3.2.1 Viability assay

In the viability assay, the MDA-MB-231 triple-negative breast cancer cell model and a normal-like HB4a (mammary duct immortalized cell line) were used. Results from the assay with the normal-like HB4a cell line showed that the GlcEtSn-300 fraction exhibited minimal cytotoxicity, affecting only around 20% of the cells at the highest concentration tested (1200 μg. mL^{-1}; Figure 5A). In contrast, the assay with MDA-MB-231 cells demonstrated a dose-dependent cytotoxic effect, with cell viability reduced to 40% at the highest concentration (Figure 5B). These differences indicate that the GlcEtSn-300 fraction exhibits a selective cytotoxic effect, which may be linked to the presence or overexpression of specific cellular receptors in tumor cells (Ferreira et al., 2021). This selective interaction suggests that the soluble and high *O*-6 substituted glucan (GlcEtSn-300) could preferentially target pathways that are more active in cancer cells, thereby reducing their viability while sparing normal-like cells. In fact, it was already demonstrated that some cellular receptors are overexpressed in tumor cells. Feigin et al. (2014) demonstrated through genomic analysis that the G protein-coupled receptor 161 (GPR161) is overexpressed in triple-negative breast cancer (TNBC) cells, correlating with poor prognosis, particularly by promoting increased cell proliferation and

migration. According to Raj et al. (2024), several cell-specific proteins are overexpressed in TNBC, including Intercellular Adhesion Molecule 1 (ICAM-1), αVβ3 integrin, Transmembrane Glycoprotein Mucin 1 (MUC-1), Glucose Transporter 5 (GLUT5), and Epidermal Growth Factor Receptor (EGFR). These proteins could serve as targets for specific ligands through ligand-receptor interactions for therapeutic purposes.

In contrast, the GlcEt-Pp fraction displayed cytotoxic effects in both MDA-MB-231 and HB4a cell lines (Fig. 5C and D), suggesting that its cytotoxicity may operate through mechanisms different from those of GlcEtSn-300. This broader cytotoxic activity indicates that the insoluble glucan (GlcEt-Pp) may act via less selective pathways, affecting both tumor and normal-like cells similarly. Similar results were reported by Pires et al. (2013), who compared the anticancer activities of a (1→6)-β-D-glucan and a (1→3), (1→6)-β-D-glucan. The findings indicate that the *O*-6 substituted glucan exhibited higher cytotoxic effects on hepatocellular carcinoma cells (HepG2) but also affected primary hepatocytes, whereas the linear polysaccharide showed cytotoxicity exclusively towards HepG2 cells, suggesting cell selectivity. Therefore, we understand that the presence of (1→6)-linked side chains may be a key factor in determining selective cytotoxicity in (1→3), (1→6)-β-D-glucans.

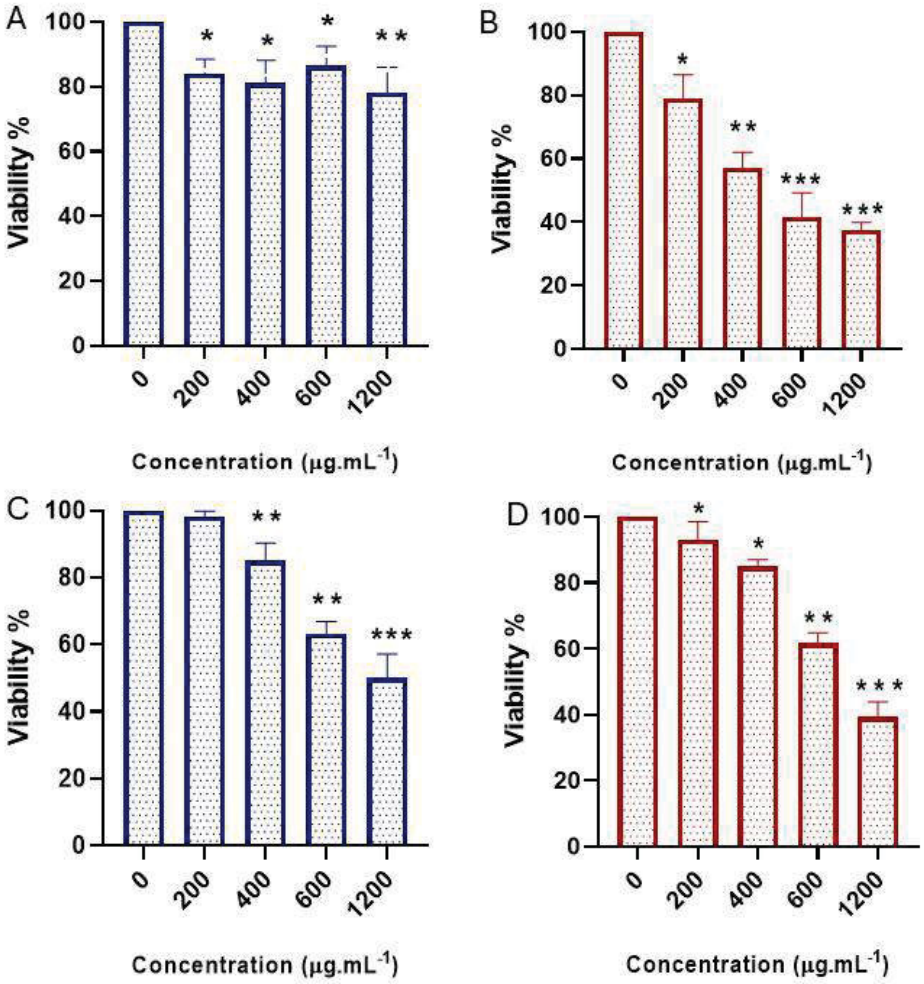

Figure 5. Viability assay of breast cell lines after treatment with the GlcEtSn-300 and GlcEt-Pp glucans. **(A)** HB4a and **(B)** MDA-MB-231 cells treated with GlcEtSn-300; **(C)** HB4a and **(D)** MDA-MB-231 cells treated with GlcEt-Pp. These results represent the set of at least three independent experiments. The data were plotted as mean ± SD and statistical analyses were indexed as * *p< 0,05, ***<0,01 ***<0,001.* The asterisks are relative to the mock group (0).

For the cell migration assays, we initially used a concentration of 800 µg. mL^{-1} for both samples. However, no effect was observed. Therefore, we repeated the assays at a concentration of 1.200 µg. mL^{-1} for both fractions. Even at higher concentrations, no effects were observed (data not shown) for the GlcEt-Pp fraction. In contrast, the use of 1200 µg. mL^{-1} of the GlcEtSn-300 fraction reduced the migration of the MDA-MB-231 breast cancer cell line by almost 60% (Figure 6), indicating that this fraction also has antimetastatic properties.

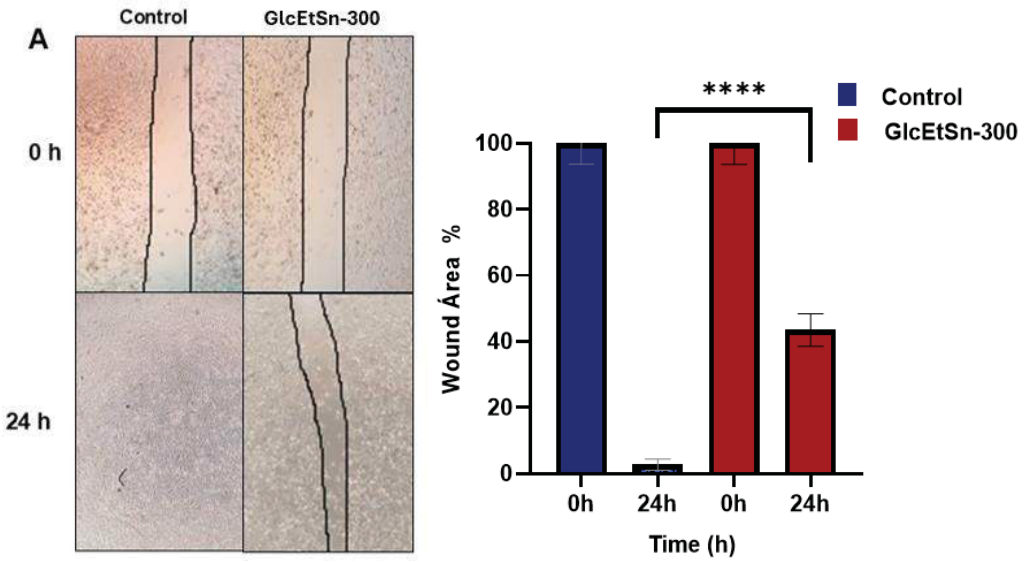

Figure 6. GlcEtSn-300 inhibits migration ability of MDA-MB-231 breast cancer cell line. (A) Optical micrography images (x10 magnification) of the wounded area at 0 and 24 h. **(B)** Wounded area measurement for control (blue) and GlcEtSn-300 (red). These results represent the set of at least three independent experiments. The data were plotted as mean ± SD and statistical analyses were indexed as ****$p<0.0001$. The asterisks are relative to the mock group (control).

Some studies exhibited similar results. Chatnarin and Thirabunyanon (2024) reported the isolation of a β-glucan from the parasitic fungus *Ophiocordyceps sinensis*, which not only reduced the viability of HepG2 liver cancer cells but also inhibited their migration. Lentinan and schizophyllan, two well-established β-glucans with (1→3)-linked backbones and varying ratios and distributions of (1→6)-linked side chains, have demonstrated antitumor effects by reducing cell viability and migration, as shown by (Randeni & Xu, 2024)). The structural similarities between these compounds and their diverse biological effects underscore the potential of β-glucans in cancer therapy

The GlcEtSn-300 fraction demonstrated a selective cytotoxic effect and significant antimetastatic properties by reducing cancer cell viability by 60% and inhibiting the migration of MDA-MB-231 cells. These promising findings highlight the potential of β-D-glucans in cancer therapy and increase interest in their therapeutic applications. They are consistent with growing evidence supporting the anticancer properties of various glucans. For instance, β-glucans derived from mushrooms have shown remarkable therapeutic potential. Shaheen et al. (2022) isolated nano β-Glucans using an acid-base procedure from *Lentinus edodes* and *Pleurotus ostreatus* and demonstrated their antitumor cytotoxic effects in MCF-7 and HCT-116 cells. Zhang et al. (2020) investigated a β-glucan also isolated from *Lentinus edodes*, which inhibited the growth of MCF-7 cells *in vitro* and, *in vivo*, impacted proteins

involved in cell migration, thereby reducing metastatic potential. Similarly, Morales et al. (2020) analyzed (1-6) and (1-3) glucans obtained from the same mushroom, showing selective cytotoxicity by inhibiting MDA-MB-231 cancer cells without affecting normal MCF-10A cells. Furthermore, Yang et al. (2024) reported antitumor effects from a β-(1→3)-glucan isolated from *Lactarius hatsudake*, which inhibited HCT-116 cell growth, further supporting the *Lactarius* genus as a promising source of bioactive polysaccharides for cancer treatment.

Additionaly, Bu et al. (2024) demonstrated that a β-(1→3)-glucan from the *Ganoderma lucidum* mushroom helps reduce tumor growth and mitigates the adverse effects of chemotherapy resistance in breast cancer when co-administered with gemcitabine. These and other reported properties of glucans highlight their potential as therapeutic molecules with versatile biological activities.

4. Conclusion

The structural analysis of the GlcEt-Pp and GlcEtSn-300 fractions revealed distinct chemical characteristics. Despite both being (1→3), (1→6)-β-D-glucans, the GlcEtSn-300 fraction displayed a main chain (1→3)-linked that is highly substituted at the *O*-6 position by (1→6)-linked or non-reducing terminal units of Glc*p*. This extensive substitution differentiates GlcEtSn-300 from GlcEt-Pp and contributes to its unique chemical profile. Given these distinct structural features, we identified GlcEtSn-300 as a previously unreported polysaccharide. Both glucan fractions demonstrated significant cytotoxic effects, but only the GlcEtSn-300 fraction exhibited selective cytotoxicity against MDA-MB-231 breast cancer cells. Additionally, this fraction significantly inhibited the migration of MDA-MB-231 cells, indicating its potential antimetastatic properties, which makes GlcEtSn-300 a promising candidate for targeted breast cancer therapy. Therefore, future studies aiming to elucidate the mechanism of action of this molecule, as well as its detailed physicochemical characteristics, are essential to fully understand its therapeutic potential.

Acknowledgments

This work was supported by the Brazilian funding agencies: Conselho Nacional de Desenvolvimento Científico e Tecnológico (CNPq, Process 403295/2021-1 and 310731/2021-6) and Fundação Coordenação de Aperfeiçoamento de Pessoal de Nível Superior (CAPES, Finance Code 001). The authors are also grateful to the NMR Center of UFPR for recording the NMR spectra.

5. References

Abreu, H., Zavadinack, M., Smiderle, F. R., Cipriani, T. R., Cordeiro, L. M. C., & Iacomini, M. (2021). Polysaccharides from Pleurotus eryngii: Selective extraction methodologies and their modulatory effects on THP-1 macrophages. *Carbohydrate Polymers*, *252*, 117177. https://doi.org/10.1016/j.carbpol.2020.117177

Bu, Y., Liu, Q., Shang, Y., Zhao, Z., Sun, H., Chen, F., Ma, Q., Song, J., Cui, L., Sun, E., Luo, Y., Shu, L., Jing, H., & Tan, X. (2024). Ganoderma lucidum spores-derived particulate β-glucan treatment improves antitumor response by regulating myeloid-derived suppressor cells in triple-negative breast cancer. *International Journal of Biological Macromolecules*, *270*, 131949. https://doi.org/10.1016/j.ijbiomac.2024.131949

Cantu-Jungles, T. M., Ruthes, A. C., El-Hindawy, M., Moreno, R. B., Zhang, X., Cordeiro, L. M. C., Hamaker, B. R., & Iacomini, M. (2018). In vitro fermentation of Cookeina speciosa glucans stimulates the growth of the butyrogenic Clostridium cluster XIVa in a targeted way. *Carbohydrate Polymers*, *183*, 219-229. https://doi.org/10.1016/j.carbpol.2017.12.020

Carbonero, E. R., Ruthes, A. C., Freitas, C. S., Utrilla, P., Gálvez, J., Silva, E. V. d., Sassaki, G. L., Gorin, P. A. J., & Iacomini, M. (2012). Chemical and biological properties of a highly branched β-glucan from edible mushroom Pleurotus sajor-caju. *Carbohydrate Polymers*, *90*(2), 814-819. https://doi.org/10.1016/j.carbpol.2012.06.005

Chatnarin, S., & Thirabunyanon, M. (2024). Potential of β-D-glucan polysaccharide from Ophiocordyceps sinensis OS8 cultivated mycelium on anticancer activity via inducing liver cancer cell death apoptosis. *Process Biochemistry*, *145*, 243-249. https://doi.org/10.1016/j.procbio.2024.07.009

Cognigni, V., Ranallo, N., Tronconi, F., Morgese, F., & Berardi, R. A.-O. (2021). Potential benefit of β-glucans as adjuvant therapy in immuno-oncology: a review. (2692-3114 (Electronic)).

da Silva Milhorini, S., de Lima Bellan, D., Zavadinack, M., Simas, F. F., Smiderle, F. R., de Santana-Filho, A. P., Sassaki, G. L., & Iacomini, M. (2022a). Antimelanoma effect of a fucoxylomannan isolated from Ganoderma lucidum fruiting bodies. *Carbohydrate Polymers*, *294*, 119823. https://doi.org/10.1016/j.carbpol.2022.119823

da Silva Milhorini, S., Simas, F. F., Smiderle, F. R., Inara de Jesus, L., Rosado, F. R., Longoria, E. L., & Iacomini, M. (2022b). β-Glucans from the giant mushroom Macrocybe titans: Chemical characterization and rheological properties. *Food Hydrocolloids*, *125*, 107392. https://doi.org/10.1016/j.foodhyd.2021.107392

Feigin, M. E., Xue, B., Hammell, M. C., & Muthuswamy, S. K. (2014). G-protein–coupled receptor GPR161 is overexpressed in breast cancer and is a promoter of cell proliferation and invasion. *Proceedings of the National Academy of Sciences*, *111*(11), 4191-4196. 10.1073/pnas.1320239111

Ferreira, D., Barbosa, J., Sousa, D. A., Silva, C., Melo, L. D. R., Avci-Adali, M., Wendel, H. P., & Rodrigues, L. R. (2021). Selection of aptamers against triple negative breast cancer cells using high throughput sequencing. *Scientific Reports*, *11*(1), 8614. 10.1038/s41598-021-87998-y

Gantner, B. N., Simmons, R. M., Canavera, S. J., Akira, S., & Underhill, D. M. (2003). Collaborative Induction of Inflammatory Responses by Dectin-1 and Toll-like Receptor 2. *Journal of Experimental Medicine*, *197*(9), 1107-1117. 10.1084/jem.20021787

Gao, W., Zhang, L., Wu, J., Xu, Y., Qi, S., Liu, W., Liu, P., Shi, S., Wang, H., Zhang, Q., Wang, Y., & Wang, S. (2023). Extraction, characterization, and anti-nonalcoholic steatohepatitis activity of a (1,3) (1,6)-β-D-glucan from the Polyporus umbellatus (Pers.) Fries. *International Journal of Biological Macromolecules*, *230*, 123252. https://doi.org/10.1016/j.ijbiomac.2023.123252

Goodridge, H. S., Reyes, C. N., Becker, C. A., Katsumoto, T. R., Ma, J., Wolf, A. J., Bose, N., Chan, A. S. H., Magee, A. S., Danielson, M. E., Weiss, A., Vasilakos, J. P., & Underhill, D. M. (2011). Activation of the innate immune receptor Dectin-1 upon formation of a 'phagocytic synapse'. *Nature*, *472*(7344), 471-475. 10.1038/nature10071

Gorin, P. A. J., & Iacomini, M. (1984). Polysaccharides of the lichens Cetraria islandica and Ramalina usnea. *Carbohydrate Research*, *128*(1), 119-132. https://doi.org/10.1016/0008-6215(84)85090-9

Grosse, C., Noack, P., Grosse, A., Preuss, C. I., Schwarz, H. K., Gitter, T., Schrenk, P., Frauchiger-Heuer, H., Papassotiropoulos, B., Tausch, C., Maccio, U., Moch, H., Langer, R., & Varga, Z. (2024). Prognostic impact of histological subtyping in triple-negative breast cancer. *Human Pathology*, *152*, 105640. https://doi.org/10.1016/j.humpath.2024.105640

Jones, J. K. N., & Stoodley, R. J. (1965). Fractionation using copper complexes. *Methods in carbohydrate chemistry*, *5*, 36-38.

Leong, Y. K., Yang, F.-C., & Chang, J.-S. (2021). Extraction of polysaccharides from edible mushrooms: Emerging technologies and recent advances. *Carbohydrate Polymers*, *251*, 117006. https://doi.org/10.1016/j.carbpol.2020.117006

Liu, N., Zou, S., Xie, C., Meng, Y., & Xu, X. (2023). Effect of the β-glucan from Lentinus edodes on colitis-associated colorectal cancer and gut microbiota. *Carbohydrate Polymers*, *316*, 121069. https://doi.org/10.1016/j.carbpol.2023.121069

Lowman, D. W., West, L. J., Bearden, D. W., Wempe, M. F., Power, T. D., Ensley, H. E., Haynes, K., Williams, D. L., & Kruppa, M. D. (2011). New Insights into the Structure of (1→3,1→6)-β-D-Glucan Side Chains in the Candida glabrata Cell Wall. *PLOS ONE*, *6*(11), e27614. 10.1371/journal.pone.0027614

Lu, H., Lou, H., Hu, J., Liu, Z., & Chen, Q. (2020). Macrofungi: A review of cultivation strategies, bioactivity, and application of mushrooms [https://doi.org/10.1111/1541-4337.12602]. *Comprehensive Reviews in Food Science and Food Safety*, *19*(5), 2333-2356. https://doi.org/10.1111/1541-4337.12602

Mazzeo, R., Sears, J., Palmero, L., Bolzonello, S., Davis, A. A., Gerratana, L., & Puglisi, F. (2024). Liquid biopsy in triple-negative breast cancer: unlocking the potential of precision oncology. *ESMO Open*, *9*(10), 103700. https://doi.org/10.1016/j.esmoop.2024.103700

536 Meng, X., Liang, H., & Luo, L. (2016). Antitumor polysaccharides from mushrooms: a review on the
537 structural characteristics, antitumor mechanisms and immunomodulating activities. *Carbohydrate*
538 *Research*, *424*, 30-41. https://doi.org/10.1016/j.carres.2016.02.008

539 Mizuno, M., & Minato, K.-i. (2024). Anti-inflammatory and immunomodulatory properties of
540 polysaccharides in mushrooms. *Current Opinion in Biotechnology*, *86*, 103076.
541 https://doi.org/10.1016/j.copbio.2024.103076

542 Morales, D., Rutckeviski, R., Villalva, M., Abreu, H., Soler-Rivas, C., Santoyo, S., Iacomini, M., &
543 Smiderle, F. R. (2020). Isolation and comparison of α- and β-D-glucans from shiitake mushrooms
544 (Lentinula edodes) with different biological activities. *Carbohydrate Polymers*, *229*, 115521.
545 https://doi.org/10.1016/j.carbpol.2019.115521

546 Oliveira, K. S. M., Di Bastiani, M., Cordeiro, L. M. C., Costa, M. F., Toledo, K. A., Iacomini, M.,
547 Babosa, A. M., Dekker, R. F. H., & Nascimento, V. M. G. (2015). (1→6)- and (1→3)(1→6)-β-glucans
548 from Lasiodiplodia theobromae MMBJ: Structural characterization and pro-inflammatory activity.
549 *Carbohydrate Polymers*, *133*, 539-546. https://doi.org/10.1016/j.carbpol.2015.07.060

550 Pérez-Bassart, Z., Fabra, M. J., Martínez-Abad, A., & López-Rubio, A. (2023). Compositional
551 differences of β-glucan-rich extracts from three relevant mushrooms obtained through a sequential
552 extraction protocol. *Food Chemistry*, *402*, 134207. https://doi.org/10.1016/j.foodchem.2022.134207

553 Pires, A. d. R. A., Ruthes, A. C., Cadena, S. M. S. C., Acco, A., Gorin, P. A. J., & Iacomini, M. (2013).
554 Cytotoxic effect of Agaricus bisporus and Lactarius rufus β-d-glucans on HepG2 cells. *International*
555 *Journal of Biological Macromolecules*, *58*, 95-103. https://doi.org/10.1016/j.ijbiomac.2013.03.040

556 Raj, A., Chandran C, S., Dua, K., Kamath, V., & Alex, A. T. (2024). Targeting overexpressed surface
557 proteins: A new strategy to manage the recalcitrant triple-negative breast cancer. *European Journal*
558 *of Pharmacology*, *981*, 176914. https://doi.org/10.1016/j.ejphar.2024.176914

559 Randeni, N., & Xu, B. (2024). New insights into signaling pathways of cancer prevention effects of
560 polysaccharides from edible and medicinal mushrooms. *Phytomedicine*, *132*, 155875.
561 https://doi.org/10.1016/j.phymed.2024.155875

562 Reddy Shetty, P., Batchu, U. R., Buddana, S. K., Sambasiva Rao, K. R. S., & Penna, S. (2021). A
563 comprehensive review on α-D-Glucans: Structural and functional diversity, derivatization and
564 bioapplications. *Carbohydrate Research*, *503*, 108297. https://doi.org/10.1016/j.carres.2021.108297

565 Rodrigues Barbosa, J., dos Santos Freitas, M. M., da Silva Martins, L. H., & de Carvalho, R. N.
566 (2020). Polysaccharides of mushroom Pleurotus spp.: New extraction techniques, biological activities
567 and development of new technologies. *Carbohydrate Polymers*, *229*, 115550.
568 https://doi.org/10.1016/j.carbpol.2019.115550

569 Rutckeviski, R., Corso, C. R., Román-Ochoa, Y., Cipriani, T. R., Centa, A., & Smiderle, F. R. (2022).
570 Agaricus bisporus β-(1 → 6)-d-glucan induces M1 phenotype on macrophages and increases
571 sensitivity to doxorubicin of triple negative breast cancer cells. *Carbohydrate Polymers*, *278*, 118917.
572 https://doi.org/10.1016/j.carbpol.2021.118917

573 Ruthes, A. C., Carbonero, E. R., Córdova, M. M., Baggio, C. H., Santos, A. R. S., Sassaki, G. L.,
574 Cipriani, T. R., Gorin, P. A. J., & Iacomini, M. (2013). Lactarius rufus (1→3),(1→6)-β-d-glucans:
575 Structure, antinociceptive and anti-inflammatory effects. *Carbohydrate Polymers*, *94*(1), 129-136.
576 https://doi.org/10.1016/j.carbpol.2013.01.026

577 Ruthes, A. C., Smiderle, F. R., & Iacomini, M. (2015). d-Glucans from edible mushrooms: A review
578 on the extraction, purification and chemical characterization approaches. *Carbohydrate Polymers*,
579 *117*, 753-761. https://doi.org/10.1016/j.carbpol.2014.10.051

580 Ruthes, A. C., Smiderle, F. R., & Iacomini, M. (2016). Mushroom heteropolysaccharides: A review
581 on their sources, structure and biological effects. *Carbohydrate Polymers*, *136*, 358-375.
582 https://doi.org/10.1016/j.carbpol.2015.08.061

583 Sahasrabudhe, N. M., Dokter-Fokkens, J., & de Vos, P. (2016). Particulate β-glucans synergistically
584 activate TLR4 and Dectin-1 in human dendritic cells. *Molecular Nutrition & Food Research*, *60*(11),
585 2514-2522. https://doi.org/10.1002/mnfr.201600356

586 Shaheen, T. I., Hussien, G. M. A., Mekawey, A. A., Ghalia, H. H. A., youssry, A. A., & El Mokadem,
587 M. T. (2022). Facile extraction of nanosized β-glucans from edible mushrooms and their antitumor
588 activities. *Journal of Food Composition and Analysis*, *111*, 104607.
589 https://doi.org/10.1016/j.jfca.2022.104607

590 Smiderle, F. R., Olsen, L. M., Carbonero, E. R., Baggio, C. H., Freitas, C. S., Marcon, R., Santos, A.
591 R. S., Gorin, P. A. J., & Iacomini, M. (2008). Anti-inflammatory and analgesic properties in a rodent
592 model of a (1→3),(1→6)-linked β-glucan isolated from Pleurotus pulmonarius [Article]. *European*
593 *Journal of Pharmacology*, *597*(1-3), 86-91. 10.1016/j.ejphar.2008.08.028

594 Stamps, A. C., Davies, S. C., Burman, J., & O'Hare, M. J. (1994). Analysis of proviral integration in
595 human mammary epithelial cell lines immortalized by retroviral infection with a temperature-sensitive
596 SV40 T-antigen construct. *International Journal of Cancer*, *57*(6), 865-874.
597 https://doi.org/10.1002/ijc.2910570616

598 Steimbach, L., Borgmann, A. V., Gomar, G. G., Hoffmann, L. V., Rutckeviski, R., de Andrade, D. P.,
599 & Smiderle, F. R. (2021). Fungal beta-glucans as adjuvants for treating cancer patients - A systematic
600 review of clinical trials. (1532-1983 (Electronic)).

601 Sulieman, A. A., Zhu, K.-X., Peng, W., Hassan, H. A., Obadi, M., Siddeeg, A., & Zhou, H.-M. (2019).
602 Rheological and quality characteristics of composite gluten-free dough and biscuits supplemented
603 with fermented and unfermented Agaricus bisporus polysaccharide flour. *Food Chemistry*, *271*, 193-
604 203. https://doi.org/10.1016/j.foodchem.2018.07.189

605 Tondolo, J. S. M., Ledur, P. C., Loreto, É. S., Verdi, C. M., Bitencourt, P. E. R., de Jesus, F. P. K.,
606 Rocha, J. P., Alves, S. H., Sassaki, G. L., & Santurio, J. M. (2017). Extraction, characterization and
607 biological activity of a (1,3)(1,6)-β-d-glucan from the pathogenic oomycete Pythium insidiosum.
608 *Carbohydrate Polymers*, *157*, 719-727. https://doi.org/10.1016/j.carbpol.2016.10.053

609 Vaz da Luz, K. T., Gonçalves, J. P., de Lima Bellan, D., Visnheski, B. R. C., Schneider, V. S., Cortes
610 Cordeiro, L. M., Vargas, J. E., Puga, R., da Silva Trindade, E., de Oliveira, C. C., & Simas, F. F.
611 (2024). Molecular weight-dependent antitumor effects of prunes-derived type I arabinogalactan on

612 human and murine triple wild-type melanomas. *Carbohydrate Research*, *535*, 108986.
613 https://doi.org/10.1016/j.carres.2023.108986

614 Webb, A. (2012). Increasing the Sensitivity of Magnetic Resonance Spectroscopy and Imaging.
615 *Analytical Chemistry*, *84*(1), 9-16. 10.1021/ac201500v

616 World Health Organization (, 2024). *Breast Cancer*. [WHO]. Retrieved 06/2024 from
617 https://www.who.int/news-room/fact-sheets/detail/breast-cancer

618 Yang, Q., Chang, S.-L., Tian, Y.-M., Li, W., & Ren, J.-L. (2024). Glucan polysaccharides isolated
619 from Lactarius hatsudake Tanaka mushroom: Structural characterization and in vitro bioactivities.
620 *Carbohydrate Polymers*, *337*, 122171. https://doi.org/10.1016/j.carbpol.2024.122171

621 Zavadinack, M., Cantu-Jungles, T. M., Abreu, H., Ozturk, O. K., Cordeiro, L. M. C., de Freitas, R.
622 A., Hamaker, B. R., & Iacomini, M. (2024). (1 → 3),(1 → 6) and (1 → 3)-β-D-glucan physico-
623 chemical features drive their fermentation profile by the human gut microbiota. *Carbohydrate*
624 *Polymers*, *327*, 121678. https://doi.org/10.1016/j.carbpol.2023.121678

625 Zavadinack, M., de Lima Bellan, D., da Rocha Bertage, J. L., da Silva Milhorini, S., da Silva Trindade,
626 E., Simas, F. F., Sassaki, G. L., Cordeiro, L. M. C., & Iacomini, M. (2021). An α-D-galactan and a β-
627 D-glucan from the mushroom Amanita muscaria: Structural characterization and antitumor activity
628 against melanoma. *Carbohydrate Polymers*, *274*, 118647.
629 https://doi.org/10.1016/j.carbpol.2021.118647

630 Zavadinack, M., de Lima Bellan, D., Fernandes Bonaldi, M. P., da Silva Milhorini, S., Cordeiro, L.
631 M. C., Fogagnoli Simas, F., & Iacomini, M. (2024). Polysaccharide fractions extracted from Lactarius
632 quieticolor mushroom exhibit immune stimulatory activities on macrophages. *Food Research*
633 *International*, *197*, 115205. https://doi.org/10.1016/j.foodres.2024.115205

634 Zhang, H., Li, C., Lai, P. F. H., Xie, F., Xia, Y., & Ai, L. (2022). NMR elucidation of a water-soluble
635 β-(1→3, 1→6)-glucan from Russula vinosa Lindblad. *Bioactive Carbohydrates and Dietary Fibre*,
636 *27*, 100311. https://doi.org/10.1016/j.bcdf.2022.100311

637 Zhang, S., Lei, L., Zhou, Y., Ye, F.-y., & Zhao, G.-h. (2022). Roles of mushroom polysaccharides in
638 chronic disease management. *Journal of Integrative Agriculture*, *21*(7), 1839-1866.
639 https://doi.org/10.1016/S2095-3119(21)63871-6

640 Zhang, X., Li, T., Liu, S., Xu, Y., Meng, M., Li, X., Lin, Z., Wu, Q., Xue, Y., Pan, Y., & Alitongbieke,
641 G. (2020). β-glucan from Lentinus edodes inhibits breast cancer progression via the Nur77/HIF-1α
642 axis. *Bioscience Reports*, *40*(12). https://doi.org/10.1042/BSR20201006

643

644

Supplementary material

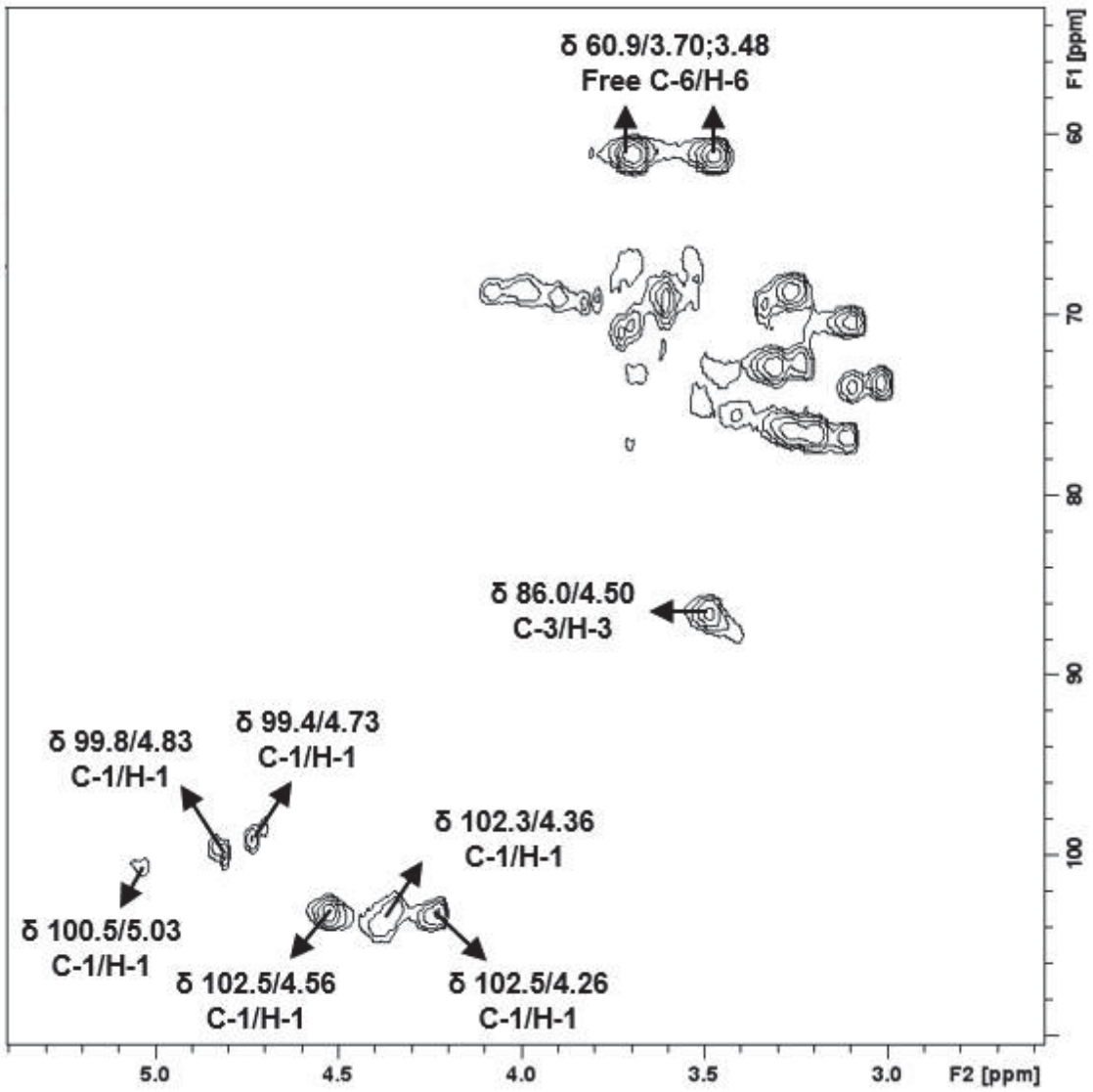

Supplementary Figure 1. Crude alkaline extract obtained from the *Lactarius quieticolor* mushroom. The Sample was analyzed in Me_2SO-d_6, at 70 °C (calibration parameters: δ 39.7/ 2.50 for C/H), and the chemical shifts are expressed in δ ppm.

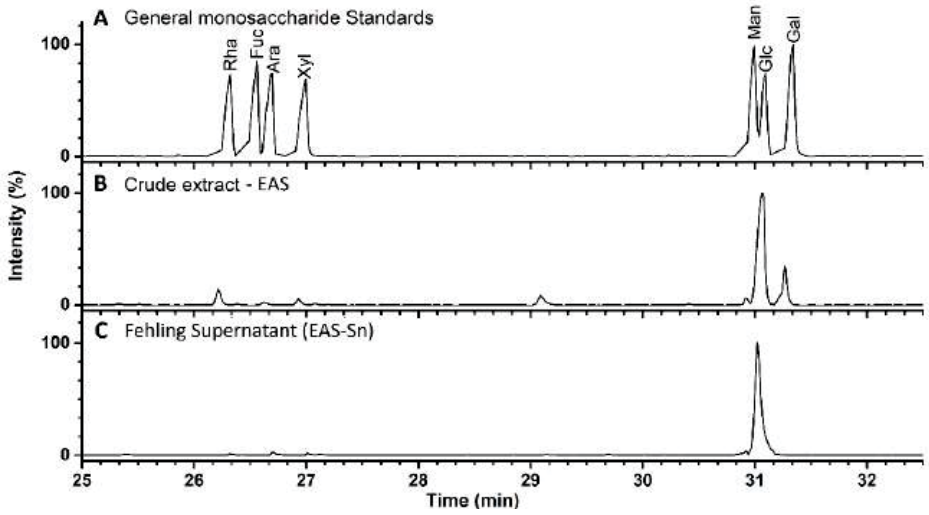

Supplementary Figure 2. Chromatograms obtained from the monosaccharide standards. (A); General monosaccharide standards; **(B)** Crude extract obtained after alkaline extraction; **(C)** Glc-Feh fraction.

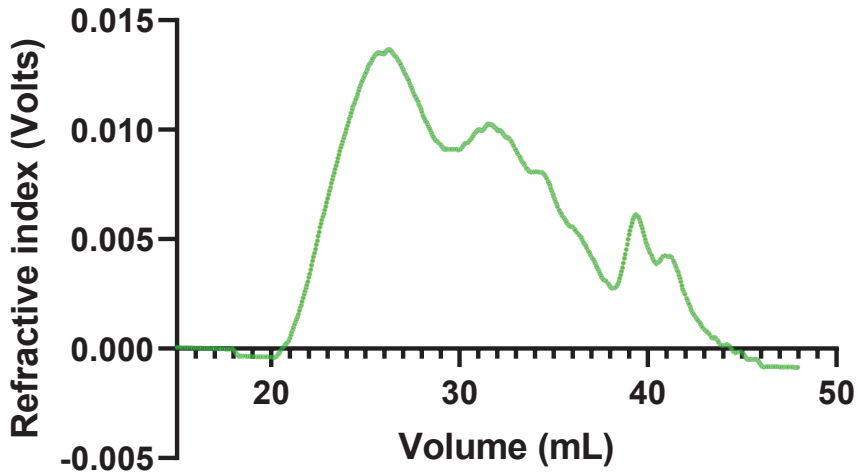

Supplementary Figure 3. Glc-Feh elution profile in HPSEC coupled to a Refractive Index (RI) detector.

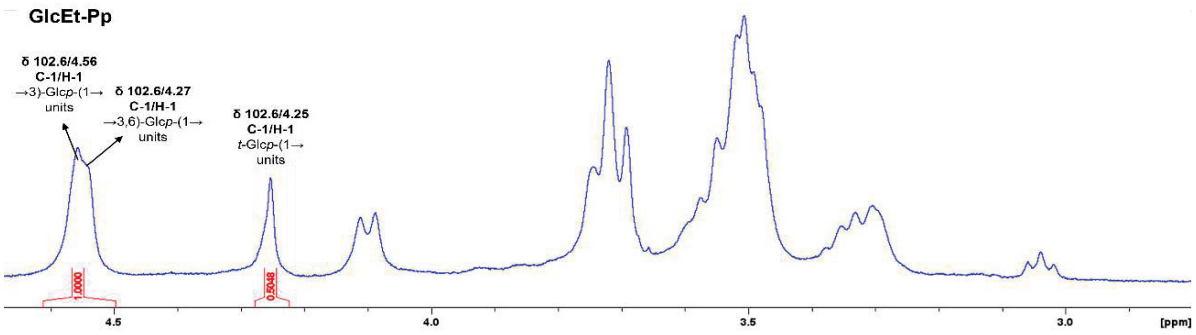

Supplementary Figure 4. 1H-NMR of the GlcEt-Pp fraction obtained from the *Lactarius quieticolor* mushroom. Integrated values (in red) obtained through ^{1}H-NMR spectra.The sample was analyzed in Me_2SO-d_6 (calibration parameters: δ 2.50) at 70°C and the results are expressed in ppm (δ). The analysis and peak assignments were performed using TopSpin software, version 3.6.5.

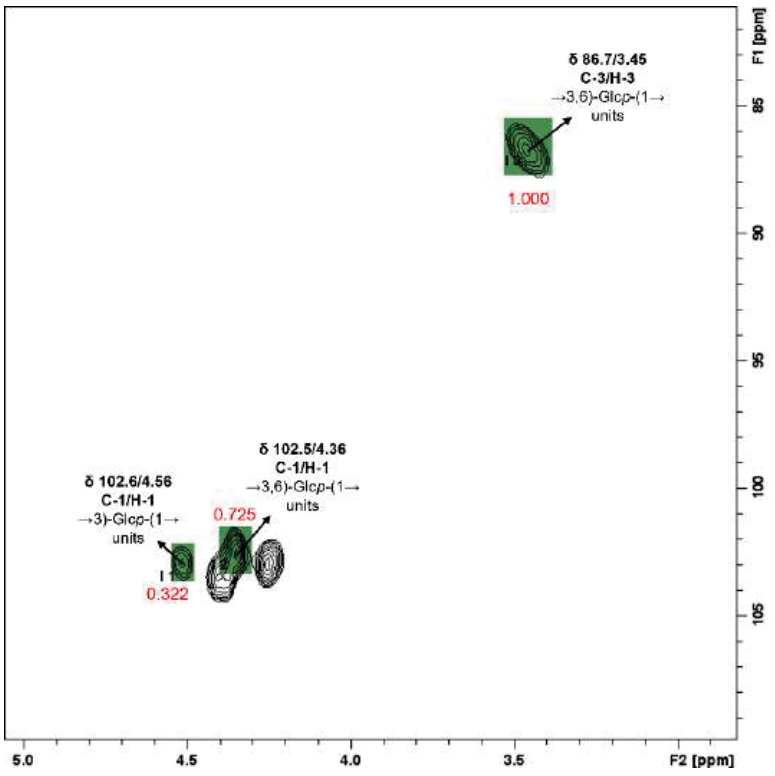

Supplementary Figure 5. HSQC-NMR of the GlcEt-Pp and the GlcEtSn-300 fractions obtained from the *Lactarius quieticolor* mushroom. The integrated values (highlighted in red) correspond to the areas marked in green on the anomeric and linkage signals in the HSQC-NMR spectrum. The samples were analyzed in Me_2SO-d_6 (calibration parameters: δ 2.50) at 70°C and the results are expressed in ppm (δ). The analysis and peak assignments were performed using TopSpin software, version 3.6.5.

5. CONCLUSÕES

A purificação do extrato alcalino do cogumelo *Lactarius quieticolor* deu origem a três polissacarídeos distintos, sendo um heteropolissacarídeo e duas β-glucanas com diferentes estruturas e solubilidade.

O heteropolissacarídeo, uma ramnogalactana composta por 72,6% de α-galactose e 27,4% de β-ramnose, foi isolado a partir do precipitado obtido após tratamento com a solução de Fehling e apresentou perfil homogêneo nas análises de HPSEC, com uma massa molecular estimada em 1,53 x 10^4 Da. A molécula possui uma estrutura formada por unidades de α-D-galactopiranose (1→6) em sua cadeia principal, com substituições em *O*-2 por unidades terminais de ramnose. Esta molécula demonstrou significativo efeito antitumoral ao inibir a viabilidade de células de câncer de mama da linhagem MDA-MB-231 em aproximadamente 50% na maior concentração testada, enquanto mostrava efeitos mínimos em células normais HB4-a. A molécula também demonstrou efeito sinérgico em combinação com paclitaxel, resultando em uma inibição das células MDA-MB-231 superior à observada com os componentes isolados.

Da fração sobrenadante obtida após tratamento com solução de Fehling foram obtidas duas glucanas distintas, as quais foram isoladas por meio de precipitação etanólica fracionada, atingindo uma concentração de etanol de 41% (v/v) e separando-se o precipitado por centrifugação, originando a fração GlcEt-Pp. O sobrenadante etanólico foi posteriormente dialisado utilizando-se membranas de 300 kDa, recuperando-se e concentrando o eluído, originando a fração GlcEtSn-300. Ambas as frações mostraram efeito citotóxico contra as células de câncer MDA-MB-231. No entanto, a fração GlcEtSn-300 apresentou efeitos superiores, pois inibiu as células tumorais de maneira mais seletiva, afetando menos as células normais HB4-a em comparação com a fração GlcEt-Pp. Adicionalmente, enquanto a fração GlcEt-Pp não inibiu a migração das células cancerígenas, a fração GlcEtSn-300 foi capaz de reduzir essa migração em quase 60%. Essas diferenças na atividade biológica podem ser atribuídas às características estruturais das frações: ambas possuem uma estrutura de (1→3), (1→6)-β-D-glucopiranose, mas a fração GlcEtSn-300 apresenta uma maior quantidade de ramificações, com substituições mais intensas na posição O-6 em comparação à GlcEt-Pp. Esses achados destacam as diversas e promissoras propriedades bioativas dos polissacarídeos de *Lactarius quieticolor*, com cada fração contribuindo de forma única para potenciais aplicabilidades destas moléculas.

6. REFERÊNCIAS

ABREU, H.; SMIDERLE, F. R.; SASSAKI, G. L.; SOVRANI, V.; CORDEIRO, L. M. C.; IACOMINI, M. Naturally methylated mannogalactans from the edible mushrooms Pholiota nameko and Pleurotus eryngii. **Journal of Food Composition and Analysis**, 102, p. 103985, 2021.

ADAMS, G. A. Complete acid hydrolysis. **Methods Carbohydr. Chem.**, 5, p. 269-276, 1965.

ALBERSHEIM, P.; NEVINS, D. J.; ENGLISH, P. D.; KARR, A. A method for the analysis of sugars in plant cell-wall polysaccharides by gas-liquid chromatography. **Carbohydrate Research**, 5, n. 3, p. 340-345, 1967.

ARAÚJO-RODRIGUES, H.; SOUSA, A. S.; RELVAS, J. B.; TAVARIA, F. K.; PINTADO, M. An Overview on Mushroom Polysaccharides: Health-promoting Properties, Prebiotic and Gut Microbiota Modulation Effects and Structure-function Correlation. **Carbohydrate Polymers**, 333, p. 121978, 2024.

BONALDI, M. P. F. **Caracterização Estrutural de Polissacarídeos do Cogumelo *Lactarius quieticolor***. 2021. (Mestrado) - Departamento de Bioquímica e Biologia Celular, Universidade Federal do Paraná - UFPR.

BOWMAN, S. M.; FREE, S. J. The structure and synthesis of the fungal cell wall. **BioEssays**, 28, n. 8, p. 799-808, 2006.

BRIDGE, P. D.; SPOONER, B. M.; ROBERTS, P. J. The Impact of Molecular Data in Fungal Systematics. *In*: CALLOW, J. A. (Ed.). **Advances in Botanical Research**: Academic Press, 2005. v. 42, p. 33-67.

BUCZACKI, S.; SHIELDS, C.; OVENDEN, D. **Collins Fungi Guide: The most complete field guide to the mushrooms and toadstools of Britain & Ireland**. HarperCollins Publishers, 2012. 9780007413430.

BUENO, D. J.; SILVA, J. O. FUNGI | The Fungal Hypha. *In*: BATT, C. A. e TORTORELLO, M. L. (Ed.). **Encyclopedia of Food Microbiology (Second Edition)**. Oxford: Academic Press, 2014. p. 11-19.

CHENG, J.; SONG, J.; WANG, Y.; WEI, H.; HE, L.; LIU, Y.; DING, H.; HUANG, Q.; HU, C.; HUANG, X.; JIANG, Y.; WU, Y. Conformation and anticancer activity of a novel mannogalactan from the fruiting bodies of Sanghuangporus sanghuang on HepG2 cells. **Food Research International**, 156, p. 111336, 2022.

CIUCANU, I.; KEREK, F. A simple and rapid method for the permethylation of carbohydrates. **Carbohydrate Research**, 131, n. 2, p. 209-217, 1984.

COGNIGNI, V.; RANALLO, N.; TRONCONI, F.; MORGESE, F.; BERARDI, R. Potential benefit of β-glucans as adjuvant therapy in immuno-oncology: a review. **Exploration of Targeted Anti-tumor Therapy**, p. 122-138, 2021.

DA SILVA MILHORINI, S.; DE LIMA BELLAN, D.; ZAVADINACK, M.; SIMAS, F. F.; SMIDERLE, F. R.; DE SANTANA-FILHO, A. P.; SASSAKI, G. L.; IACOMINI, M. Antimelanoma effect of a fucoxylomannan isolated from Ganoderma lucidum fruiting bodies. **Carbohydrate Polymers**, 294, p. 119823, 2022a.

DA SILVA MILHORINI, S.; SIMAS, F. F.; SMIDERLE, F. R.; INARA DE JESUS, L.; ROSADO, F. R.; LONGORIA, E. L.; IACOMINI, M. β-Glucans from the giant mushroom Macrocybe titans: Chemical characterization and rheological properties. **Food Hydrocolloids**, 125, p. 107392, 2022b.

GARCIA, J.; RODRIGUES, F.; SAAVEDRA, M. J.; NUNES, F. M.; MARQUES, G. Bioactive polysaccharides from medicinal mushrooms: A review on their isolation, structural characteristics and antitumor activity. **Food Bioscience**, 49, p. 101955, 2022.

GOLOVCHENKO, V. V.; NARANMANDAKH, S.; GANBAATAR, J.; PRILEPSKII, A. Y.; BURYGIN, G. L.; CHIZHOV, A. O.; SHASHKOV, A. S. Structural investigation and comparative cytotoxic activity of water-soluble polysaccharides from fruit bodies of the medicinal fungus quinine conk. **Phytochemistry**, 175, p. 112313, 2020.

GORIN, P. A. J.; IACOMINI, M. Polysaccharides of the lichens Cetraria islandica and Ramalina usnea. **Carbohydrate Research**, 128, n. 1, p. 119-132, 1984.

GOW, N. A. R.; LENARDON, M. D. Architecture of the dynamic fungal cell wall. **Nature Reviews Microbiology**, 21, n. 4, p. 248-259, 2023.

HALL, I. R.; NEW ZEALAND INSTITUTE FOR, C.; FOOD RESEARCH, L. **Edible and Poisonous Mushrooms: An Introduction**. New Zealand Institute for Crop & Food Research, 1998. 9780478046977.

HAN, D.; YANG, L.; LIANG, Q.; SUN, H.; SUN, Y.; YAN, G.; ZHANG, X.; HAN, Y.; WANG, X.; WANG, X. Natural resourced polysaccharides: Preparation, purification, structural elucidation, structure-activity relationships and regulating intestinal flora, a system review. **International Journal of Biological Macromolecules**, 280, p. 135956, 2024.

HIBBETT, D. A Phylogenetic overview of the Agaricomycotina. **Mycologia**, 98, p. 917-925, 2006.

HU, X.; GOFF, H. D. Fractionation of polysaccharides by gradient non-solvent precipitation: A review. **Trends in Food Science & Technology**, 81, p. 108-115, 2018.

HYDE, K. D.; XU, J.; RAPIOR, S.; JEEWON, R.; LUMYONG, S.; NIEGO, A. G. T.; ABEYWICKRAMA, P. D.; ALUTHMUHANDIRAM, J. V. S.; BRAHAMANAGE, R. S.; BROOKS, S.; CHAIYASEN, A.; CHETHANA, K. W. T.; CHOMNUNTI, P.; CHEPKIRUI, C.; CHUANKID, B.; DE SILVA, N. I.; DOILOM, M.; FAULDS, C.; GENTEKAKI, E.; GOPALAN, V.; KAKUMYAN, P.; HARISHCHANDRA, D.; HEMACHANDRAN, H.; HONGSANAN, S.; KARUNARATHNA, A.; KARUNARATHNA, S. C.; KHAN, S.; KUMLA, J.; JAYAWARDENA, R. S.; LIU, J.-K.; LIU, N.; LUANGHARN, T.; MACABEO, A. P. G.; MARASINGHE, D. S.; MEEKS, D.; MORTIMER, P. E.; MUELLER, P.; NADIR, S.; NATARAJA, K. N.; NONTACHAIYAPOOM, S.; O'BRIEN, M.; PENKHRUE, W.; PHUKHAMSAKDA, C.; RAMANAN, U. S.; RATHNAYAKA, A. R.; SADABA, R. B.; SANDARGO, B.; SAMARAKOON, B. C.; TENNAKOON, D. S.; SIVA, R.; SRIPROM, W.; SURYANARAYANAN, T. S.; SUJARIT, K.; SUWANNARACH, N.; SUWUNWONG, T.; THONGBAI, B.; THONGKLANG, N.; WEI, D.; WIJESINGHE, S. N.; WINISKI, J.; YAN, J.; YASANTHIKA, E.; STADLER, M. The amazing potential of fungi: 50 ways we can exploit fungi industrially. **Fungal Diversity**, 97, n. 1, p. 1-136, 2019.

JONES, J. K. N.; STOODLEY, R. J. Fractionation using copper complexes. **Methods in carbohydrate chemistry**, 5, p. 36-38, 1965.

KARAKAYA, F.; BİLGİLİ, C.; SOYSAL, N.; YıLMAZ, M. Investigation of secondary school students' learning about the fungi kingdomOrtaöğretim öğrencilerinin mantarlar âlemine yönelik öğrenmelerinin incelenmesi. **Turkish Journal of Education**, 12, p. 227-242, 2023.

KIM, Y.; PRESTEGARD, J. H. Measurement of vicinal couplings from cross peaks in COSY spectra. **Journal of Magnetic Resonance (1969)**, 84, n. 1, p. 9-13, 1989.

KONO, H.; KONDO, N.; ISONO, T.; OGATA, M.; HIRABAYASHI, K. Characterization of the secondary structure and order–disorder transition of a β-(1 → 3, 1 → 6)-glucan from Aureobasidium pullulans. **International Journal of Biological Macromolecules**, 154, p. 1382-1391, 2020.

KOUR, H.; KOUR, D.; KOUR, S.; SINGH, S.; JAWAD HASHMI, S. A.; YADAV, A. N.; KUMAR, K.; SHARMA, Y. P.; AHLUWALIA, A. S. Bioactive compounds from mushrooms: Emerging bioresources of food and nutraceuticals. **Food Bioscience**, 50, p. 102124, 2022.

KRUPPA, M. D.; LOWMAN, D. W.; CHEN, Y.-H.; SELANDER, C.; SCHEYNIUS, A.; MONTEIRO, M. A.; WILLIAMS, D. L. Identification of (1→6)-β-d-glucan as the major carbohydrate component of the Malassezia sympodialis cell wall. **Carbohydrate Research**, 344, n. 18, p. 2474-2479, 2009.

LATGÉ, J.-P. The cell wall: a carbohydrate armour for the fungal cell. **Molecular Microbiology**, 66, n. 2, p. 279-290, 2007.

LEONG, Y. K.; YANG, F.-C.; CHANG, J.-S. Extraction of polysaccharides from edible mushrooms: Emerging technologies and recent advances. **Carbohydrate Polymers**, 251, p. 117006, 2021.

LI, D.; CHEN, M.; MENG, X.; SUN, Y.; LIU, R.; SUN, T. Extraction, purification, structural characteristics, bioactivity and potential applications of polysaccharides from Avena sativa L.: A review. **International Journal of Biological Macromolecules**, 265, p. 130891, 2024.

LI, H.; TIAN, Y.; MENOLLI JR, N.; YE, L.; KARUNARATHNA, S. C.; PEREZ-MORENO, J.; RAHMAN, M. M.; RASHID, M. H.; PHENGSINTHAM, P.; RIZAL, L.; KASUYA, T.; LIM, Y. W.; DUTTA, A. K.; KHALID, A. N.; HUYEN, L. T.; BALOLONG, M. P.; BARUAH, G.; MADAWALA, S.; THONGKLANG, N.; HYDE, K. D.; KIRK, P. M.; XU, J.; SHENG, J.; BOA, E.; MORTIMER, P. E. Reviewing the world's edible mushroom species: A new evidence-based classification system. **Comprehensive Reviews in Food Science and Food Safety**, 20, n. 2, p. 1982-2014, 2021. https://doi.org/10.1111/1541-4337.12708.

LI, K.; WANG, L.; HU, Y.; ZHU, Z. Structural characterization and protective effect on PC12 cells against H2O2-induced oxidative damage of a polysaccharide extracted from mycelia of Lactarius deliciosus Gray. **International Journal of Biological Macromolecules**, 209, p. 1815-1825, 2022.

LIN, S.-R.; CHANG, C.-H.; HSU, C.-F.; TSAI, M.-J.; CHENG, H.; LEONG, M. K.; SUNG, P.-J.; CHEN, J.-C.; WENG, C.-F. Natural compounds as potential adjuvants to cancer therapy: Preclinical evidence. **British Journal of Pharmacology**, 177, n. 6, p. 1409-1423, 2020.

LU, H.; LOU, H.; HU, J.; LIU, Z.; CHEN, Q. Macrofungi: A review of cultivation strategies, bioactivity, and application of mushrooms. **Comprehensive Reviews in Food Science and Food Safety**, 19, n. 5, p. 2333-2356, 2020. https://doi.org/10.1111/1541-4337.12602.

MAITY, P.; SEN, I. K.; CHAKRABORTY, I.; MONDAL, S.; BAR, H.; BHANJA, S. K.; MANDAL, S.; MAITY, G. N. Biologically active polysaccharide from edible mushrooms: A review. **International Journal of Biological Macromolecules**, 172, p. 408-417, 2021.

MANDAL, S.; MAITY, K. K.; BHUNIA, S. K.; DEY, B.; PATRA, S.; SIKDAR, S. R.; ISLAM, S. S. Chemical analysis of new water-soluble (1→6)-, (1→4)-α, β-glucan and water-insoluble (1→3)-, (1→4)-β-glucan (Calocyban) from alkaline extract of an edible mushroom, Calocybe indica (Dudh Chattu). **Carbohydrate Research**, 345, n. 18, p. 2657-2663, 2010.

MILHORINI, S. d. S.; SMIDERLE, F. R.; BISCAIA, S. M. P.; ROSADO, F. R.; TRINDADE, E. S.; IACOMINI, M. Fucogalactan from the giant mushroom Macrocybe titans inhibits melanoma cells migration. **Carbohydrate Polymers**, 190, p. 50-56, 2018.

MILHORINI, S. d. S.; ZAVADINACK, M.; SANTOS, J. F. d.; LARA, E. L. d.; SMIDERLE, F. R.; IACOMINI, M. Structural variety of glucans from Ganoderma lucidum fruiting bodies. **Carbohydrate Research**, 538, p. 109099, 2024.

MUELLER, G. M.; SCHMIT, J. P.; LEACOCK, P. R.; BUYCK, B.; CIFUENTES, J.; DESJARDIN, D. E.; HALLING, R. E.; HJORTSTAM, K.; ITURRIAGA, T.; LARSSON, K.-H.; LODGE, D. J.; MAY, T. W.; MINTER, D.; RAJCHENBERG, M.; REDHEAD, S. A.; RYVARDEN, L.; TRAPPE, J. M.; WATLING, R.; WU, Q. Global diversity and distribution of macrofungi. **Biodiversity and Conservation**, 16, n. 1, p. 37-48, 2007.

NAVARRO-SIMARRO, P.; GÓMEZ-GÓMEZ, L.; AHRAZEM, O.; RUBIO-MORAGA, Á. Food and human health applications of edible mushroom by-products. **New Biotechnology**, 81, p. 43-56, 2024.

PARK, G. S.; SHIN, J.; HONG, S.; GOPAL, J.; OH, J.-W. Anticarcinogenic potential of the mushroom polysaccharide lentinan on gastric and colon cancer cells: Antiproliferative, antitumorigenic, Mu-2-related death-inducing gene, MUDENG ramifications. **Journal of Industrial and Engineering Chemistry**, 135, p. 122-130, 2024.

PENG, F.; REN, J.-L.; XU, F.; BIAN, J.; PENG, P.; SUN, R.-C. Comparative Study of Hemicelluloses Obtained by Graded Ethanol Precipitation from Sugarcane Bagasse. **Journal of Agricultural and Food Chemistry**, 57, n. 14, p. 6305-6317, 2009.

PIRES, A. d. R. A.; RUTHES, A. C.; CADENA, S. M. S. C.; ACCO, A.; GORIN, P. A. J.; IACOMINI, M. Cytotoxic effect of Agaricus bisporus and Lactarius rufus β-d-glucans on HepG2 cells. **International Journal of Biological Macromolecules**, 58, p. 95-103, 2013.

REDDY SHETTY, P.; BATCHU, U. R.; BUDDANA, S. K.; SAMBASIVA RAO, K. R. S.; PENNA, S. A comprehensive review on α-D-Glucans: Structural and functional diversity, derivatization and bioapplications. **Carbohydrate Research**, 503, p. 108297, 2021.

ROMAGNESI, H. Recherches sur les Lactaires a lait rouge (Dapetes Fr.). **Revue de mycologie**, 23, n. 3, 1958.

RUTCKEVISKI, R.; CORSO, C. R.; ROMÁN-OCHOA, Y.; CIPRIANI, T. R.; CENTA, A.; SMIDERLE, F. R. Agaricus bisporus β-(1 → 6)-d-glucan induces M1 phenotype on macrophages and increases sensitivity to doxorubicin of triple negative breast cancer cells. **Carbohydrate Polymers**, 278, p. 118917, 2022.

RUTHES, A. C.; CARBONERO, E. R.; CÓRDOVA, M. M.; BAGGIO, C. H.; SANTOS, A. R. S.; SASSAKI, G. L.; CIPRIANI, T. R.; GORIN, P. A. J.; IACOMINI, M. Lactarius rufus (1→3),(1→6)-β-d-glucans: Structure, antinociceptive and anti-inflammatory effects. **Carbohydrate Polymers**, 94, n. 1, p. 129-136, 2013.

RUTHES, A. C.; SMIDERLE, F. R.; IACOMINI, M. d-Glucans from edible mushrooms: A review on the extraction, purification and chemical characterization approaches. **Carbohydrate Polymers**, 117, p. 753-761, 2015.

RUTHES, A. C.; SMIDERLE, F. R.; IACOMINI, M. Mushroom heteropolysaccharides: A review on their sources, structure and biological effects. **Carbohydrate Polymers**, 136, p. 358-375, 2016.

SAKDASRI, W.; ARNUTPONGCHAI, P.; PHONSAVAT, S.; BUMRUNGTHAICHAICHAN, E.; SAWANGKEAW, R. Pressurized hot water extraction of crude polysaccharides, β-glucan, and phenolic compounds from dried gray oyster mushroom. **LWT**, 168, p. 113895, 2022.

SAMANTA, S.; NANDI, A. K.; SEN, I. K.; MAITY, P.; PATTANAYAK, M.; DEVI, K. S. P.; KHATUA, S.; MAITI, T. K.; ACHARYA, K.; ISLAM, S. S. Studies on antioxidative and immunostimulating fucogalactan of the edible mushroom Macrolepiota dolichaula. **Carbohydrate Research**, 413, p. 22-29, 2015.

SHEN, Q.; SUN, L.; HE, Z.; XIE, J.; ZHUANG, Y. Isolation, taste characterization and molecular docking study of novel umami peptides from Lactarius volemus (Fr.). **Food Chemistry**, 401, p. 134137, 2023.

SHI, L. Bioactivities, isolation and purification methods of polysaccharides from natural products: A review. **Int J Biol Macromol**, 92, p. 37-48, 2016.

SILVA-FILHO, A.; SULZBACHER, M.; GREBENC, T.; WARTCHOW, F. Not every edible orange milkcap is Lactarius deliciosus: first record of *Lactarius quieticolor* (sect. Deliciosi) from Brazil. **Journal of Applied Botany and Food Quality**, 93, p. 289-299, 2020.

SINNOTT, M. **Carbohydrate Chemistry and Biochemistry: Structure and Mechanism**. The Royal Society of Chemistry, 2007. 978-0-85404-256-2.

SMIDERLE, F. R.; ALQUINI, G.; TADRA-SFEIR, M. Z.; IACOMINI, M.; WICHERS, H. J.; VAN GRIENSVEN, L. J. L. D. Agaricus bisporus and Agaricus brasiliensis (1→6)-β-d-glucans show immunostimulatory activity on human THP-1 derived macrophages. **Carbohydrate Polymers**, 94, n. 1, p. 91-99, 2013.

STEIMBACH, L.; BORGMANN, A. V.; GOMAR, G. G.; HOFFMANN, L. V.; RUTCKEVISKI, R.; DE ANDRADE, D. P.; SMIDERLE, F. R. Fungal beta-glucans as adjuvants for treating cancer patients – A systematic review of clinical trials. **Clinical Nutrition**, 40, n. 5, p. 3104-3113, 2021.

SULIEMAN, A. A.; ZHU, K.-X.; PENG, W.; HASSAN, H. A.; OBADI, M.; SIDDEEG, A.; ZHOU, H.-M. Rheological and quality characteristics of composite gluten-free dough and biscuits supplemented with fermented and unfermented Agaricus bisporus polysaccharide flour. **Food Chemistry**, 271, p. 193-203, 2019.

TJAHJANINGSIH, W.; PITUTUR, P. S. P.; PATMAWATI; MUBARAK, A. S.; HUSEIN, M. A. A.; RASEETHA; ELKAVANTO, M. G. P.; RACHMANSYAH, M. R.; HANIF, F. Z. Effect of NaOH-based deproteinisation on chemical and biological properties of Moina sp. chitosan. **Food Res.**, 7, n. Supplementary 4, p. 1-9, 2023.

TU, J.; ADHIKARI, B.; BRENNAN, M. A.; LUO, S.; CHENG, P.; BAI, W.; BRENNAN, C. S. Acidic polysaccharides from black ear and silver ear mushrooms modulated the release and transport of glucose from gelatinised sorghum starch during digestion. **Food Chemistry**, 411, p. 135426, 2023.

WANG, W.; TAN, J.; NIMA, L.; SANG, Y.; CAI, X.; XUE, H. Polysaccharides from fungi: A review on their extraction, purification, structural features, and biological activities. **Food Chemistry: X**, 15, p. 100414, 2022.

WANG, Y.; AZHAR, S.; LINDSTRÖM, M.; HENRIKSSON, G. Stabilization of Polysaccharides During Alkaline Pre-Treatment of Wood Combined with Enzyme-Supported Extractions in a Biorefinery. **Journal of Wood Chemistry and Technology**, 35, 2015.

WANG, Z.; ZHOU, X.; SHU, Z.; ZHENG, Y.; HU, X.; ZHANG, P.; HUANG, H.; SHENG, L.; ZHANG, P.; WANG, Q.; WANG, X.; LI, N. Regulation strategy, bioactivity, and physical property of plant and microbial

polysaccharides based on molecular weight. **International Journal of Biological Macromolecules**, 244, p. 125360, 2023.

WEBSTER, J.; WEBER, R. **Introduction to Fungi**. 3 ed. Cambridge: Cambridge University Press, 2007. 9780521014830.

WORLD HEALTH ORGANIZATION **Cancer**. , 2022. Disponível em: https://www.who.int/news-room/fact-sheets/detail/cancer. Acesso em: 06/2024.

WORLD HEALTH ORGANIZATION **Breast Cancer**. , 2024. Disponível em: https://www.who.int/news-room/fact-sheets/detail/breast-cancer. Acesso em: 06/2024.

YANG, Q.; CHANG, S.-L.; TIAN, Y.-M.; LI, W.; REN, J.-L. Glucan polysaccharides isolated from Lactarius hatsudake Tanaka mushroom: Structural characterization and in vitro bioactivities. **Carbohydrate Polymers**, 337, p. 122171, 2024.

YAO, H.-Y.-Y.; WANG, J.-Q.; YIN, J.-Y.; NIE, S.-P.; XIE, M.-Y. A review of NMR analysis in polysaccharide structure and conformation: Progress, challenge and perspective. **Food Research International**, 143, p. 110290, 2021.

YIN, C.; NORATTO, G. D.; FAN, X.; CHEN, Z.; YAO, F.; SHI, D.; GAO, H. The Impact of Mushroom Polysaccharides on Gut Microbiota and Its Beneficial Effects to Host: A Review. **Carbohydrate Polymers**, 250, p. 116942, 2020.

YU, Y.; LIU, Z.; SONG, K.; LI, L.; CHEN, M. Medicinal value of edible mushroom polysaccharides: a review. **Journal of Future Foods**, 3, n. 1, p. 16-23, 2023.

YUGUEROS, S. I.; PELÁEZ, J.; STAJICH, J. E.; FUERTES-RABANAL, M.; SÁNCHEZ-VALLET, A.; LARGO-GOSENS, A.; MÉLIDA, H. Study of fungal cell wall evolution through its monosaccharide composition: An insight into fungal species interacting with plants. **The Cell Surface**, 11, p. 100127, 2024.

ZAVADINACK, M.; DE LIMA BELLAN, D.; DA ROCHA BERTAGE, J. L.; DA SILVA MILHORINI, S.; DA SILVA TRINDADE, E.; SIMAS, F. F.; SASSAKI, G. L.; CORDEIRO, L. M. C.; IACOMINI, M. An α-D-galactan and a β-D-glucan from the mushroom Amanita muscaria: Structural characterization and antitumor activity against melanoma. **Carbohydrate Polymers**, 274, p. 118647, 2021.

ZAVADINACK, M.; DE LIMA BELLAN, D.; FERNANDES BONALDI, M. P.; DA SILVA MILHORINI, S.; CORDEIRO, L. M. C.; FOGAGNOLI SIMAS, F.; IACOMINI, M. Polysaccharide fractions extracted from *Lactarius quieticolor* mushroom exhibit immune stimulatory activities on macrophages. **Food Research International**, 197, p. 115205, 2024.

ZHANG, H.; LI, C.; LAI, P. F. H.; XIE, F.; XIA, Y.; AI, L. NMR elucidation of a water-soluble β-(1→3, 1→6)-glucan from Russula vinosa Lindblad. **Bioactive Carbohydrates and Dietary Fibre**, 27, p. 100311, 2022.

ZHANG, S.; LEI, L.; ZHOU, Y.; YE, F.-y.; ZHAO, G.-h. Roles of mushroom polysaccharides in chronic disease management. **Journal of Integrative Agriculture**, 21, n. 7, p. 1839-1866, 2022.

ZHONG, R.-F.; YANG, J.-J.; GENG, J.-H.; CHEN, J. Structural characteristics, anti-proliferative and immunomodulatory activities of a purified polysaccharide from Lactarius volemus Fr. **International Journal of Biological Macromolecules**, 192, p. 967-977, 2021.